



AER4855

PROJET INTÉGRATEUR IV: DESIGN D'AÉRONEF

FINAL REPORT



CHRISTIAN CRUZ-SANCHEZ (1538976)
FRANÇOIS DESGROSEILLIERS (1581221)
MATTIEU GEMME (1630618)
TONY LAC (1521876)
MARTIN LAFRANCE (1529087)
MARTIN LEFEBVRE (1437052)
SIMON MOLGAT LAURIN (1536399)
MENA NASHED (1525781)
MATTIEU PARENTEAU (1525599)

PRESENTED TO:

STÉPHANE DUFRESNE

April 24, 2015





Abstract

The present report will describe the conceptual design of two aircrafts developed in order to comply with the future needs of the regional aviation field. At the start of the first term, a Marketing Requirement & Objectives document was presented to the teams to set the target values with regard of the different fields of aircraft design. Mainly, both aircrafts are required to transport at least 76 and 100 passengers at a range of 1800 and 1200 nautical miles respectively. Thus, two aircrafts with unprecedented open rotor propellers and MEA systems have been designed to replace the aging regional aircraft fleet in the coming years.

The current term saw the integration of two teams from the previous term to increase human resources in order to allow us to increase the quality of the preliminary design. Therefore, two aircraft families were merged into a design that respected the design philosophy of all team members. This philosophy is translated by the integration of innovative engines and a more electric approach with regard of systems. Integration of such technologies will allow regional aviation to gain more technical appeal. The aircraft design has been optimized in order to meet the requirements of the MR&O and also in order to introduce a marketable product line in a competitive environment. The numerous optimization changes have been continuously approved by the project manager and the various specialities among the team. The design process was completed by integrating the end product of the different disciplines into a uniform aircraft family representation. Table 1 indicates the team member assignment for the final report.

Department	Team Members	Report Part
Project Management	Christian Cruz-Sanchez	Abstract, Introduction (1), Comparative Study (2.1, 2.2), Design Process (4.1, 4.1.2, 4.1.3), Top-level Schedule (3), Conclusion (14)
Economics	Simon Molgat-Laurin	Comparative Study (2.3), Economics (13)
Configuration & CAD	Matthieu Gemme	Configuration (5)
Engines & Systems	Mena Nashed François Desgroseilliers	Engines (8) , Systems (7)
Performance, S&C	Tony Lac	Design Process (4.1.1, 4.2.1, 4.2.2), Performance (10), Stability & Control (12.1, 12.2, 12.4, 12.5)
Aerodynamics	Matthieu Parenteau	Design Process (4.2.3), Aerodynamics (9)
Weights & Balance	Martin Lafrance	Weights & CG Envelope (11), Stability & Control (12.3)
Structure	Martin Lefebvre	Structure (6)

Table 1: Role of Team Members



Acknowledgements

The ORCA design team would like to thank the Bombardier Aerospace representatives for the help that was provided throughout the conception process. Their insight during the weekly meetings was indispensable throughout our project and allowed the team to deepen our knowledge about aircraft development, particularly regarding the interactions between the various aspects and teams in aircraft design.

We would also like to thank Stéphane Dufresne in particular for his valuable theoretical courses, as well as for his guidance throughout the entire project.



Contents

1	Introduction	1
2	Comparative Study	2
2.1	MR&O Comparison	2
2.2	Competitors Comparison	4
2.3	Market Share Analysis	7
3	Top-Level Schedule	10
4	Design Process	12
4.1	Overall Design Process	13
4.1.1	Data Center	14
4.1.2	Systems	16
4.1.3	Structure	16
4.2	Optimisation	16
4.2.1	Cruise Altitude & Speed	16
4.2.2	Climb Speed	17
4.2.3	Wing Area	18
5	Configuration	22
5.1	Morphology	22
5.1.1	Engine	22
5.1.2	Wing	23
5.1.3	Fuselage	24
5.1.4	Empennage	24
5.1.5	Landing Gear	25
5.2	Detailed Configuration	27
5.2.1	Overall Configuration	28
5.2.2	Cargo Capacity	33
5.2.3	Ground Servicing	34
5.2.4	Turning Radius	36
5.3	Interior	37
5.3.1	Floor Plan	38
5.3.2	Cross Sections	40
6	Structure	43
6.1	Materials	44
6.2	Fuselage Structure	46
6.3	Wing Junction	50
6.4	Wing Structure	51
6.4.1	Wing & Fuselage	53



6.5	Landing Gear	54
7	Systems	56
7.1	Overall System Architecture	56
7.2	Electrical System	58
7.3	Hydraulic System	60
7.4	Pneumatic System	62
7.5	Fuel Reserve	65
7.5.1	Refuel and Defuel	67
7.5.2	Engine and APU Feed	67
7.5.3	Fuel Transfer and Jettison System	68
7.5.4	Fuel Measurement and Management	68
7.6	Flight Controls	68
7.7	Avionics	70
7.7.1	Auto Land Category IIIB	74
7.7.2	Auto-Throttle	74
7.7.3	Head-Up Display Visual Guidance System (HVGS)	75
7.8	Ice Protection	76
7.9	APU	77
8	Engines	80
8.1	Noise and Emissions	82
8.2	Position	83
8.3	Fuel Consumption	83
8.4	Thrust Reversers	84
8.5	Electrical Generators	85
9	Aerodynamics	86
9.1	Airfoil	86
9.2	Wing Characteristics	87
9.2.1	Clean Wing	87
9.2.2	High Lift Devices	89
9.3	Drag Breakdown	94
9.3.1	Takeoff	94
9.3.2	Cruise	95
9.3.3	Landing	97
10	Performance	100
10.1	Takeoff	100
10.2	Landing	101
10.3	Climb	101
10.4	Cruise	102
10.5	Mission Profile	102
10.6	Payload Range	104
10.7	High Density Configuration	104



11 Weights and CG Envelope	106
11.1 Weight Breakdown	106
11.2 CG Envelope	111
11.3 Wing Position & Plugs	113
11.4 High Density Configuration	113
12 Stability & Control	115
12.1 Initial Tail Sizing	115
12.2 Stability Coefficients	116
12.3 Longitudinal Stability - AFT/FWD CG Limit	116
12.4 Directional Stability	117
12.5 Control Surfaces	118
13 Economics	121
13.1 Cash Operating Cost Evaluation	121
13.2 COC Presentation	123
13.2.1 Competitor Comparison	124
13.3 Fixed Costs: Research, Development, Test and Evaluation Cost	125
13.4 Variable Costs: Acquisition Costs	128
13.5 ORCA77 and ORCA101 RDTE and Acquisition Costs Overview	129
13.6 Unit Price per Aircraft and Competitor Comparison	132
13.7 Break-Even Analyses	133
13.8 Virtual Budget Evaluation	135
14 Conclusion	138
14.1 Commonality	138
14.2 Last Words	139
A ANNEX	145
A.1 Materials	145
A.2 Structure	148
A.3 Barrel and Panel Design Analysis	151
A.4 Landing Gear Design	158



List of Figures

1	Global GDP Growth	7
2	Projected Program Market Share	8
3	Projected Program Market Share	9
4	Top-Level Program Schedule	10
5	Overall Design Process	12
6	Design Process Interactions	13
7	Design Flow	14
8	Performance - Weight Loop Convergence	14
9	Mission Profile	15
10	Reserve Profile	15
11	Cost vs Mach number at 26 000ft	17
12	Cost vs Mach number at 36 000ft	17
13	Design Process Interactions	19
14	Wing Surface Optimization - BFL with 12000 thrust/engine	20
15	Wing Surface Optimization - BFL with 13000 thrust/engine	20
16	Wing Surface Optimization - BFL with 14000 thrust/engine	20
17	Wing Surface Optimization - COC with 13000 thrust/engine	20
18	Wing Surface Optimization - Alt=36 000 ft; Mach=0.66; Aircraft: ORCA101; 13 000 lbf thrust/engine	21
19	Nose Landing Gear Design	26
20	Main Landing Gear Design	26
21	Nose Landing Gear Position	27
22	Main Landing Gear Position	27
23	3 Views Drawing of ORCA77 Design	29
24	3 Views Drawing of ORCA101 Design	30
25	Control Surfaces	32
26	Rotor Burst Zones	33
27	Cargo Integration	34
28	Ground Servicing - ORCA77	35
29	Ground Servicing - ORCA101	36
30	Turning Radius	37
31	Floor Plan	39
32	Business Class Section View	41
33	Economy Class Section View	41
34	Complete Structural Isometric View	44
35	Aircraft Material	46
36	Fuselage Structure	47
37	Fuselage Panel Configuration	49
38	Wing Junction	51
39	Wing Structure	52
40	Wing Section Along with Baffle Rib	52
41	H-Tail Structure	53
42	V-Tail Structure	53



43	Material and Functional Analysis	54
44	Overall System Architecture	57
45	Electrical Architecture	58
46	Electrical Layout	60
47	Hydraulic Architecture	61
48	Hydraulic Layout	62
49	Pneumatic Architectures	63
50	Air Distribution - Business Cross View	64
51	Pneumatic Layout	65
52	Fuel Storage and Venting System[29]	66
53	Surge Tank	67
54	Avionics System Disposition [42]	71
55	Top Level Architecture of the Avionics System	72
56	Avionics Domain [42]	73
57	Avionics Cabinet	74
58	HVGS [12]	75
59	Enhanced Vision System (EVS) [12]	76
60	APU[2]	79
61	APU Location	79
62	Engine Dimension	82
63	Pylon Design	83
64	SFC vs Thrust @ M0.66	84
65	SFC vs Thrust @ M0.68	84
66	Thrust vs Delta in Takeoff	84
67	Airfoil Analysis - C_d vs α [8]	86
68	Airfoil Analysis - C_l vs α [8]	86
69	Airfoil Analysis - C_d vs C_l [8]	86
70	Airfoil SC(2)-0612	87
71	Leading Edge Device	90
72	Bombardier CRJ-700 High-Lift design (ICAS Congress[26])	91
73	Effect of Flap Gap on Lift Coefficient of a Two-element Airfoil at $\alpha = 0^\circ$, $Re = 3.7\text{million}$, $M_\infty = 0.2$ [22]	92
74	High-Lift Geometry Definitions	93
75	Drag Breakdown - Takeoff ORCA77	95
76	Drag Breakdown - Takeoff ORCA101	95
77	Drag Breakdown - Cruise ORCA77	96
78	Drag Breakdown - Cruise ORCA101	97
79	Drag Breakdown - Landing ORCA77	98
80	Drag Breakdown - Landing ORCA101	99
81	BFL vs TOW - ORCA77	101
82	BFL vs TOW - ORCA101	101
83	Payload Range - ORCA77	104
84	Payload Range - ORCA101	104
85	Structure Weight Breakdown	109
86	Systems Weight Breakdown	110



87	Operating Weight Empty Breakdown	110
88	CG Location for Individual Components	111
89	CG Envelope - ORCA 77	112
90	CG Envelope - ORCA 101	112
91	X-plot Longitudinal Stability - ORCA 77	117
92	X-plot Longitudinal Stability - ORCA 101	117
93	X-plot Directional Stability - ORCA 77	118
94	X-plot Directional Stability - ORCA 101	118
95	Control Surfaces Dimensions	120
96	ORCA77 COC Distribution	123
97	ORCA101 COC Distribution	124
98	ORCA77 COC Competition Comparison	124
99	ORCA101 COC Competition Comparison	125
100	ORCA77 RDTE Cost Distribution	130
101	ORCA101 RDTE Cost Distribution	130
102	ORCA77 Manufacturing Cost Distribution	131
103	ORCA101 Manufacturing Cost Distribution	132
104	ORCA Family Weighted Break Even Analysis	134
105	ORCA Family Payback Period Analysis	134
106	Weekly Personal Work Hours	135
107	Departmental Budget Spending Distribution	136
108	Overall Budget Distribution	137
109	Weekly Budget Tracker	137
110	Cost and Weight Impact Based on Conservative Assumptions	146
111	Range of Potential Weight and Cost Savings	147
112	Thickness Along a Sample Panel	147
113	Initial Conventional Structure	148
114	Barrel Design	151
115	Three Sections Panels with Plugs	152
116	Full Panels Design with Plugs	153
117	Full Length Panel Design	154
118	Top View Load Path	156
119	Frontal Load Path	157
120	Longitudinal Load Path	157
121	Landing Gear Weight Breakdown	159
122	Landing Gear Weight Initial Sizing	160





List of Tables

1	Role of Team Members	I
2	Specifications Comparison with MR&O	3
3	ORCA 77 Specifications Comparison with Competitors	5
4	ORCA 101 Specifications Comparison with Competitors	6
5	Fixed Fuel-Time Allowances	15
6	Climb Speed Optimization	18
7	Design Characteristics	22
8	Wing Characteristics	23
9	Tail Specifications	25
10	Gears Dimensions	26
11	Underfloor Bulk Cargo	34
12	Meal Requirements Estimations	38
13	Overhead Bins Luggage (Number of Luggages)	42
14	Material Pugh Matrix	45
15	Electrical Load per Mission Phase	59
16	Fresh Air Flow Requirement	64
17	Actuators Analysis	69
18	Number of Actuators per Control Surfaces	69
19	Engine Failure Analysis [42]	78
20	Engines Criteria	80
21	Marketing Requirements and Objectives	80
22	General Characteristics	81
23	Airfoil Characteristics	87
24	Wing Geometry	88
25	Wing Aerodynamic's Characteristics at Mach=0.66	88
26	Competitors Wing Comparison[62]	89
27	Slat Competitor Comparison[62]	89
28	Trailing-edge High-lift Devices on Several Civil Transport Airplanes[51]	92
29	High Lift Devices Characteristics	93
30	Total Drag Breakdown - Takeoff	94
31	Profile Drag Breakdown - Takeoff	94
32	Total Drag Breakdown - Cruise	96
33	Profile Drag Breakdown - Cruise	96
34	Total Drag Breakdown - Landing	98
35	Profile Drag Breakdown - Landing	98
36	Takeoff Performance	100
37	Landing Performance	101
38	Climb Performance	102
39	Cruise Mach Number	102
40	Mission Profile	103
41	Reserve Fuel Requirements Optimization	103
42	High Density Impact on Performance - ORCA77	105
43	High Density Impact on Performance - ORCA101	105



44	Author Comparison for Weights Estimation	106
45	Competitor Weight Analysis	107
46	Weight breakdown for ORCA77 and ORCA101	108
47	Design Weights Summary	108
48	CG Location for Individual Components	111
49	High Density configuration weight impact for ORCA77	113
50	High Density configuration weight impact for ORCA101	114
51	Tail Comparison	115
52	Stability Derivatives	116
53	Control Surfaces DImensions	118
54	COC Breakdown	123
55	RDTE Cost Breakdown	129
56	Manufacturing Cost Breakdown	131
57	Unit Price - ORCA77	132
58	Unit Price - ORCA101	133
59	Structural Components Commonality	138
60	Systems Components Commonality	138
61	Fuselage Structure Competitor Comparison	145
62	Fuselage Structure Competitor Comparison	145
63	Fuselage Structure Competitor Comparison	149
64	Wing & Tail Structure Competitor Analysis	149
65	Control Surfaces Competitor Analysis	150
66	Panel & Barrel Comparison	155
67	Actuator Initial Sizing	158
68	Landing Gear Sizing	158
69	Landing Gear Sizing Electrical Motor Integration Analysis	159
70	Landing Gear Weight Breakdown	159



Acronyms

- AED** Airframe Engineering and Design.
- AFDX** Avionics Full-Duplex Switched Ethernet.
- AFRP** Aramid Fiber Reinforced Polymer.
- AIMS** Airplane Information Management System.
- APC** Airplane Program Production Cost.
- APU** Auxiliary Power Unit.
- ARINC** Aeronautical Radio, Incorporated.
- ATRU** Auto Transformer Rectifier Unit.
- BES** Bombardier Engineering System.
- BFL** Balanced Field Length.
- CAD** Computer-Aided Design.
- CAEP** Committee on Aviation Environmental Protection.
- CAST** Complete Airframe Static Test.
- CEF** Cost Escalation Factor.
- CFRP** Carbon Fiber Reinforced Polymer.
- CG** Center of Gravity.
- CI** Cost Index.
- COC** Cash Operating Cost.
- CPIOM** Core Processor Input/Output Module.
- CRJ** Canadair Regional Jet.
- ECS** Environmental Control System.
- EDP** Engine Driven Pump.
- EHA** Electro-Hydraulic Actuator.
- EIS** Entry Into Service.
- ELA** Electrical Load Analysis.
- EMP** Electric Motor Pump.
- ERJ** Embraer Regional Jet.



EVS Enhanced Vision System.

FAA Federal Aviation Administration.

FAR Federal Aviation Regulations.

FTA Flight Test Airplanes.

FTO Flight Test Operations.

GDP Gross Domestic Product.

GFRP Glass Fiber Reinforced Polymer.

HD High Density.

HVGS Heads-Up Display Visual Guidance System.

IATA International Air Transport Association.

IFR Instrument Flight Rules.

IMA Integrated Modular Avionics.

ISA International Standard Atmosphere.

LE Leading Edge.

LFL Landing Field Length.

LRC Long Range Cruise.

M Mach Number.

MAC Mean Aerodynamic Chord.

MEA More Electric Aircraft.

MHA Mechanical-Hydraulic Actuator.

MLG Main Landing Gear.

MLW Maximum Landing Weight.

MRJ Mitsubishi Regional Jet.

MRO Marketing Requirements & Objectives.

MRW Maximum Runway Weight.

MTOW Maximum Takeoff Weight.

MWE Manufacturer Weight Empty.



MZFW Maximum Zero-Fuel Weight.

NaN Not a Number.

NASA National Aeronautics and Space Administration.

NLG Nose Landing Gear.

ORCA Open Rotor Commercial Aircraft.

OWE Operating Weight Empty.

PAX Passengers.

PDU Power Drive Unit.

RAT Ram Air Turbine.

RATDP Ram Air Turbine Driven Pump.

RDTE Research, Development, Testing and Evaluation.

SEP Specific Excess Power.

SL Sea Level.

TC Transport Canada.

TSF Test and Simulation Facilities.

UDF Unducted Fan.

VMD Minimum Drag Speed.





1 Introduction

In recent years, aircraft manufacturers have been examining the forthcoming need to satisfy the increasing worldwide demand for commercial aviation. Regional airliners have been operating a wide range of aging aircrafts and fleet renewal is expected in the coming years. Moreover, these companies are subject to a significant amount of pressure regarding the economic side of operations. Therefore, a product family with a high regard for economic efficiency as well as customer experience satisfaction will be the principal considerations for lead airline companies in the purchase of new aircrafts. Hence, the objective of this project is to design a certifiable product line of two aircrafts that will carry at least 76 and 100 passengers with a specific range of 1800 and 1200 nautical miles respectively. A marketing requirements & objectives document has been provided to establish the thresholds that will lead us to a satisfactory design. Additionally, continual comparison with competitors will be taken into account to achieve a competitive design.

The current design is the result of a merge of two aircraft families coming from different teams. The merge was not a difficult task since the team decided to choose a single pre-defined design to establish the baseline configuration in order to save time and costs. Also, the main strategy to define the initial configuration was to establish a common design philosophy among all team members. Therefore, the design philosophy remains the same as the one specified in the past as described by three expressions: competitive, environmentally friendly and innovative. Ensuring compliance with regards of numerous technical constraints will allow the team to design a compelling aircraft family that will become a viable option for airliners. Both products will need to be environmentally friendly, because an important amount of requirements in the MR&O are related to possible new environmental restrictions to be applied in the near future. Innovation is another feature incorporated into the design process seeing that it would be compelling to bring novelty to the commercial aviation market. More specifically, the introduction of an unconventional propulsion system showcases how the aircraft design aims to implement an unprecedented feature in commercial aviation. In the following report, all these aspects will be visible with respect to every subject associated with conceptual aircraft design. The various aeronautical disciplines will be addressed, starting with configuration, structure and systems. Afterwards, the technical aspects of propulsion, aerodynamics, performance, weights & CG envelope and stability & control will be presented to validate overall integration. An economic study of the program will conclude the design. Beforehand, the initial comparative study and the design process will be dissected to ensure understanding of the numerous interactions between all disciplines. On that account, the team is proud to present the Open Rotor Commercial Aircraft (ORCA) family.



2 Comparative Study

Before introducing the numerous technical specifications of both ORCA aircrafts, it is pertinent to specify the constraints and the environment which will limit the design scope. Since both aircrafts are fully designed, comparative data tables will be presented in Section 2.1 & 2.2 with the final values. This analysis will situate both aircrafts in the regional aircraft market. The justification of each of the end product characteristics will be presented progressively in the report.

2.1 MR&O Comparison

The starting point of the project evolved around the study of an MR&O document. The constant evolution of both aircrafts was permanently subject to comparison to the numerous constraints mentionned in said document. After completing the design, one of the most important tasks was to conclude the validation of our data by comparing our specifications with the initials values from the MR&O. Table 2 highlights the areas that satisfy the numerous criteria.



Comparison Criteria	MR&O 77 PAX	ORCA 77	MR&O 101 PAX	ORCA 101
Cabin				
Minimum Seat Pitch	32 in	Economy: 32 in Business: 34 in	32 in	Economy: 32 in Business: 34 in
Checked Baggage Volume Required	616 ft ³	676 ft ³	808 ft ³	930 ft ³
Minimum Percentage of passengers that can store carry-on baggage inside overhead bins	80 %	Attained	80%	Attained
Minimum Seat Width	18 in	Economy: 18 in Business: 21 in	18 in	Economy: 18 in Business: 21 in
Minimum Aisle Width	19 in	Economy: 20 in Business: 25 in	19 in	Economy: 20 in Business: 25 in
Minimum Cabin Height	77 in	88 in	77 in	88 in
Performance				
Range	1 800 nm	1 800 nm	1 200 nm	1 200 nm
Minimal Cruise Speed (Mcruse)	M0.60	M0.68	M0.60	M0.66
Maximal Cruise Speed (Mmo)	≥ Mcruise + 0.05	M0.73	≥ Mcruise + 0.05	M0.71
BFL (MTOW, SL, ISA)	4 500 ft	4 108 ft	5 000 ft	4 681 ft
BFL (MTWO, SL+5000, ISA+25)	6 000 ft	5 060 ft	6 500 ft	5 779 ft
LFL (MLW, SL, ISA, Wet Runway)	4 500 ft	4 203 ft	4 500 ft	4 441 ft
Approach Speed (MLW, SL, ISA)	≤ 120 Kts	102 KCAS	≤ 120 Kts	107 KCAS
Minimal Initial Cruise Altitude (MTOW, ISA)	25 000 ft	36 000 ft	25 000 ft	36 000 ft
Minimal Climb Speed to Reach ICA	300 fpm	454 fpm	300 fpm	329 fpm
Maximum OEI Altitude (95% MTOW, ISA)	≥17 000 ft @ 300 ft/min	20 000 ft	≥17 000 ft @ 300 ft/min	17 000 ft
Other				
Certification Compliance	TC CAR, FAR Part 25 & JAR Part 25	Attained	TC CAR, FAR Part 25 & JAR Part 25	Attained
Parts Commonality	90 %	Attained	90 %	Attained
Avionics Compliance	CAT IIIB, EVS / HGS, Auto-Throttle	Attained	CAT IIIB, EVS / HGS, Auto-Throttle	Attained
Systems Compliance	Miscellaneous	Attained	Miscellaneous	Attained
Structural Compliance	Miscellaneous	Attained	Miscellaneous	Attained
CO₂ Emission	-20% Competition	Attained	-20% Competition	Attained
NO_x Emission	CAEP6 - 50%	CAEP6 -75%	CAEP6 - 50%	CAEP6 -75%
Cabin Noise	77 dBA	Attained	77 dBA	Attained
Exterior Noise	- 20 EPNdB	-17 EPNdB	- 20 EPNdB	-17 EPNdB
Costs	-15% Competition	-16% Competition	-15% Competition	-20% Competition

Table 2: Specifications Comparison with MR&O



The previous table indicates that the vast majority of the requirements mentioned in the MR&O are met following the multidisciplinary design of the aircraft. Geometrical compliance with the MR&O was settled after maximal passenger comfort was achieved following the integration of systems. Subsequent to the optimization phase of the project, performance data was successfully evaluated to assert compliance with the MR&O. Finally, other various requirements were addressed during the design process to demonstrate full compliance. The exterior noise of both aircrafts is the only specification that doesn't meet the requirement of the MR&O. All the subjects presented on Table 2 will be presented throughout the report. On that account, it is conceivable to state that the aircraft design is mature enough to represent a significantly competitive product in the regional jet market.

2.2 Competitors Comparison

Following the completion of the design, an important number of specifications with regard of different aspects of the aircraft design were assessed. Afterwards, the main activity was to validate the values the team obtained. Therefore, a comparison with competitors was in order. This has been achieved by comparing ORCA 77 to Bombardier, Embraer, Comac and Sukhoi regional jets (CRJ700 STD, E-170 STD, E-175 STD, ARJ21-700 STD and SSJ 100/75 Basic). Likewise, ORCA 101 will be compared to regional jets from the same companies mentioned previously (CRJ1000 STD, E-190 STD, E-195 STD, ARJ21-900 STD and SSJ 100/75 Basic). Tables 3 & 4 will display this comparative study.



Comparison Criteria	ORCA77	CRJ700 STD	E-170 STD	E-175 STD	ARJ21-700 STD	SSJ 100/75 Basic
General						
Flight Crew	2	2	2	2	2	2
Seating capacity	77 (2-class, typical)	66 (2-class, typical)	70 (2-class, standard)	78 (2-class, standard)	78 (2-class)	78 (1-class, standard)
Engine						
Engine	Conceptual	GE CF34-8C5B1	GE CF34-85E	GE CF34-85E	GE CF34-10A	PowerJet SaM146
Engine Type	Open Rotor	Turbofan	Turbofan	Turbofan	Turbofan	Turbofan
Engine Mount	Fuselage	Fuselage	Wing	Wing	Fuselage	Wing
TO thrust (per Engine)	13 000 lbf	12 670 lbf	14 200 lbf	14 200 lbf	17 640 lbf	13 000 lbf
Performance						
Range	1 800 nm	1 092 nm	1 800 nm	1 800 nm	1 200 nm	1 570 nm
Basic Cruise Speed	M0.68	M0.78	M0.78	M0.78	M0.78	M0.78
Maximum Cruise Speed	M0.73	M0.825	M0.82	M0.82	M0.82	M0.81
Takeoff Field Length	4 108 ft	4 975 ft	4 865 ft	5 289 ft	5 600 ft	4 970 ft
Landing Field Length	4 203 ft	5 040 ft	4 029 ft	4 131 ft	-	-
Service Ceiling	41 000 ft	41 000 ft	41 000 ft	41 000 ft	39 000 ft	-
External Dimensions						
Length	110 ft 1 in	106 ft 1 in	98 ft 1 in	103 ft 11 in	109 ft 9 in	86 ft 9 in
Wingspan	100 ft 1 in	76 ft 3 in	85 ft 4 in	85 ft 4 in	89 ft 6 in	91 ft 2 in
Height	29 ft 7 in	24 ft 10 in	32 ft 4 in	32 ft 4 in	27 ft 8 in	33 ft 9 in
Wing Area	1000 ft ²	760 ft ²	-	-	860 ft ²	-
Weights						
OWE	47 300 lb	43 499 lb	46 610 lb	48 080 lb	55 116 lb	-
MZFW	64 600 lb	62 300 lb	66 447 lb	69 887 lb	-	-
MTOW	75 500 lb	72 750 lb	79 344 lb	82 673 lb	89 300 lb	85 580 lb
MLW	69 100 lb	67 000 lb	72 312 lb	74 957 lb	-	77 000 lb

Table 3: ORCA 77 Specifications Comparison with Competitors



Comparison Criteria	ORCA101	CRJ1000 STD	E-190 STD	E-195 STD	ARJ21-900	SSJ 100/95 Basic
General						
Flight Crew	2	2	2	2	2	2
Seating capacity	101 (2-class, typical)	100 (1-class, typical)	94 (2-class, typical)	106 (2-class, standard)	98 (2-class)	98 (1-class, standard)
Engine						
Engine	Conceptual	GE CF34-8C5A1	GE CF34-10E	GE CF34-10E	GE CF34-10A	PowerJet SaM146
Engine Type	Open Rotor	Turbofan	Turbofan	Turbofan	Turbofan	Turbofan
Engine Mount	Fuselage	Fuselage	Wing	Wing	Fuselage	Wing
TO thrust (per Engine)	13 000 lbf	13 630 lbf	20 000 lbf	20 000 lbf	18 500 lbf	16 000 lbf
Performance						
Range	1 200 nm	1 425 nm	1 800 nm	1 600 nm	1 200 nm	1590 nm
Basic Cruise Speed	M0.66	M0.78	M0.78	M0.78	M0.78	M0.78
Maximum Cruise Speed	M0.71	M0.82	M0.82	M0.82	M0.82	M0.81
Takeoff Field Length	4 681 ft	6 695 ft	5 243 ft	5 715 ft	5 740 ft	5 033 ft
Landing Field Length	4 441 ft	5 740 ft	4 022 ft	4 134 ft	-	-
Service Ceiling	41 000 ft	41 000 ft	41 000 ft	41 000 ft	39 000 ft	-
External Dimensions						
Length	124 ft 9 in	128 ft 5 in	118 ft 11 in	126 ft 10 in	119 ft 3 in	98 ft 3 in
Wingspan	100 ft 1 in	85 ft 11 in	94 ft 3 in	94 ft 3 in	89 ft 6 in	91 ft 2 in
Height	29 ft 7 in	24 ft 6 in	34 ft 7 in	34 ft 7 in	27 ft 8 in	33 ft 9 in
Wing Area	1000 ft ²	833 ft ²	-	-	860 ft ²	-
Weights						
OWE	49 400 lb	51 120 lb	61 910 lb	63 870 lb	57 920 lb	-
MZFW	72 100 lb	77 500 lb	90 169 lb	93 696 lb	-	-
MTOW	80 600 lb	90,000 lb	105 360 lb	107 564 lb	96 157 lb	101 150 lb
MLW	76 600 lb	81,500 lb	94 800 lb	99 208 lb	-	90 000 lb

Table 4: ORCA 101 Specifications Comparison with Competitors



Both tables substantiate that the values obtained are within the range of acceptance. For both aircrafts, engine specifications vary according to the morphology adopted by the companies. Takeoff thrust is in the ballpark range among all regional jets presented. In contrast, external dimensions of both ORCA aircrafts seem oversized in comparison to other regional jets. This can be explained by our technical limitations associated with optimization. Overall weights of the design are slightly lower than most competitors. This can be attributed to the implementation of different weight reduction strategies, such as the use of advanced composite materials. Hence, the aircraft design specifications are in the correct range for validation.

2.3 Market Share Analysis

Various economic studies have demonstrated a significant correlation between Gross Domestic Product (GDP) growth and the demand for commercial aircrafts, largely due to the association between a population's propensity to travel and the corresponding country's economic growth. As seen in Figure 1 below, global GDP is expected to rise by 3.3% between 2013 and 2033, particularly due to important economic growth in certain regions such as China and India. It is therefore reasonable to assume the commercial aircraft market will continue to grow and remain lucrative in the coming years [15].

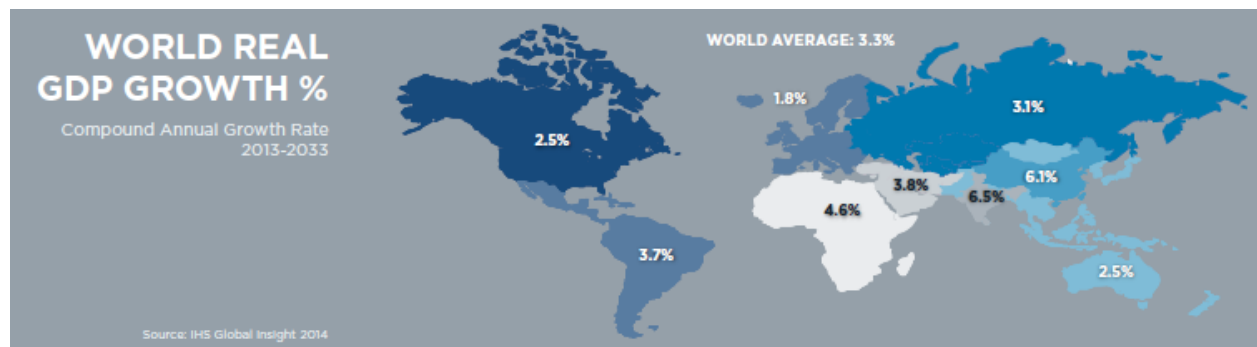


Figure 1: Global GDP Growth

According to various market analyses, the 70 to 140 passenger regional aircraft market is expected to see a substantial rise in orders as airlines start retiring older aircraft models for newer and more technologically advanced models; 9475 regional aircraft in this passenger range are expected to be delivered over the course of the next 20 years [15] [16]. While approximately 95% of this market was previously controlled by Bombardier and Embraer [11], new aircraft from companies such as Comac, Sukhoi and Mitsubishi have created a highly competitive market where customer experience and fuel efficiency are at the forefront of product development; the Mitsubishi



Regional Jet (MRJ) program in particular is estimated to claim as much as 22% of the regional aircraft market [11].

Using these projections, and accounting for the heightened competitiveness of the market, it is estimated that the ORCA program will claim 12% of the 70 to 140 passenger regional aircraft market over the course twenty years from the 2021 launch date. This projection would result in approximately 474 deliveries for the ORCA77 and 663 deliveries for the ORCA101, for a total of 1137 aircraft as shown in Figure 2 below:

2021 – 2041 MARKET SHARE ANALYSIS				
Market Projections		Our Possible Market Share		
PAX Range	Expected Deliveries	10%	12%	15%
75-95	3950	395	474	593
95-140	5525	553	663	829
Total	9475	948	1137	1421

Our Projected Market Share

Figure 2: Projected Program Market Share

Using this information, the sales of the ORCA family over the course of the 20 year program are projected to be distributed as seen in Figure 3.



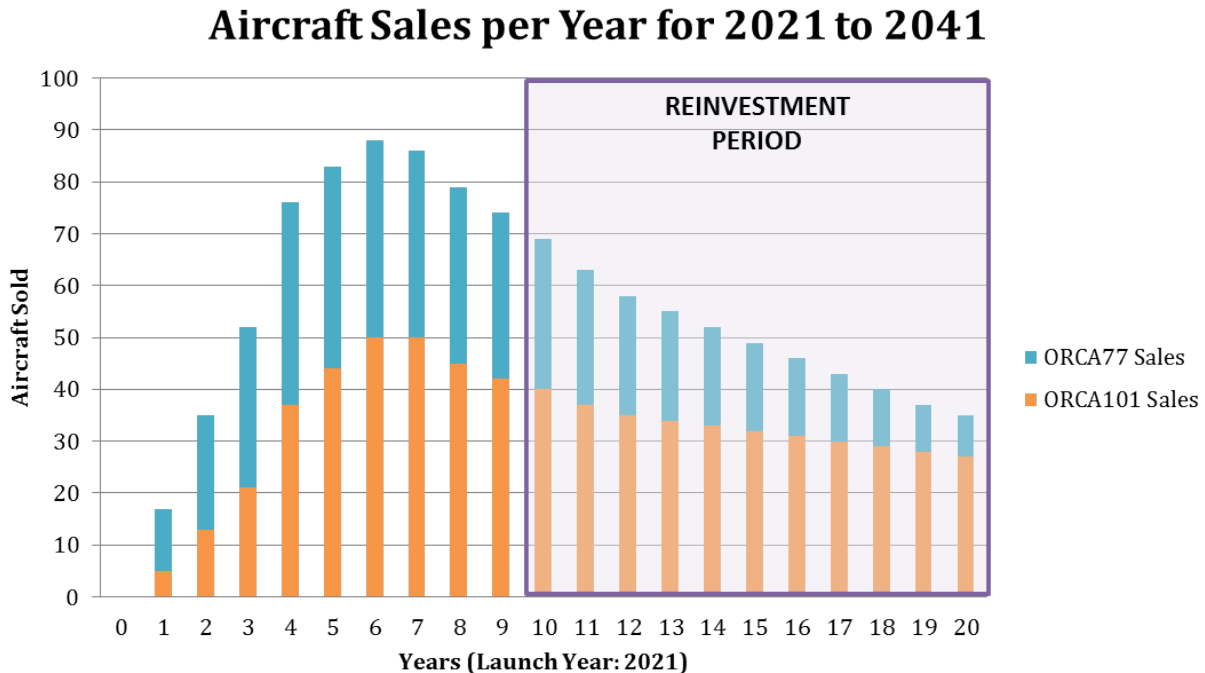


Figure 3: Projected Program Market Share

It is estimated that the ORCA77 will sell more units in the first years after entry into service as it replaces old turbojets as well as a portion of the 60-90 seat turboprop market. Following the first years of sales, customer confidence will build as our novel open rotor aircraft's efficiency is proven. This will lead to a rapid rise in ORCA101 sales since several market analyses predict that the majority of regional aircraft deliveries will consist of 100+ seat aircraft, particularly in regions such as the Middle East, India and China. Finally, as the ORCA77 sales decline, the ORCA101 sales will remain relatively constant since it is projected that 100+ seat aircrafts will remain in high demand for years to come.

Figure 3 above also presents a Reinvestment Period starting the 10th year after entry into service of the ORCA family. This period represents the time at which new configurations must be considered in order maintain the company's profitability as ORCA family sales decline.

It is this team's belief that the ORCA family will meet these marketing and economic objectives due to the innovation and technological prowess that fuel the top-level efficiency and comfort of these aircraft.



3 Top-Level Schedule

The ORCA aircraft family is scheduled for Entry Into Service (EIS) in the year 2021. To respect such a restrictive deadline, the development of a top-level program schedule is mandatory. The task that the team has completed during both terms corresponds to an accelerated version of the conceptual design and launch preparation phases. The conceptual design was completed last term by presenting a product line that possessed satisfactory specifications to meet the program's goal, which is to design a competitive aircraft family that fully complies with the MR&O. In reality, an additional study regarding potential partners and suppliers should be conducted at the conceptual design phase. Subsequently, the current term is focused on advancing the design to prepare for the official program launch. The launch preparation phase distinguishes itself from the conceptual phase by increasing the amount of details by using optimization tools and by adding cost and schedule assessments. The remaining phases were set to respect an EIS for the year 2021 using a backward planning methodology. Their lengths were determined by approximating the time required to complete the tasks involved in each phase. Since EIS is scheduled for 2021, the suggested timeline is rigorous and highly optimistic. The schedule, which was built according to the Bombardier Engineering System (BES) [20] as a benchmark, can be seen on Figure 4.

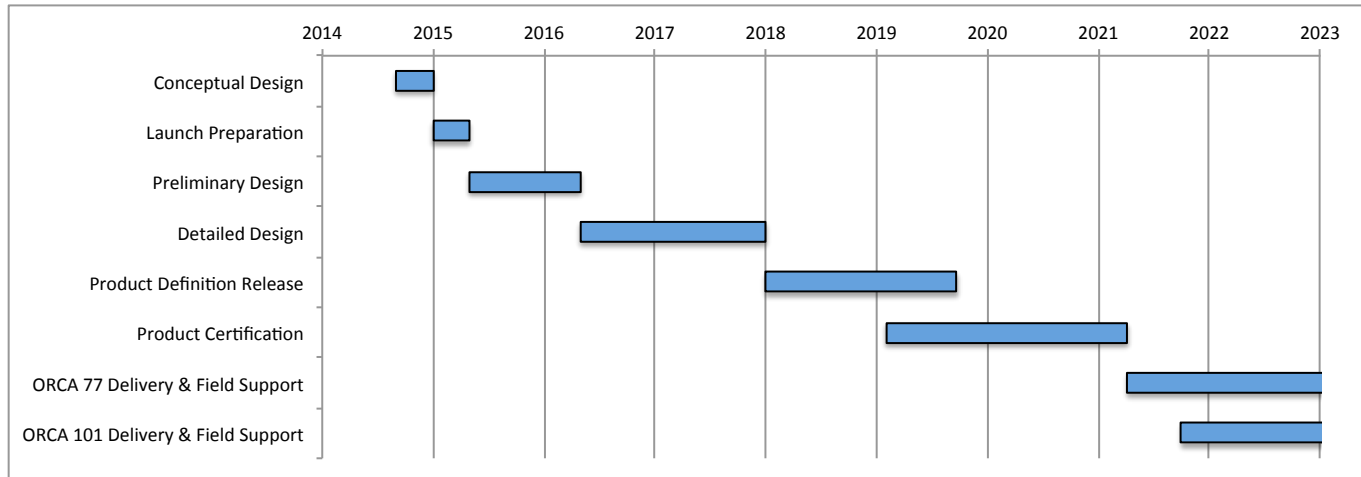


Figure 4: Top-Level Program Schedule

The conceptual design and launch preparation phases usually take up more time than shown, but they will be represented as stages covering both terms for academic purposes. Following the launch completion, which will be official after the final presentation, the preliminary definition phase can begin. This phase will allow the designers to freeze the main components. Also, optimization will continue with regard of life-cycle cost analysis. The inception of the manufacturing and assembly



documents will allow to reach a milestone where partners and suppliers can be reached to distribute work shares. During this phase, it is recommended to go through reviews to guarantee that compliance with initial requirements are still ensured. Once the preliminary design is complete, the development of production drawings will set off the detailed definition phase. It is clear that the progression of different phases results in additional refinements of the design. In order to complete this phase, an important milestone has to be reached and approved: the critical design review. Prior to this event, numerous design reviews are set to be carried out, but the critical design review will represent the final step to validate the compliance of the aircraft family with regard of technical, marketing, cost, weights and performance requirements to name a few.

The product definition release phase will see the beginning of the manufacturing stage with the development of tooling and first article assembly. Progressively, some major structural parts will be produced to allow the next phase to take place simultaneously. The engineering department will be consulted repeatedly for reviews throughout this phase to validate major deliverables, such as engineering configuration statements and nomenclature documentation. After the approval of the final engineering design, the product certification phase will commence in order to prepare for the various certification tests. It is important to note that production shall be subject to inspection at that point in order to approve the manufacturers' quality control system that will replicate the approved design documents. Specifically, this phase will include the development of the Complete Airframe Static Test (CAST) and the first flight certification tests. In fact, there are two important milestones during this phase that need to be addressed rigorously in order to respect the initial timeline. The first one is the first flight readiness review. At this stage, different certification authorities will assess the readiness to initiate flight tests. Subsequently, the type certificate readiness review will ensure that airworthiness standards are met to initiate EIS. Furthermore, the certification phase will conclude and product delivery and field support will begin. A time shift was adopted to simulate the delay between EIS for the ORCA77 and ORCA101 aircrafts.



4 Design Process

In order to complete a competitive multidisciplinary aircraft design, eight different groups were created among the team: project management, economics, configuration, engines & systems, performance, aerodynamics, weights and structure. Distinct processes were developed to manage the numerous interactions that were required to advance the design in an orderly manner. Thus, a design process was established to direct the involvement of the groups. Afterwards, the optimization phase utilized the fixed design process to improve the end product quality. Figure 5 presents a summary of the iterative methodology that was applied to achieve the aircraft design. Hence, this section will detail the tools that lead the team throughout the design process and the optimization phase.

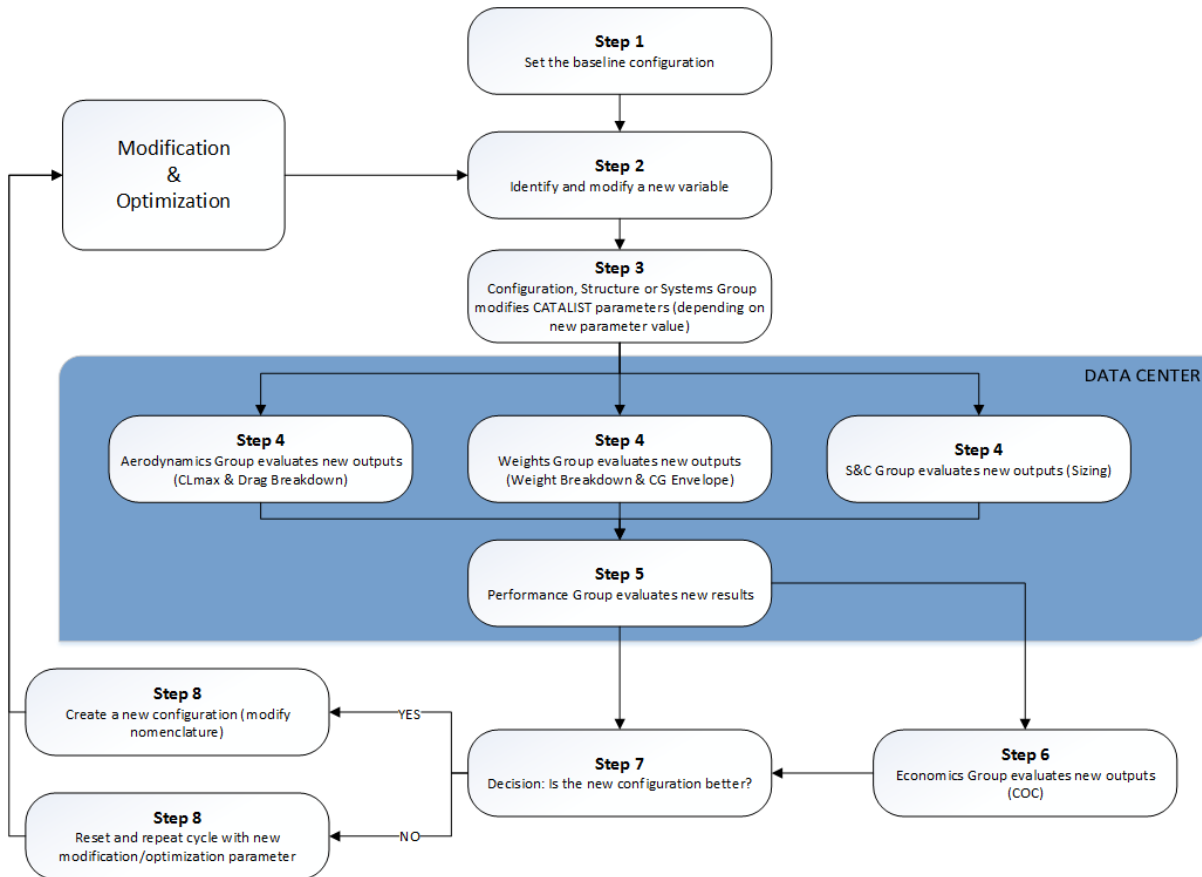


Figure 5: Overall Design Process



4.1 Overall Design Process

The main objective of developing a design process is to organise the interactions between the eight groups. All team members impact the evolution of the aircraft family, so a systematic approach is needed to manage the maturing design. This meant that most groups required direct contact with the configuration team member. Hence, the first decision was to merge the functionalities of the following three groups: performance, aerodynamics and weights. These three factions were merged into a code called the Data Center. Section 4.1.1 will address the technical aspects of that merger. The other two interactions to be described in Section 4.1.2 and 4.1.3 are the ones that involve the systems and structure groups with the configuration team member. The complete coordination was directed and overseen by the project manager to ensure a high level of synergy to productively advance the aircraft design. The overall team design process interactions can be seen on Figure 6.

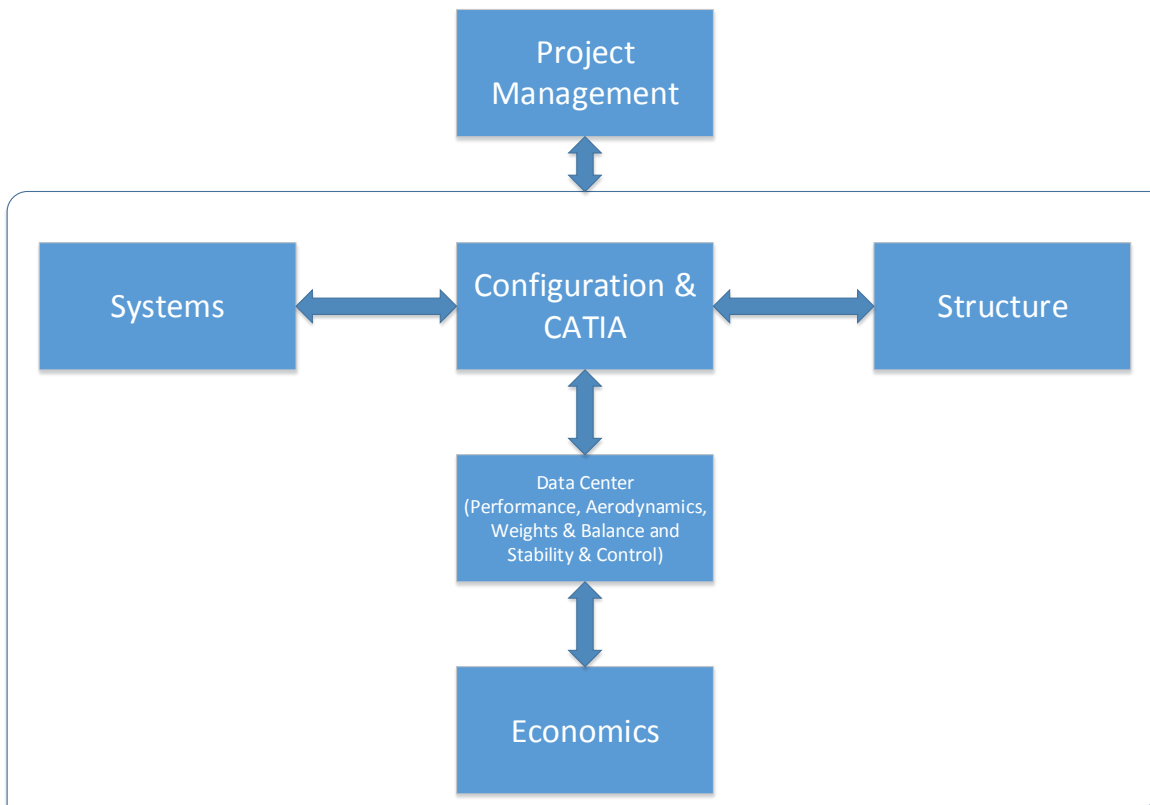


Figure 6: Design Process Interactions

Thereby, the main interactions visible on Figure 6 will be addressed in the following sections. Additionally, the optimization process will be explained in Section 4.2 to highlight the methodology



applied to design the aircrafts.

4.1.1 Data Center

Upon receiving the aircraft design geometry file from the configuration group, the objective of the performance group is to select optimal cruise speed, cruise altitude, climb speeds and wing surface area. The optimization process accounts for five possible variables of optimization. In order to minimize optimization time, the calculations are done separately and they follow a linear process as illustrated in Figure 7.

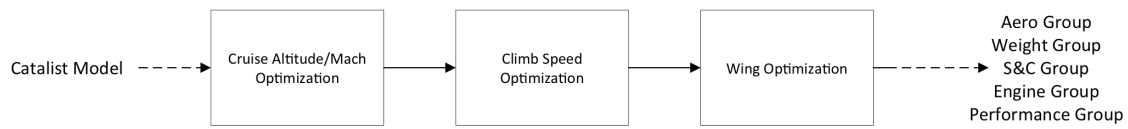


Figure 7: Design Flow

Firstly, the code uses two “for” loops to select cruise speed and altitude for the designed Cost Index. Secondly, according to MR&O OEI and AEO ceiling’s specific excess power, two climb speed variables are selected by observation in order to minimize climb time. Finally, the program verifies that the BFL/LFL requirements are satisfied. If the ground performance requirements are not satisfied, a wing area optimization is entailed. For a better understanding of the code, Figure 8 illustrates the performance-weight convergence loop.

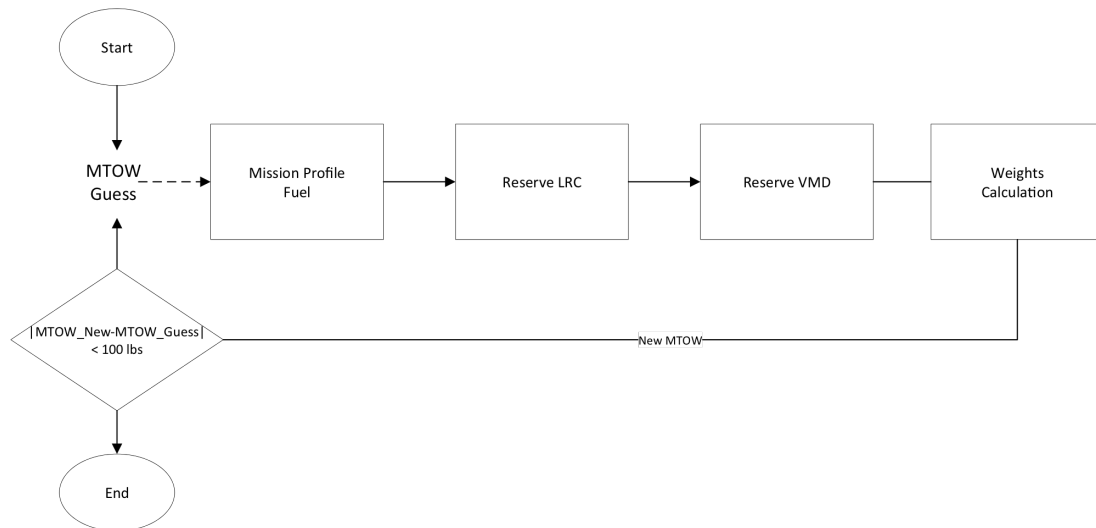


Figure 8: Performance - Weight Loop Convergence

For each iteration, the performance code calculates the required fuel weight for the primary and Instrument Flight Rules (IFR) mission profile which is then processed by the weight code to outputs a new guess for MTOW and OWE. The code is stopped once the guessed value and the evaluated value difference is below 100 lbm. In order to simulate the complete mission of the aircraft, the performance code attempts to simulate the mission profile and the reserve profile as illustrated in Figure 9 and Figure 10 given the fixed fuel-time allowances as shown in Table 5.

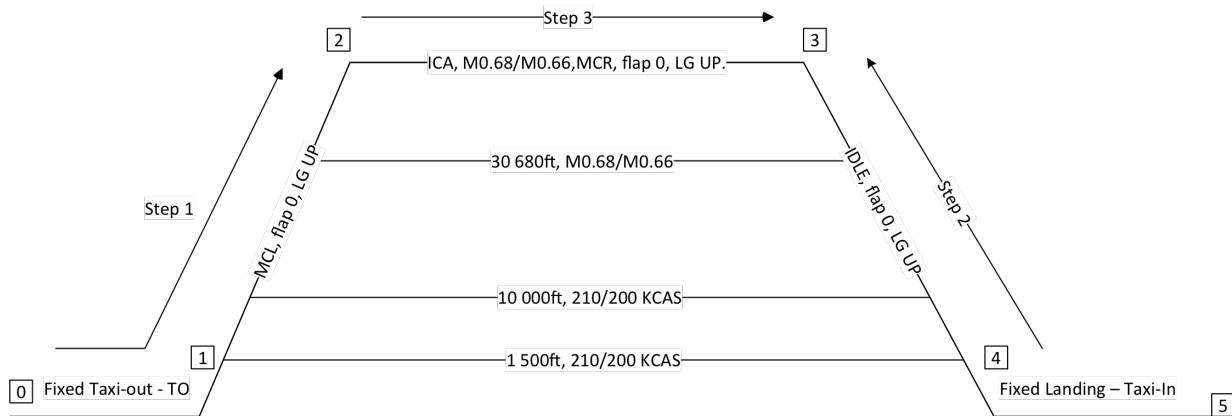


Figure 9: Mission Profile

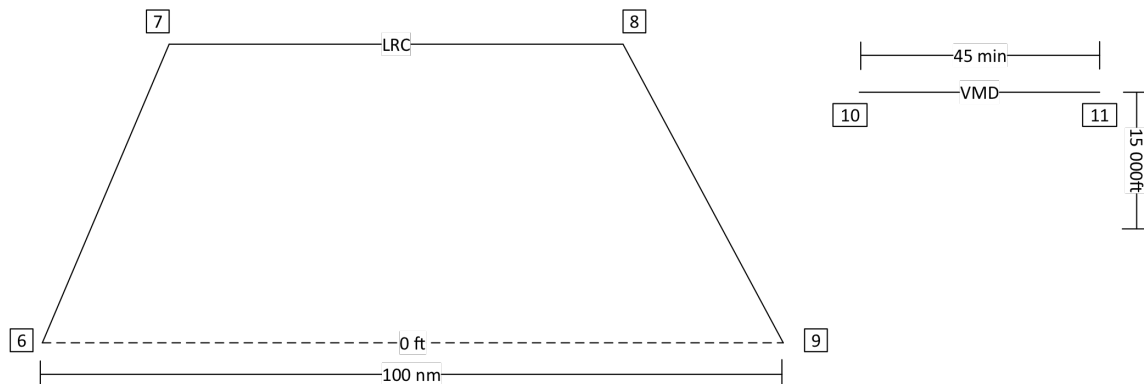


Figure 10: Reserve Profile

	Time (mins)	Fuel (lbs)
Taxi-out	10	148
Takeoff	2	150
Landing	3	IDLE flight
Taxi-in	5	90

Table 5: Fixed Fuel-Time Allowances



4.1.2 Systems

As it was seen on Figure 6, the systems group had numerous contacts with the configuration group to continually approve its progress. During the project, the systems team members conceptually developed system architectures and layouts to implement into the aircrafts. The evaluation of volumes for various parts were required for integration. After reaching the milestone of design completion, the systems had to be implemented into the 3D model to verify if passenger comfort and space management wasn't compromised. Hence, the interaction between the systems and configuration groups was iterative. The same type of activities were carried out with the weights group to validate the systems of the ORCA aircrafts.

4.1.3 Structure

The interaction between the structure group and the configuration team member required a significant amount of communication because the design criteria of structural components depended on the current configuration of both aircrafts. The configuration group was permanently implicated in modification activities with regard to the numerous group requests. Hence, the structure group had to keep track of the frequent changes that were implemented into the ORCA design. This also implies that this interaction was iterative throughout the design process.

4.2 Optimisation

4.2.1 Cruise Altitude & Speed

The fuel cost can be estimated by assuming the following data: IATA's jet fuel price for North America (updated since February 15 2015) = 185.5 cents/gallon [34]. Two main grades of turbine fuel is commonly around the world: Jet A and Jet A-1.

However, since the Jet A is usually not available outside the United States, the Jet A-1 physical properties will be used for the cost evaluation of the mission. Knowing the density of Jet A-1, (6.71 lbs /US gal) [34], the fuel-related cost can be calculated as follows:

$$Cost_{fuel} = 185.5 \frac{\text{cents}}{\text{gallon}} \times \frac{\text{gallon}}{6.79 \text{lbs}} \times \frac{\text{dollar}}{100 \text{cents}} = 0.2732 \frac{\text{dollar}}{\text{lbs}} \quad (1)$$

Next, the time-related cost relies on the set CI (Cost Index) from the company. CI is the ratio of



the time related cost and the fuel cost. A zero cost index determines a flight for minimum trip fuel and maximum range. A maximum cost index determines a flight for maximum flight envelope speeds. The optimal CI is determined to be 12 for all 737 models and 22 for the MD-80 [19]. The passenger capacity of the 737 and MD-80 are typically larger than the ORCA.

Based on IATA jet fuel price analyses, the current price is approximately 40% lower than last year. The assumed CI will be 50 which gives more importance to flight time as compared to the 737's and the MD-80's cost index. Therefore, the time-related cost can be calculated with the following equation:

$$Cost_{time} = \frac{CI}{Cost_{fuel}} = 181.8 \frac{\text{dollar}}{\text{hr}} \quad (2)$$

Figure 11 and Figure 12 illustrates the computed cost vs mach number for the start and final value of iteration for two altitudes: 26 000 ft and 36 000 ft.

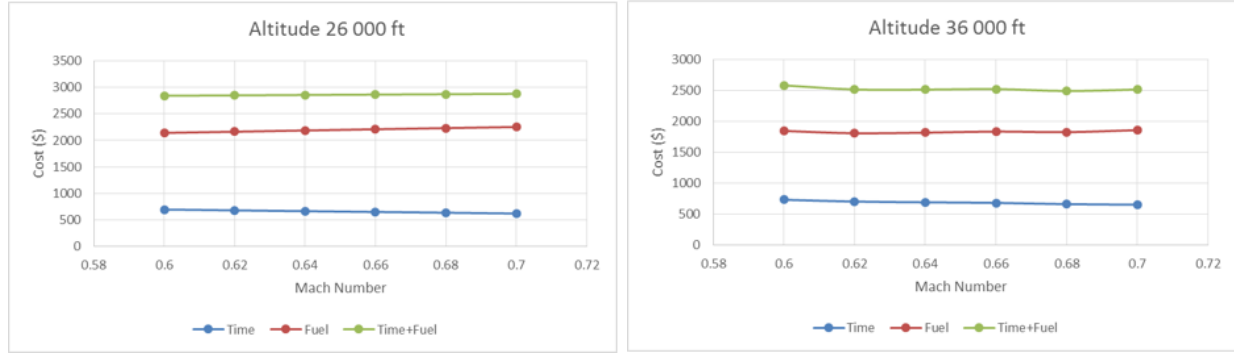


Figure 11: Cost vs Mach number at 26 000ft

Figure 12: Cost vs Mach number at 36 000ft

It is noted that an increasing cruise altitude causes a significant change in total cost. The simulation is stopped at 36 000 ft because at 38 000 ft and M0.7, the results would report a NaN for the fuel flow. The NaN output means that the current thrust tables cannot interpolate a fuel flow for the given drag parameter and flight conditions. Although an increase of Mach number causes an increase of fuel consumption, the Mach number does not significantly change the total cost of mission. The underlying cause is the assumption of CI = 50.

4.2.2 Climb Speed

As per MR&O, ORCA is required to have a SEP (Specific Excess Power) of at least 300 fpm at 17 000 ft during OEI climb. During AEO climb, a minimum of 300 fpm at the initial cruise altitude is required. Climb Speed Optimization is done through observation of the calculated results. Knowing that, NaN values start at M0.68 and 38000ft. Optimization started at M0.66 and 36 000ft as a



safety margin.

Table 6 illustrates the optimization for the ORCA101. Orange values indicates the change between each evaluation. As opposed to green values, red values indicate values where the MR&O are not attained.

Optimization Variables				Evaluated Components				Validation
Evaluation	Speed Combination	Cruise Altitude (ft)	Cruise Mach	OEI at 300fpm (ft)	SEP at Cruise Altitude (fpm)	Time (mins)	Block Fuel (lbs)	MR&O
1	180/200/M	36k	0.68	18k	263	220	6551	No
2	180/200/M	36k	0.66	17.5k	350	227	6590	Yes
3	180/210/M	36k	0.66	11k	350	227	6613	No
4	185/200/M	36k	0.66	17.5k	350	227	6586	Yes
5	190/200/M	36k	0.66	18k	350	226	6582	Yes
6	200/200/M	36k	0.66	17.5k	350	226	6577	Yes, Optimal
7	210/210/M	36k	0.66	11k	350	221	6458	No

Table 6: Climb Speed Optimization

The logic behind the optimization is to maximize the climb speed and evaluate the changes in time and fuel burn. The optimal climb speed is found at evaluation 6. As the climb speed increases past 200 KCAS, the OEI ceiling starts to drop dramatically. Whether the 210 KCAS climb speed was set before or after 10 000 ft, evaluation 3 and 7 shows a similar OEI ceiling drop. Therefore, by observation for ORCA101, optimized climb speed schedule is

200/200/M0.66/36kft. Similar analysis is performed for the ORCA77 and optimized climb speed schedule is 210/210/M0.68/36kft.

4.2.3 Wing Area

The algorithm used to evaluate the fuel weight required to complete the mission is an iterative scheme. Thus, it is not efficient when incorporated into an optimization loop. This is the main reason why the objective function used was the total cruise drag instead of the fuel weight. But, minimizing drag in cruise is a good approximation of minimized fuel weight, because in cruise conditions the thrust must equal the drag to maintain a level flight. Therefore, if the drag is lower, a lower thrust is required which leads to lower fuel consumption. Since the wing area is the same for both aircraft, the optimization was performed with the ORCA101 configuration.

In other words, the optimization loop, showed in Figure 13, with cruise drag as the objective function, is just a first guess of the optimal wing surface to give an overview of the link between



the aircraft's wing area and it's performance for a given altitude and Mach number.

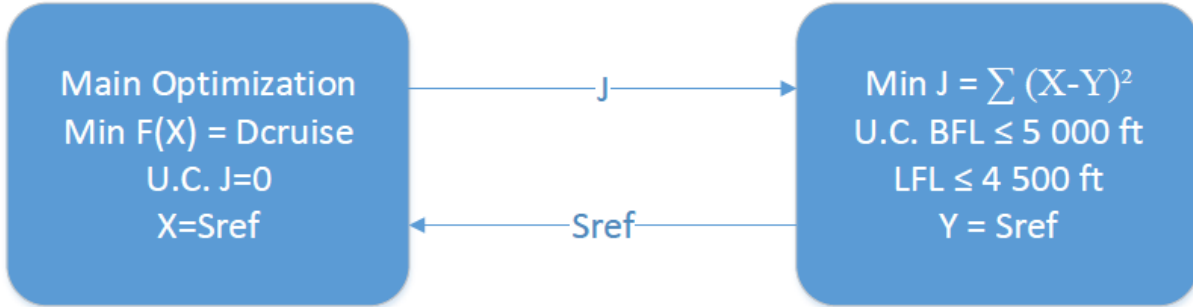


Figure 13: Design Process Interactions

The global optimization loop in Figure 13 tries to find a wing area to minimize the drag in cruise conditions and in each iteration, the weight and span of the wing is recalculated. The global optimization then sends its wing area value to a sub-optimization loop. This sub-optimization loop has two constraints, which are the MR&O BFL/LFL requirements. The sub-optimization will try to match the wing area received from the main optimization loop, while respecting these BFL/LFL constraints. The objective function of this sub-optimization is a square-difference and its value is returned to the main optimization as the variable J . If J is equal to zero, the wing area value found by the main optimization complies with the BFL/LFL requirements from the MR& O.

The reason for using two optimization loops is to create a system which is less unstable. With this scheme, the system is temporarily allowed to have two different solutions, which could be very helpful for a bigger optimization with more variables. Moreover, the objective function of the sub-optimization is a convex function because of the square-difference. A convex function always has a global minimum and will therefore always converge. This is a major benefit when doing optimization with multiple variables.

Since the numerical tools used to size the aircraft are limited, the optimization has only been done with one variable, which is the wing surface area. Figures 14, 15, 16 present the results from this optimization for three different engine thrust (12 000 lbf, 13 000 lbf, 14 000 lbf) for which the wing area yields the lowest drag in cruise condition. In Figures 14, 15, 16, the stagnation points represent the minimum wing area to comply with the BFL/LFL requirements. For example, we clearly see from Figure 14 that the minimum wing area required for a BFL under 5 000 ft is around $1\ 020\ ft^2$. Moreover, Figure 15 shows that the minimum wing area required for a LFL under 4 500 ft is $950\ ft^2$.

Base on these results, engines with 13 000 lbf of thrust were chosen because engines with



only 12 000 lbf of thrust required a minimum wing area of $1\ 020\ ft^2$ which is far too large for a design minimum. On the other hand, engines with 14 000 lbf of thrust and more are heavier and unnecessary because the minimum wing area required for LFL is $950\ ft^2$. The choice of heavier engines would also induce balancing problems. Thus, 13 000 lbf of thrust engine are chosen to comply with all the requirements.

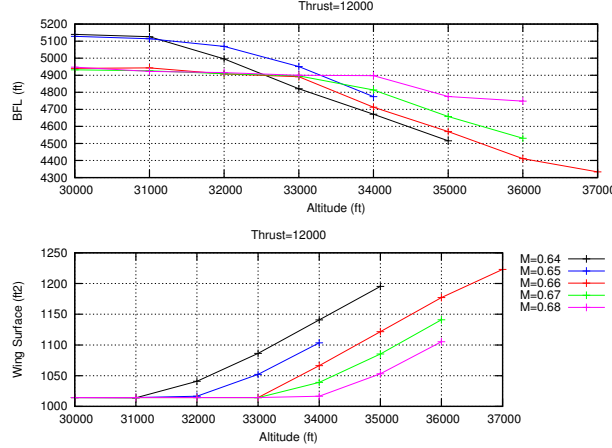


Figure 14: Wing Surface Optimization - BFL with 12000 thrust/engine

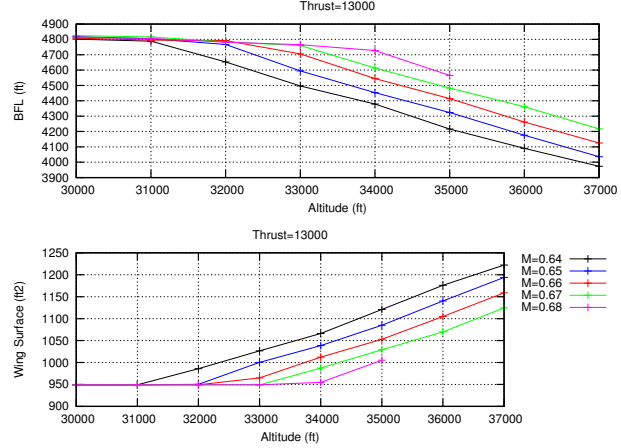


Figure 15: Wing Surface Optimization - BFL with 13000 thrust/engine

With the selection of 13 000 lbf thrust engines, a COC analysis for the 1 200 nm mission was performed at every design point from the optimization. The results are presented in Figure 17. We observe that the COC is lower for higher altitude and faster Mach number.

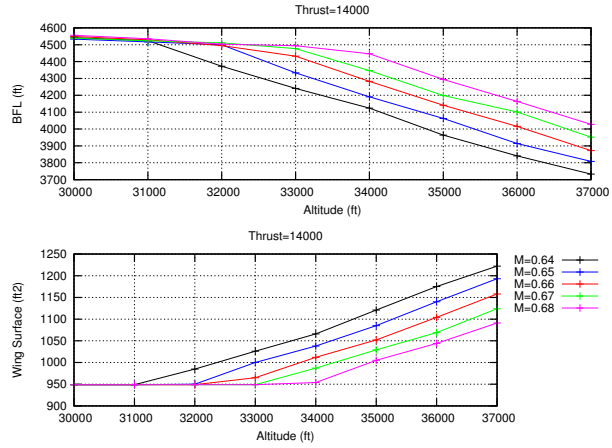


Figure 16: Wing Surface Optimization - BFL with 14000 thrust/engine

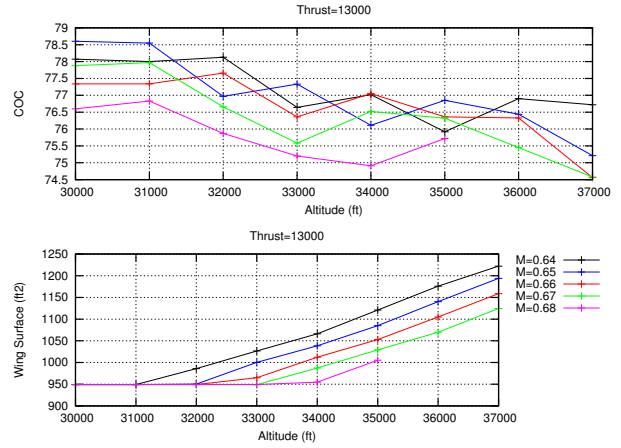


Figure 17: Wing Surface Optimization - COC with 13000 thrust/engine

Based on the previous results, the highest altitude and fastest Mach number possible were chosen as calculated by performance (Section 10), 36 000 ft and Mach 0.66 for ORCA101. Finally,



an iterative process was performed at those cruise conditions over the wing area with the complete algorithm to evaluate the lowest fuel weight possible and it is presented in Figure 18.

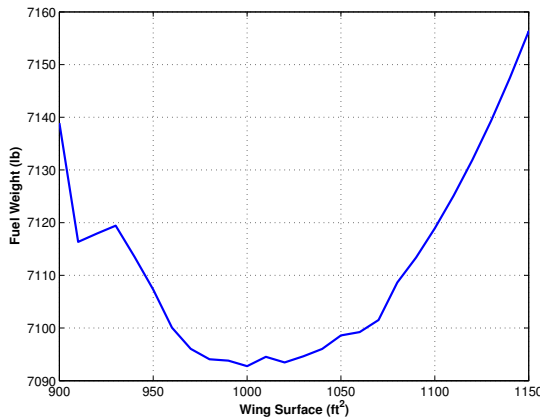


Figure 18: Wing Surface Optimization - Alt=36 000 ft; Mach=0.66; Aircraft: ORCA101; 13 000 lbf thrust/engine

Therefore, the optimal wing area, which yields the lowest fuel weight while respecting the BFL/LFL requirements, is 1000 ft^2 .

5 Configuration

5.1 Morphology

In order to refine last semester's design, the team met at the beginning of the current project phase to choose the main morphological elements to define the baseline model. Table 7 presents the design points discussed and the principal decisions.

Morphology Element	Baseline Model Characteristic
Engine Type	Open Rotor engine
Engine Location	AFT Fuselage Mounted
Wing Type	Compound with 1 kink
Wing Location	Low (Underfloor)
Empennage type	T-tail
Fuselage Type	Circular
Seat Row Configuration	5 abreast (3 left, 2 right)
Landing Gear Location	Under wing

Table 7: Design Characteristics

As a result of the optimization process, the ORCA family kept all those characteristics except for the wing that has a different sweep angle, as it will be presented further in this section.

5.1.1 Engine

The engine was the first element to be selected because its choice defined the aircraft design philosophy for the whole team. The Open Rotor engine was selected in order to build an innovative, competitive and environmentally friendly aircraft concept. The lack of historical data and the fact that no commercial aircraft is currently equipped with such an engine poses a challenge to this design, especially considering the aircraft family will enter into service in the next five years. After comparing the possible performance results between an open rotor, a turbofan and a turbo propeller, the team had high expectations considering the fuel efficiency of the open rotor. It was expected that the fuel economy over the years would compensate for the higher development cost and anticipated maintenance costs. Altitude and cruise speed limitations would lead the design of such an engine, and they will be used later as important optimization parameters.

To accommodate passengers and alleviate their probable fear of an unknown engine, it was chosen that the engine be mounted on the AFT fuselage. This decision was supported by the



rotor burst considerations because at that location, it is possible to ensure that no high energy rotating debris could pierce the pressurized cabin. Stability-wise, the open rotor has the benefit of a thrust line that is closer to the lateral CG. However, both engines' weight have a stronger pitching moment around the longitudinal CG, so its location compromises the integration of systems due to their weights.

The dimensions will be presented in the engine section of this report, but its installed orientation was dictated by the air flow coming from the wing to the inlet. Thus, the pylons have a dihedral angle of 2 degrees and the engine themselves are mounted with a tow-out angle of 3 degrees and an incidence angle of 2 degrees (refer to Figures 23 & 24).

5.1.2 Wing

Since the engine is installed in the high AFT part of the fuselage, the only possible wing position to prevent its trailing flow to alter the engine intake conditions is under the floor (low wing). As a consequence, the systems integration had to adjusted. Since there is no need for a center fuel tank, the wing box is reserved for the heavy structural components of the wing junction and the fuel system dry elements. To provide a better roll stability, a 4 degrees dihedral angle was selected according to a competitors benchmark study (5 degrees and over would cause unnecessary wing structure weight and manufacturing complexity). Table 8 shows the final wing characteristics for both family models:

Characteristics	Wing
Area	1000 sq. feet
Aspect Ratio	9.5
Taper Ratio	0.19
Sweep Angle	15 degrees
Full Span	100 feet
Winglet Presence	Yes
Kink Presence	No
Airfoil	NASA SC(2)-0612

Table 8: Wing Characteristics

A compound wing type was selected at first because it has a more modern look and its design could achieve advanced aerodynamic properties as proven by its almost unanimous presence amongst competitors' aircrafts. However, the optimisation revealed that the ORCA cruise speed is too low to even require a sweep angle over ten degrees. A sweep angle of 15 degrees was chosen to ensure



the possibility of flying faster without being significantly heavier or more expensive to build. The structural bending moment towards the aft is lower as a consequence and the lift is the value at no sweep.

5.1.3 Fuselage

Both previous design groups had chosen a circular fuselage section because of its friction drag reduction for the same length compared to a double-bubble section. As long as it allowed enough volume capacity for the cabin requirements, the cargo and systems integration, the circular fuselage was a valid and justifiable choice. This fuselage type is easier for manufacturing, and also represents a weight economy in structure reinforcement. The key resulting design parameters were the wing installation and the fuselage diameter minimization.

The economy class seat row configuration was also debated between 4 seats abreast (2-2) and 5 seats abreast (3-2). The main reason why the 3-2 rows were maintained is due to the drag savings of a shorter fuselage, and a larger fuselage would also provide a more comfortable and spacious cabin for the passengers (wider section, reduced tunnel effect, reduced displacement to facilities). It is also a logical choice considering a possible future extension of the ORCA line. For the business class, the 2-2 seat rows choice was obvious for comfort and due to the MR&O requirements. It seemed wise to keep a similar class proportion between both the ORCA77 and ORCA101 by placing 12 and 16 business passengers respectively, which represents about 15 percent of the whole cabin. This caused a major family design change because the uneven number of seats per row in the economy class resulted in a 77 passenger and a 101 passenger model by placing only complete rows as opposed to the 76 and 100 passenger versions. Consequently, enough features are available to position three flight attendants in both models.

The nose cone and tail cone design has been designed following aerodynamics guidelines (smooth curves and finesse ratios) and a longitudinal number of elements to integrate; the result will be shown on the 3 views drawing (Figures 23 & 24).

5.1.4 Empennage

Given the engine type and location, the T-Tail empennage was the natural solution to provide propeller clearance in a more compact tail design, a horizontal stabilizer out of the wing downwash and a weight reduction compared to a classic empennage - the conventional vertical stabilizer



would have had to be bigger (span-wise) for the rudder to be effective. A benchmark study begins the refinement of both stabilizers' geometry and dimensions as it will be shown further on the 3 views drawings. Table 9 summarizes the selected design specifications that evolved throughout the baseline improvement with Stability & Control analysis for the empennage:

Model	Horizontal Tail		Vertical Tail	
	ORCA77	ORCA101	ORCA77	ORCA101
Area	170 sq. feet		152 sq. feet	
Aspect Ratio	4.4		0.9	
Taper Ratio	0.4		0.51	
LE Sweep Angle	20 degrees		43 degrees	
Volume Coefficients	0.74	0.83	0.064	0.073
Airfoil	NACA-0010		NACA-0010	

Table 9: Tail Specifications

The horizontal stabilizer's sweep is adjusted to the wing's to ensure a later stall, and thus a possible recovery. A kink was integrated to the vertical stabiliser to smooth its leading edge line merging with the fuselage, composed of a short lower section with a 60 degrees sweep angle. The volume coefficients will be explained further along with the longitudinal wing position justification.

5.1.5 Landing Gear

The position of the landing gears was determined according to the wing design and structure. The landing gears themselves are a tricycle landing gear with a forward double wheel chariot under the fuselage nose and two main double wheel chariots under the wing. This applies for both aircraft designs. The main landing gears are retracted inwards with their support and swivel actuators located between the rear and auxiliary spars. This also gives the aircraft a better stability on ground and a lower form drag when stowed. Table 10 presents the sized dimensions of the gears. The selected mechanism's integration has been verified in CATIA. It is to be noted that their length design is mainly based on the tail strike, nose collapse and tip strike analysis, but limited by stowing trajectory and occupied volume.



	NLG	MLG
Rim Diameter (in)	10	16
Tire Diameter (in)	24	36
Tire Width (in)	7.75	11.5
Barrel Diameter (in)	6.5	8
Cylinder Diameter (in)	5.5	6.5
Compression Stroke (in)	16	16

Table 10: Gears Dimensions

The resulting gear design is presented in Figures 19 & 20.



Figure 19: Nose Landing Gear Design

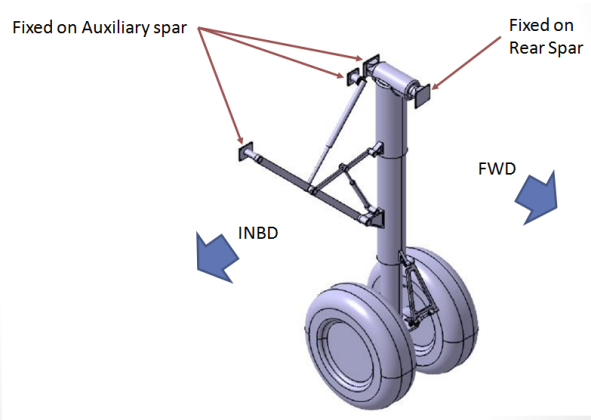


Figure 20: Main Landing Gear Design

Figures 21 & 22 show a 3D capture of the MLG stowed inside the belly fairing behind the wing center box and the NLG retracted in the nose cone.

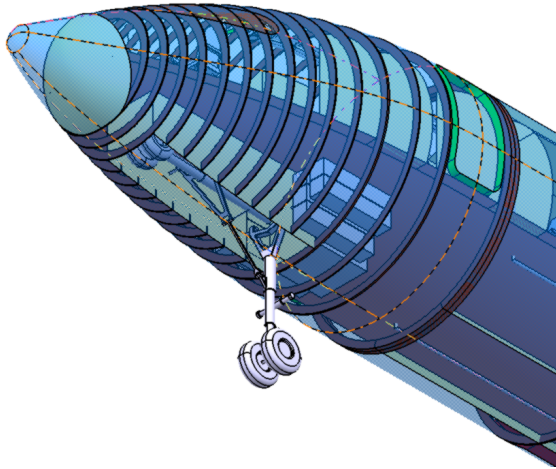


Figure 21: Nose Landing Gear Position

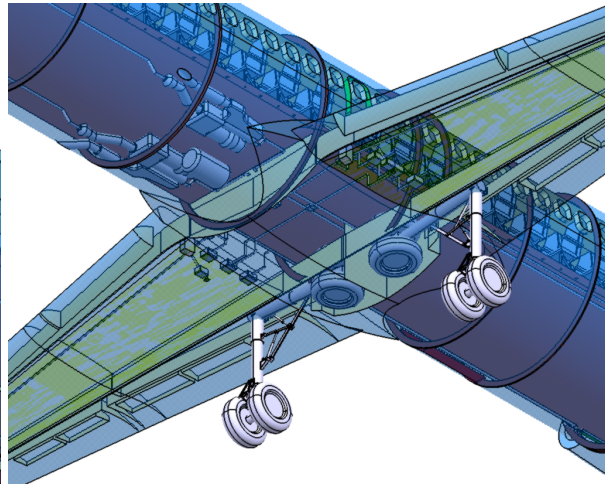


Figure 22: Main Landing Gear Position

Structural panel enclosures have been designed to provide a pressure sealing between the landing gear bays and the underfloor area. The nose door is composed of two panels that open sideways plus a small rear panel attached to the gear column. Their size is yet to be determined using drag optimization in takeoff and landing. For the main landing gear, the objective is to minimize the door surface. Thus, the design uncovers the tire area on both sides following the hole geometry in the keel panel, similar to the Boeing 737 configuration. The door panels open outwards like the Boeing design. This configuration should provide the best drag values, which is to be confirmed following an advanced aerodynamics analysis.

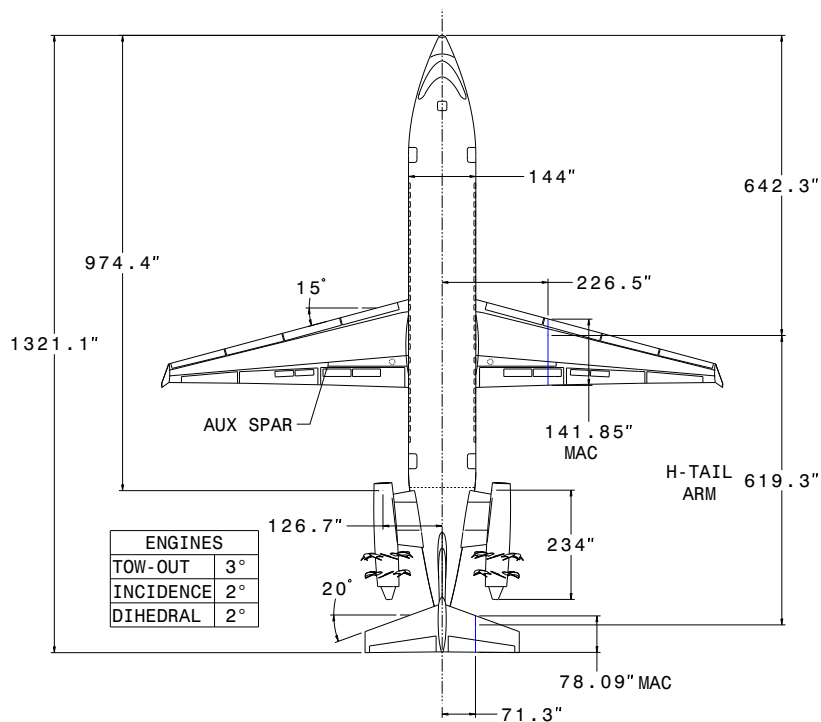
5.2 Detailed Configuration

In this section, selected design characteristics will be described in more detail and shown with help of CAD drawings and 3D modelling captures using CATIA V5. At this point, it is necessary to introduce the More Electric Aircraft (MEA) systems architecture. Since there is no pneumatic system and the modern electric components replace some of the hydraulic features, it is important to address the systems integration considering unconventional parts of the designs.

5.2.1 Overall Configuration

The 3 views comparing the two aircraft represent an overall visual reference, refer to Figures 23 & 24 throughout your reading for a better understanding of the teams concepts. The principal dimensions are shown and aircraft data is found in the tables. The three main aerodynamic chords (MAC) for the wing and the stabilizers are positioned with their lever arms. Geometrical commonality can be observed between the two models along with the 90 percent similarity requirement, except for the fuselage middle section's length and the over wing Type III door that aren't required on the ORCA77. Note that the wing junction structure is the same on both models. Also, the structure section of this report presents a more detailed fuselage description.





TYPICAL FLIGHT CONDITIONS		ORCA77
# PAX	77	
RANGE (nm)	1 800	
CRUISE SPEED (Mach)	0.68	
CRUISE ALTITUDE (ft)	36 000	
MTOW (lbm)	75 500	
OWE (lbm)	47 300	
MZFW (lbm)	64 600	
MLW (lbm)	69 100	
TOTAL ENGINES	26 000	
THRUST (lbf)	26 000	
BFL (MTOW,SL,ISA) (ft)	4 108	
LFL (MTOW,SL,ISA) (ft)	4 203	

	AREA (ft ²)	AR	TR	MAC (in)	VOLUME COEFFICIENT	AIRFOIL
WING	1000	9.5	0.19	142	-	SC(2)-0612
H-TAIL	170	4.4	0.44	78	0.74	NACA-0010
V-TAIL	152	0.9	0.51	165	0.064	NACA-0010

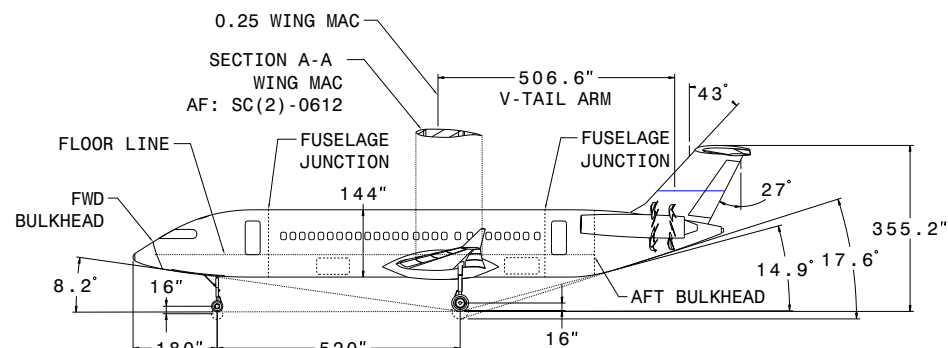
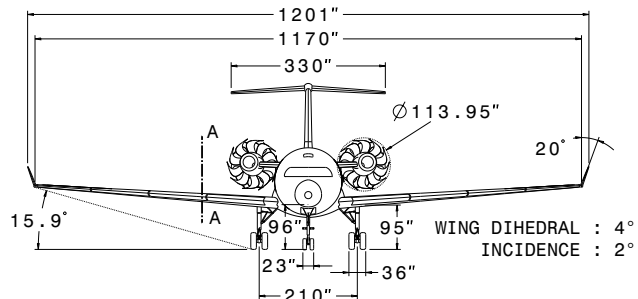
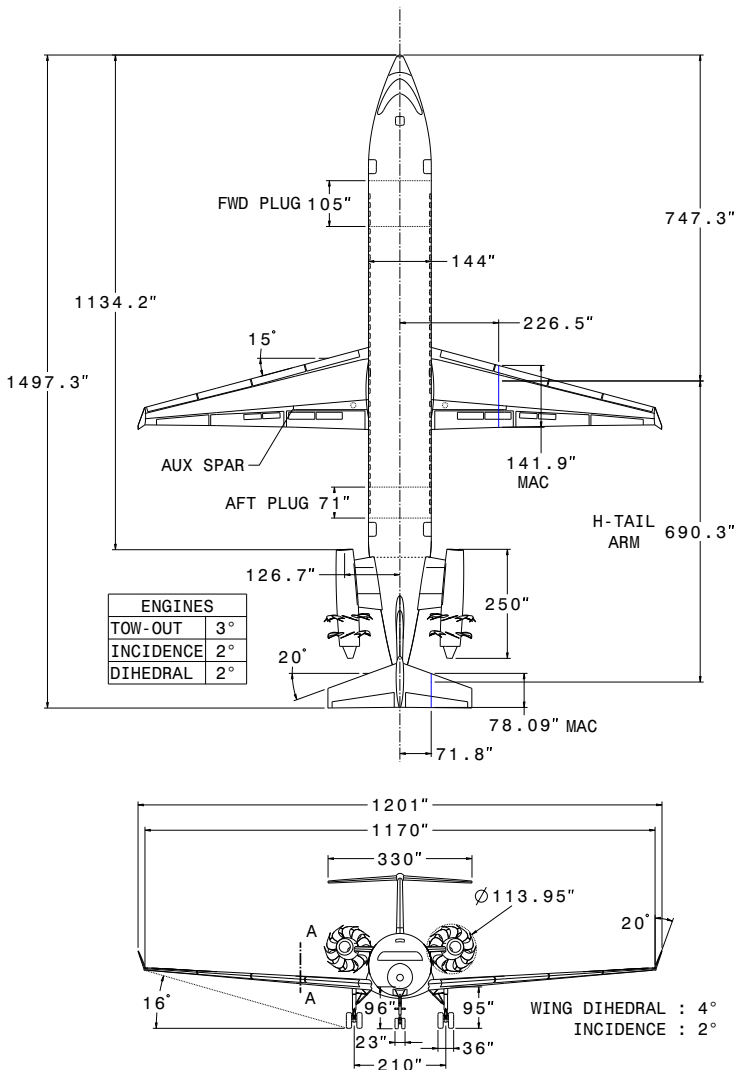


Figure 23: 3 Views Drawing of ORCA77 Design





TYPICAL FLIGHT CONDITIONS		ORCA101
# PAX	101	
RANGE (nm)	1 200	
CRUISE SPEED (Mach)	0.66	
CRUISE ALTITUDE (ft)	36 000	
MTOW (lbm)	80 600	
OWE (lbm)	49 400	
MZFW (lbm)	72 100	
MLW (lbm)	76 600	
TOTAL ENGINES		
THRUST (lbf)	26 000	
BFL (MTOW,SL,ISA) (ft)	4 681	
LFL (MTOW,SL,ISA) (ft)	4 441	

	AREA (ft ²)	AR	TR	MAC (in)	VOLUME COEFFICIENT	AIRFOIL
WING	1000	9.5	0.19	142	-	SC(2)-0612
H-TAIL	170	4.4	0.44	78	0.83	NACA-0010
V-TAIL	152	0.9	0.51	165	0.073	NACA-0010

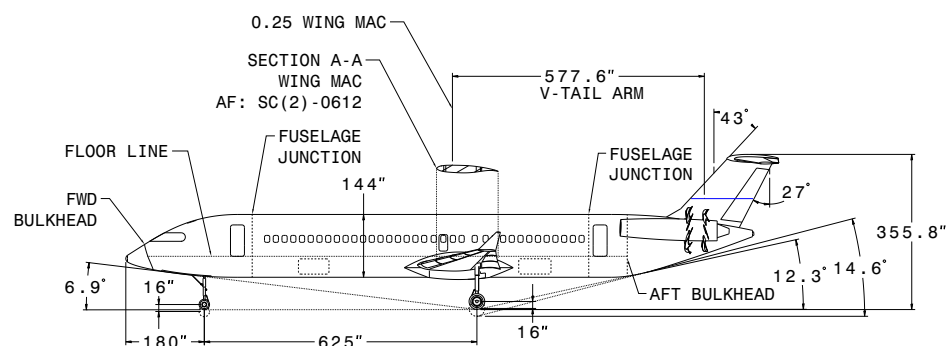


Figure 24: 3 Views Drawing of ORCA101 Design



During the optimization process, the code generated the CG envelope graphs for the ORCA family at each compilation. The team was constantly able to adjust the wing longitudinal position to verify the balancing criteria. Therefore, along with our composite panel structure configuration, there is no plug corresponding to a number of frame bays added to the mid fuselage of the ORCA77 to build the ORAC101. The plug dimensions previously presented in the 3 Views describe the fuselage length difference in reference to the wing, indicating that the middle section is common.

Figure 25 presents what was achieved as a control surfaces qualitative benchmark. All the decisions that the team made for their type, quantity, and relative position according to the actual regional aircraft market is presented. The principal references are the Bombardier CRJ family and the Embraer ERJ family. Note that the presented flaps represent the deflected area, but the cut in the upper skin starts further than the spoilers towards the trailing edge. The details of the dimensions will be shown in the Stability and Control Section (Section 12 Figure 95) as the actuation and installation properties will be described in the Structure section (Section 6).



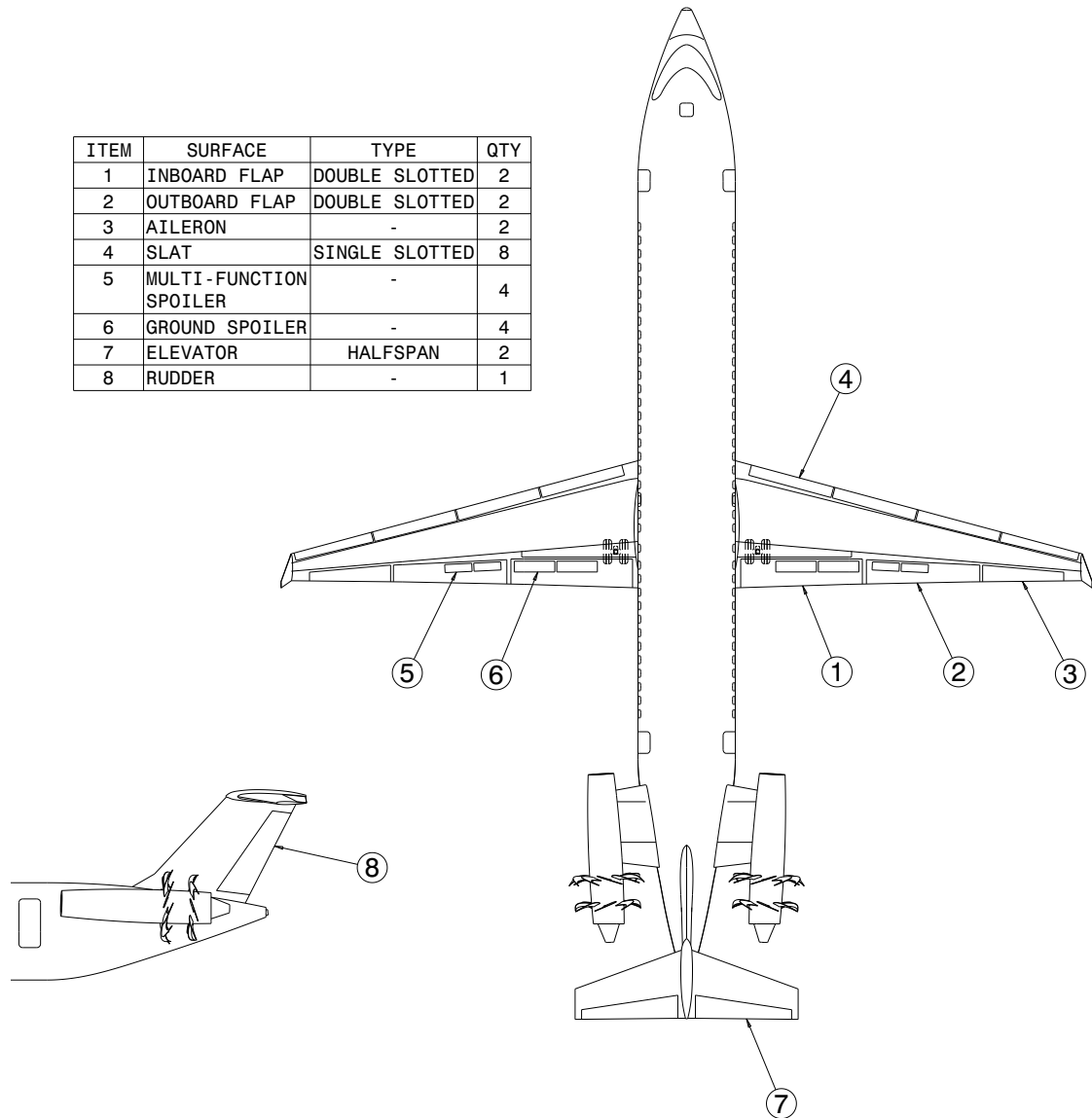


Figure 25: Control Surfaces

Finally, a Rotor Burst analysis validates the engine mount location on the tail cone (on specific frames aligned with the pylons spars and the engine structural brackets). Figure 26 defines the 5 degrees burst zones for high energy rotating parts and 15 degrees for the low energy rotating parts.

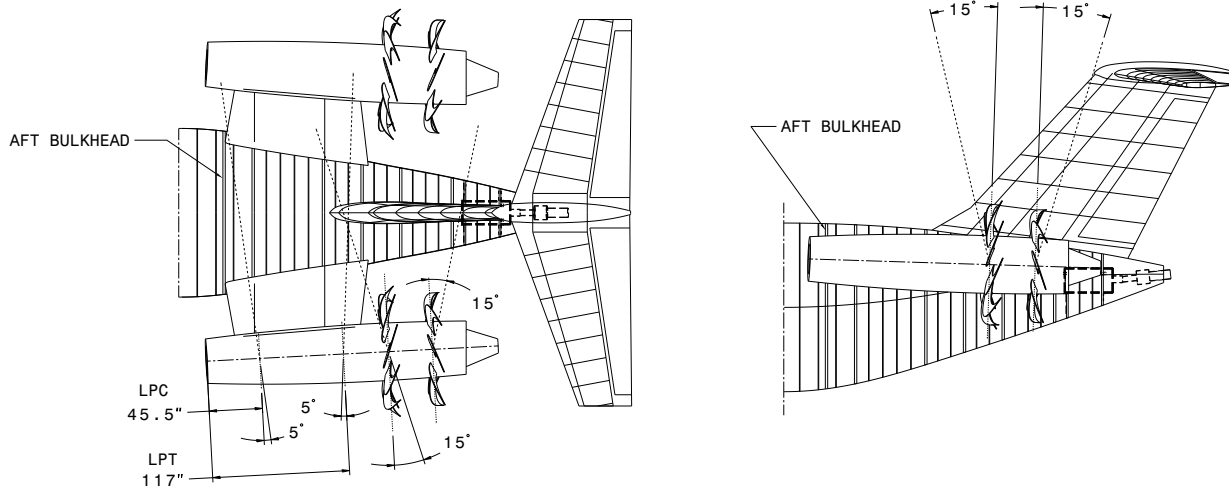


Figure 26: Rotor Burst Zones

The pressurized cabin is clear from any piercing risk, as are the rudder, the horizontal stabilizer and the APU. This indicates that the engines are well located in relation to the various elements of the tail cone. The advanced design of the ducts, harnesses and fuel lines integration in the tailcone will need to take the rotor burst trajectory into account and separate the risks of cuts for redundancy requirements.

5.2.2 Cargo Capacity

In order to plan the systems integration in the fuselage alongside with the cargo requirements, we considered placing the bulk luggage in 2 sections, one forward and one after the wing, under the cabin floor. For both aircraft, the forward section is between the battery pack in the nosecone and the ECS pack located in front of the first wing spar. The rear section goes from the MLG enclosure wall up to the rear cabin bulkhead. The underfloor cargo capacity was calculated using the section area of 19.1 square feet and 90 percent of the sections length. This coefficient was estimated in order to compensate for the missing structural and systems components in the design. According to the requirements, the minimum cargo volume to be available is 8 cubic feet per passenger.

Items such as harnesses and ducts have been considered and they are shown in the Cross-Sections Views (Figures 32, 33) found in the Interior Section 5.3 of this report. The results are presented in Table 11, and the Figure 27 shows the cargo integration in the ORCA. Cargo loading doors are represented in dotted lines on the 3 views.

	Underfloor Bulk Cargo (ft³)	
	ORCA77	ORCA101
FWD	310	462
AFT	366	468
Total	676	930
MR&O	616	808

Table 11: Underfloor Bulk Cargo

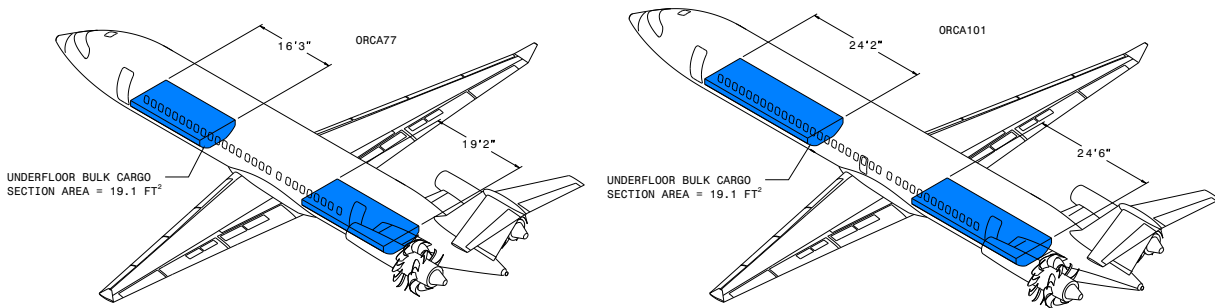


Figure 27: Cargo Integration

The current cargo space design exceeds the requirements, but the configuration detail level is not precise enough to ensure that the values are final. The margin is considered as safety volume for eventual system integration. Also, the tail cone still has a significant empty volume where a pressurized additional cargo container could be placed if needed, in the case of a High Density configuration for example.

5.2.3 Ground Servicing

In order to provide a complete study of the ORCA design, the team selected the required vehicles to ensure the ground servicing of the aircraft. If all service vehicles and tools were to be present around the aircraft at the same time, Figures 28 & 29 show an example of disposition. The vehicles and carts are positioned according to the current location of its feature on the aircraft. Thus,

the refuelling truck should be parked near the wing tip. The air conditioning vehicle is beside the ECS packs. The electric service cart goes near the nose for battery pack and electrical service plug access. The passenger loading bridge or ramp can be replaced by mobile stairs if required. The baggage carts have to be driven with care close to the cargo doors. The potable water service point has been set in the tail cone because a lot of space is available for the water tank, which is yet to be designed. The APU/Engine start cart operates on the APU to start the engines, but also to power the electrical generators or to override the electrical system. Note that galley and lavatory service vehicles have to serve the forward and rear features, so they have to rotate or alternate their position around the service doors and access traps. Indeed, the ORCA77 presents the most restrictive access around the aircraft because its fuselage is shorter.

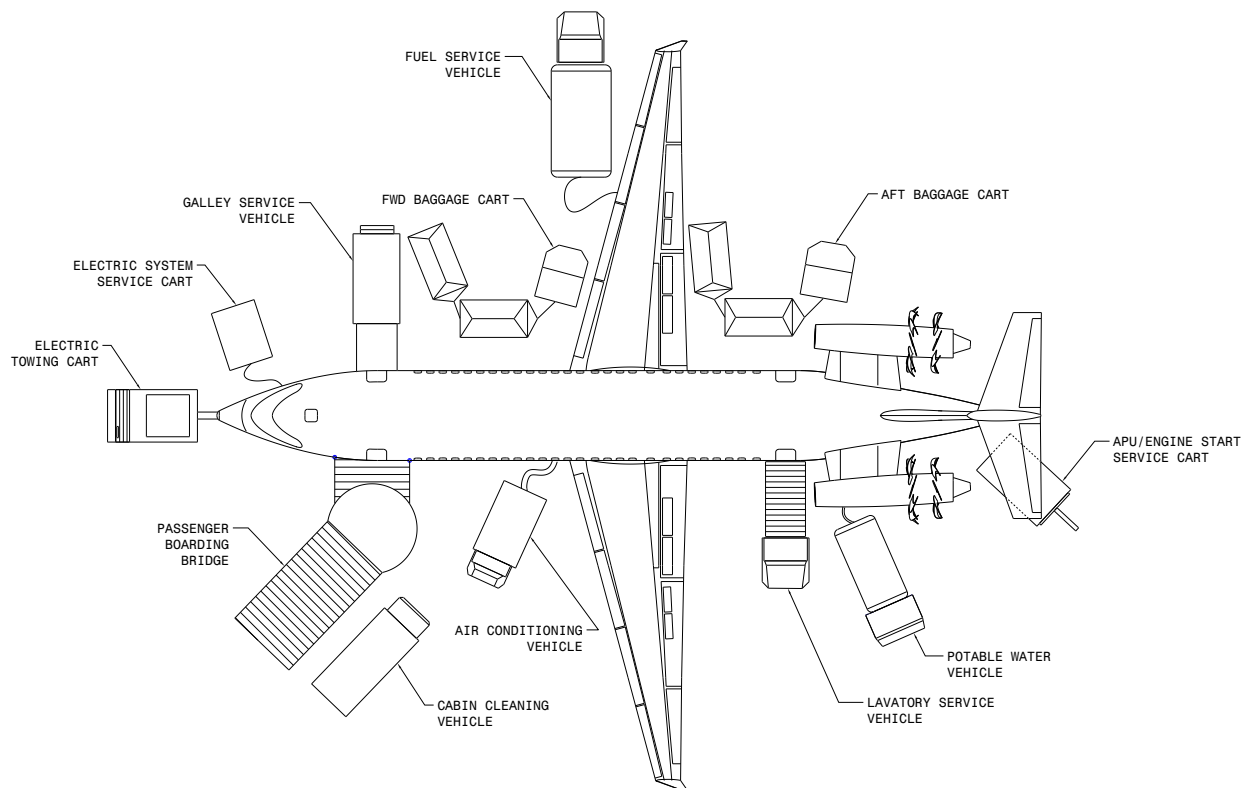


Figure 28: Ground Servicing - ORCA77

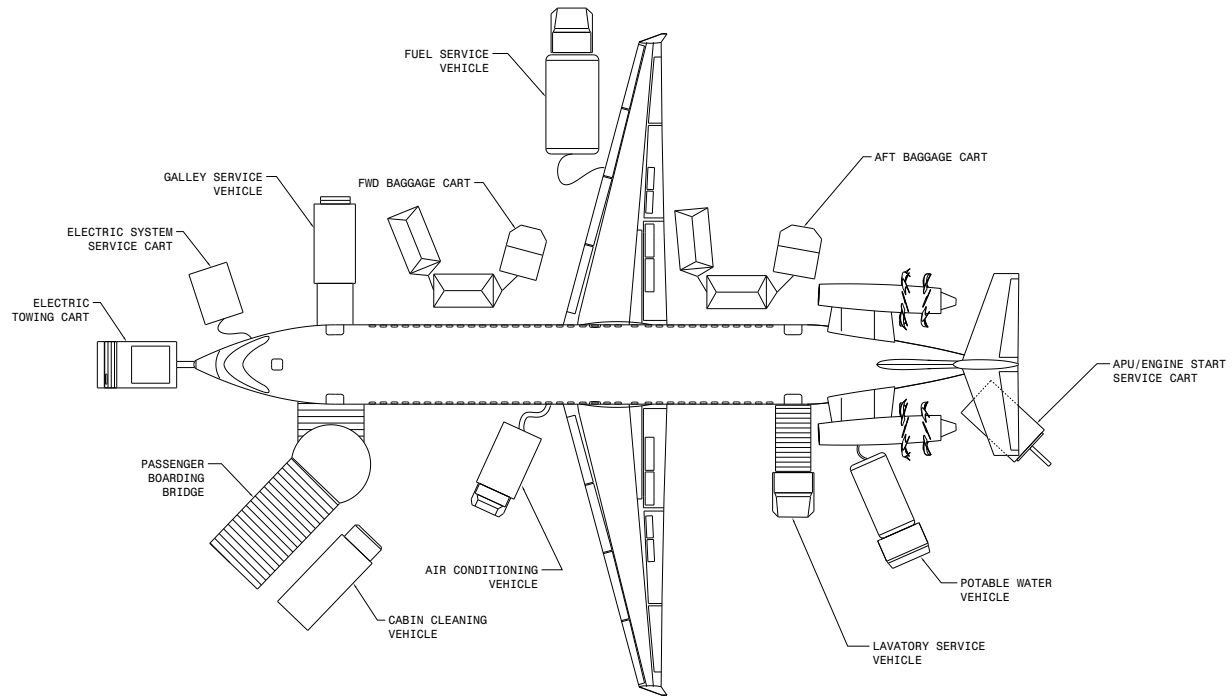


Figure 29: Ground Servicing - ORCA101

There are no precise requirements for the ground servicing except for the overall operation to be feasible and safe. No considerations were made concerning the engines operation during ground service, but an analysis is needed to prescribe the adequate limitations. However, the team is confident that this ground servicing strategy should meet the airliners' objectives in terms of aircraft preparation time and baggage loading constraints.

5.2.4 Turning Radius

The minimum turning radius is defined to validate the requirement of the minimum pavement width for a 180 degrees turn while taxiing. An 83 degrees maximum NLG steering angle was selected, and the maximum effective angle was benchmarked at the highest value of 77 degrees. The average slipping angle of 6 degrees was then adopted. Figure 30 presents the turning maneuver, which includes the swivel gear to move back, so the final width of pavement corresponds to the turning radius.

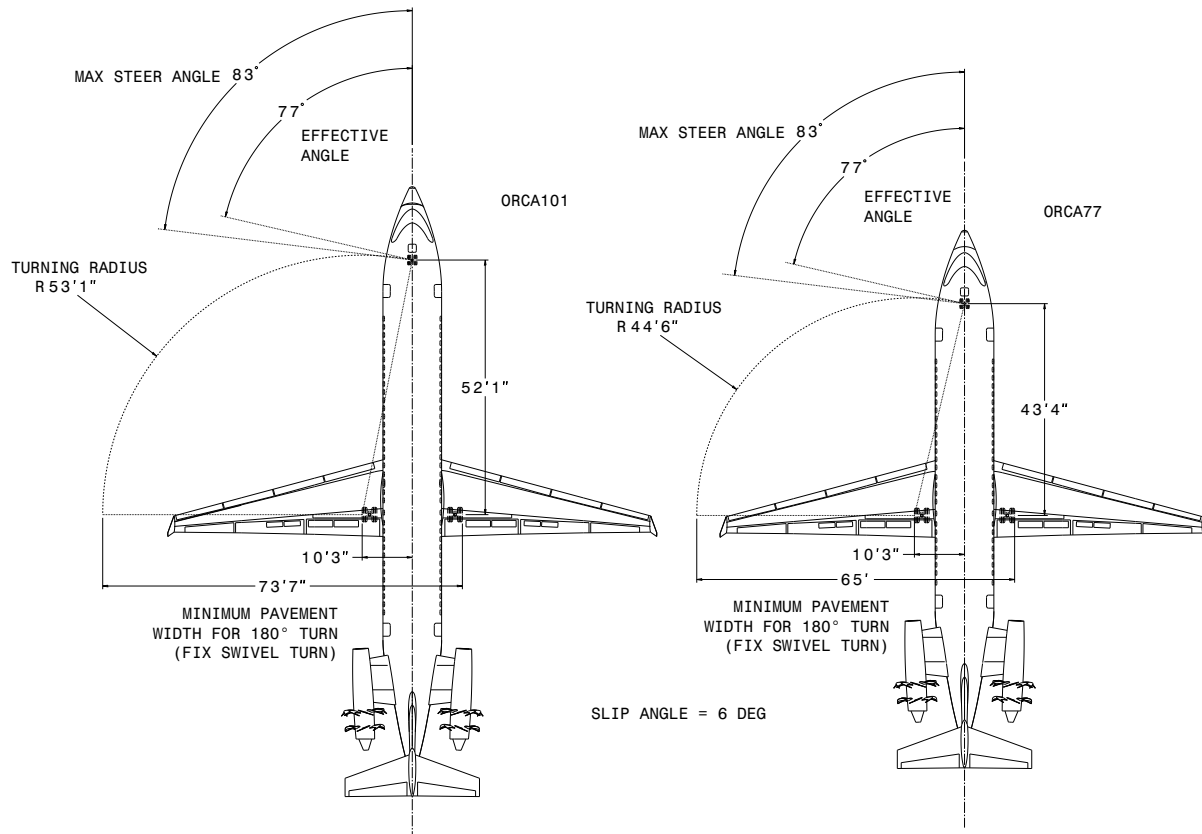


Figure 30: Turning Radius

In order to fit in most airports' taxi corridors, the width pavement is required to be under 60 feet. Both ORCA meet that objective with a respective turning radius of 45 and 53 feet. The buffer margins allow to modify the turning sequence trajectory if needed for practical considerations.

5.3 Interior

The optimized cabin design aims to provide comfort and safety to the passengers. The team arranged the features so the passengers enter a spacious environment that eliminates many negative psychological effects during the flight. The cabin is covered by a high ceiling and very large tinted windows associated to a sophisticated system of efficient LED cables provide a greater sense of open-ness. That way, the passengers will not feel any tunnel effect. The alleys width and height exceed requirements, as do the lavatory dimensions. People will be able to move freely during the safe sequences of the mission. The entertainment system is yet to be designed, but the ORCA objectives are to maximize the passengers experience within a reasonable electrical load. The floor plan and the cross-section views will provide more information.



5.3.1 Floor Plan

Both models of the ORCA family are designed to be dual passenger class, with a business class around 15% as presented in the Morphology section. The classes are separated by a transparent wall equipped with a variable opacity feature, to unify the cabin and increase the flight attendants' visibility in case of emergency. The functional elements are situated at the ends of the seats section to ease passengers and crew members displacements. There is a closet at the FWD main door, for the use of preferred business class customers. Also, the quantity of galleys needed was calculated according to the typical missions of each aircraft model. Table 12 presents the meal requirements estimations considering full size carts to be 12 x 34 x 40 inches.

	ORCA77	ORCA101
Flight Duration	4 hours	3 hours
Meal Supplied	Hot Meal and Snack	Hot Meal
Full Size Carts	7	7
Galleys	3	3

Table 12: Meal Requirements Estimations

In the three galley compartments present on the aircraft, nine full size carts are used, and the remaining space can be used for beverage and trash storage. Standard equipment such as a coffee brewer, an oven and water distributors are included in the galley modules.

The emergency exits has been sized according to the FAA regulation charts for Type I and Type III exits and the maximum distance of 60 feet between two doors is respected. The step-up height for the overwing Type III door of the ORCA101 is 12 inches (< 20 inches required) and its step-down height to the wing skin is 22 inches maximum (< 27 inches required). Front and rear doors are equipped with inflatable slides. By moving their upper body, the three seated flight attendants are able to observe every passenger. Therefore, any emergency situation or evacuation should be safe.

Figure 31 represents the actual floor configuration for both aircrafts, aligned with the wing.



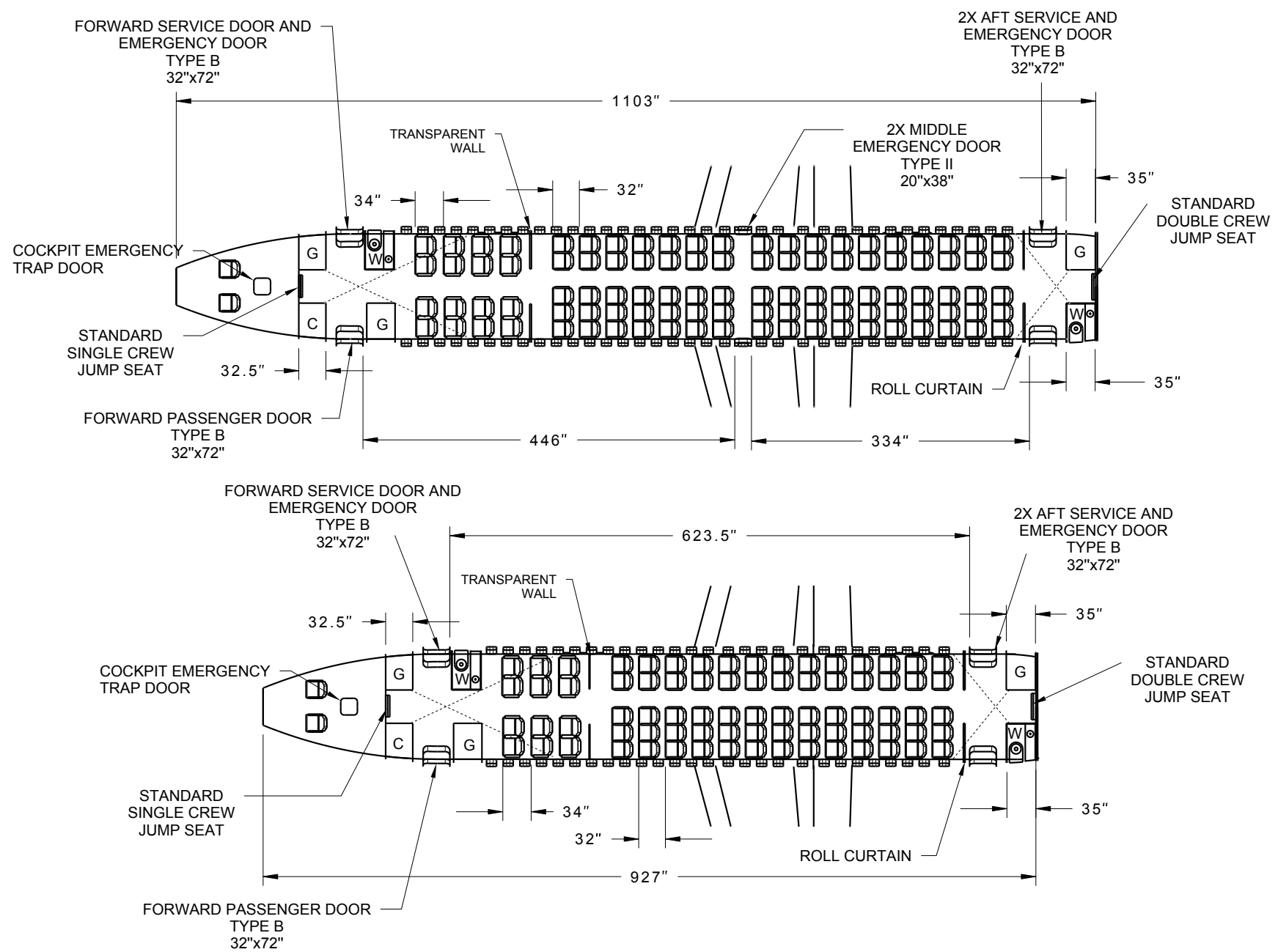


Figure 31: Floor Plan



The seat pitch of the business class is 34 inches and 32 inches for the economy class. There is a 25 inch gap between any wall and the next row to prevent head strikes. The seat design aims to allow variable comfortable passenger seating positions with the current pitch. Moreover, the retractable table and other back rest features will be designed to surpass the competition for ergonomic and pragmatic considerations.

5.3.2 Cross Sections

The cross section views of the aircraft allows the analysis of the transversal parameters and dimensions. To optimize the passenger comfort, the team used a 95 percentile American man to establish head and shoulder clearances when standing or seated. Figure 32 shows the cross section positioning for the business class as Figure 33 presents the same for economy class. Indeed, both cabin sections have the same cabin diameter and overhead bin design. The underfloor cargo area design is also the same and includes space on sides and below the floor for ducts, harnesses and fuel lines. The external skin diameter of the fuselage can be reduced with the high composites structure, but the final value is to be determined.



41

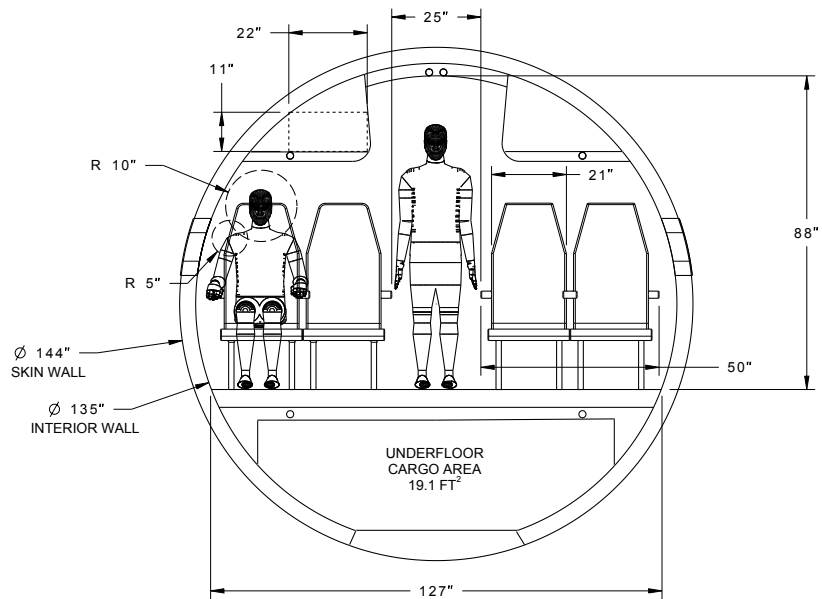


Figure 32: Business Class Section View

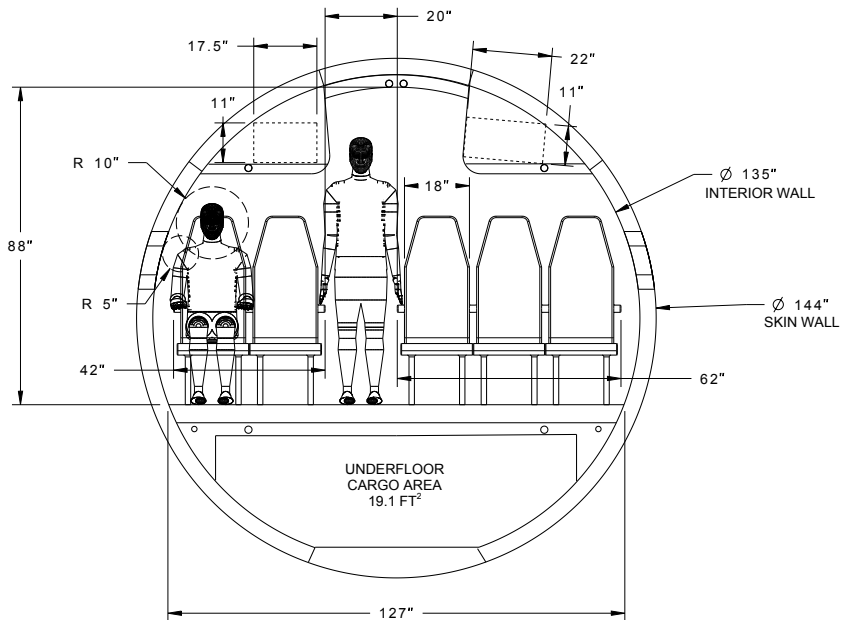


Figure 33: Economy Class Section View



The seat width of 21 inches for the business seats and their larger armrests provides a significant comfort increase for the preferred class. Every business passenger is close to amenities and the alley width of 25 inches should ease their displacements. Economy class features also meet or exceeds the requirements for those dimensions.

The overhead bins have been designed to clear a large alley ceiling and to provide accessibility to the air jet control, individual lighting and oxygen masks systems. Considering a 3 inch thickness to integrate those elements, the available luggage volume represents enough space to meet the objective of one luggage fitted for 80 percent of the passengers. The maximum size baggage was set to 11x17.5x22 inches. Table 13 presents the analysis to verify this requirement.

	ORCA77	ORCA101
Business Class	14	18
Economy Class	52	66
Total	66	84
MR&O Requirement	80%	80%

Table 13: Overhead Bins Luggage (Number of Luggages)

The number of units indicates the maximum quantity of wheels first luggage as shown on the left side of the business class or the right side of the economy class view. Their longitudinal stacking allows excess space for the business class and provides enough space for near to 80 percent of the economy section. However, the total bin volume only represents a capacity to fit bags for more than every passengers. The team believe that the requirements can be fulfilled with a margin by applying a compressibility factor of 80 percent and by considering the fact that overhead loading is generally irregular and more efficient than our conservative speculations.



6 Structure

The aircraft structure is one of the key aspects of aircraft design involving various analyses in varying flight and landing conditions, while also considering several emergency cases. The systems' interactions, the aircraft aerodynamics, the inertia loading and the control and balance of the aircraft, to name a few, alongside FAR requirements, are a few of the various inputs from other design teams that influence the structural design. Nonetheless, the primary considerations of security, manufacturing, material testing and repairs will be the primary criteria to judge the structural design - these aspects will be particularly developed in the materials selection subsection. In this section, the material selection will be explained, followed by the detailed design explanations for the structure of the fuselage, wing, empennage and their respective structural junctions, and finally the landing gear integration design. Thorough this section, the structural design has been accomplished with the help of various references [38, 58, 28, 27, 49, 48, 13, 24, 57, 21, 32, 43, 45, 25, 33, 17, 40].

Certification is one of the most critical design aspects in order ensure compliance with international regulations. In our case, FAR 25 is the basic reference along with other instances of the FAR requirements. Even though constraint analysis was not part of the conceptual design, loading distributions and load path (shown in Section A: Figure 118 & Figure 121) were used to position the component. An initial sizing was made with benchmarked values (FAR 25.301-FAR 25.571), exposed in Section A: Table 63, Table 64 & Table 65. The complete overall structure along with the systems integration is presented in the Figure 34.



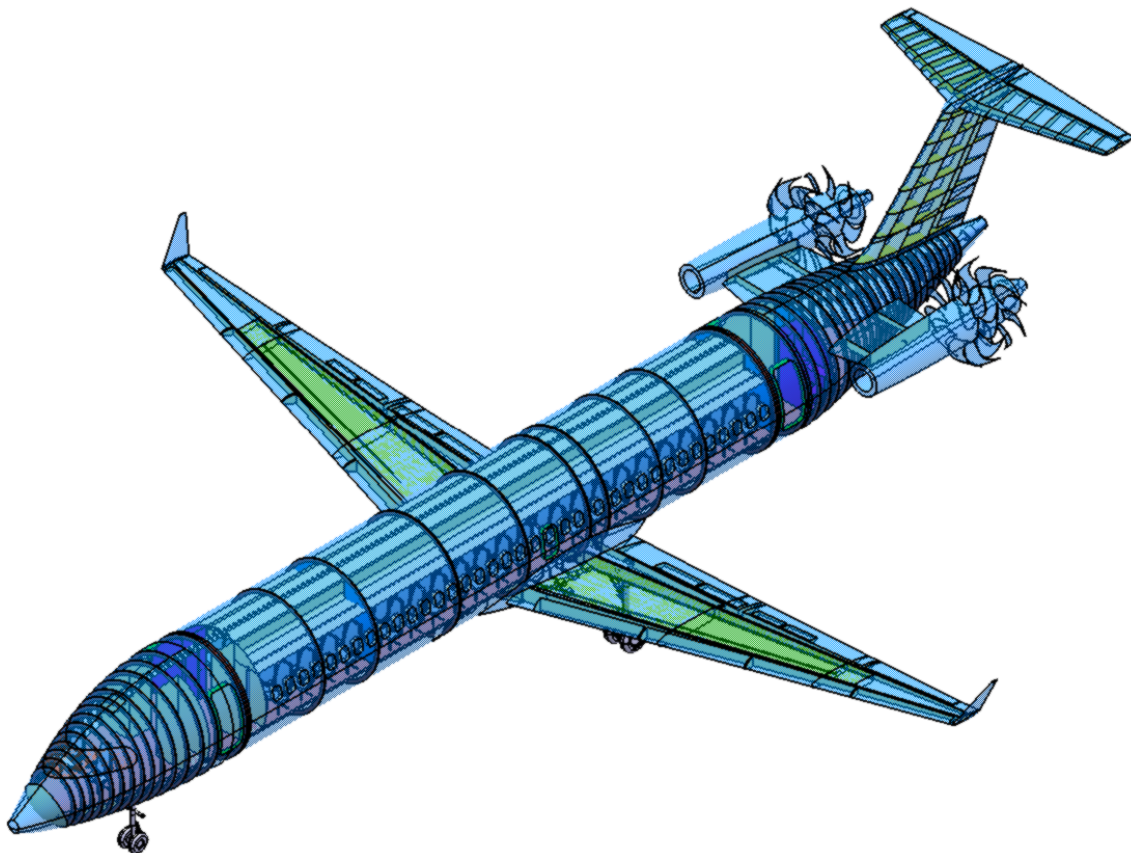


Figure 34: Complete Structural Isometric View

6.1 Materials

Material selection is a major aspect of structural design; the choice of materials must take into account various aspects such as strength, weight, economics and environmental impact. In order to make an innovative, lighter and durable structure with a lower cycle cost, a mainly composite structure was the primary option considered. Only few aircraft currently apply an expansive use of composites; the benchmark models used were the Boeing 787 and the A350. The Pugh matrix in the Table 14 below exposes the analysis of our material selection throughout the aircraft.

Material	Assembly Complexity (Part and Joint) (1-10)	Repair (1-10)	Research and Dev.Cost (B\$)	Manufacturing Cost (M\$) Mat./ labor/ tooling	Quality Control Difficulty	Weight (1000 lbs) fus/ wing /tail	Reducing Drag Count (due to Fuselage Thickness)	Recycling (1-10)	Life Cycle Cost (M USD)
Weight	0.2	0.3	1	1	0.2	1.5	1	0.1	5.3
Aluminum Lithium	5	2	2.2	7/3.4/0.4	1	10/6.7/2.5	0	1	43.4
Glare & Aluminum Lithium	6	4	2.5	8/3.4/0.5	2	9.8/6.5/2.3	0	4	45
Glare (skin) & Composite	6	6	2.8	9/3.4/0.8	4	9.6/6.0/2.1	0	6	46.4
Composite	6	6	2.7	10/3.4/1.1	4	8.5/5.4/1.9	-0.2	6	45
Composite with Foam Sandwich	2	5	2.8	10.5/2.5/1	5	9.0/5.6/1.9	-1.5	6	43.1

Table 14: Material Pugh Matrix

This Pugh matrix displays many considerations that impact the choice of materials (if further information is needed concerning our choice, it will be presented in the Annex ([A](#))). The data in the table was obtained using various sources including studies from NASA. Using this data, it was chosen to have an aircraft structure principally composed of composites, more specifically Carbon Fiber Composites. This choice is in line with our design mentality of having a technologically advanced and environmentally friendly aircraft since a lighter structure principally allows a lower fuel consumption. However, even though composite structure has great advantages (as exposed in [A: Section A.1](#)), some key issues need to be considered, and will require further analysis in later design phases: lightning protection (FAR 25.581), bird strike (FAR 25.631), structural junctions (most composite delaminate under excessive assembly constraints) and curing time and space. In addition, our green aircraft mentality comes with the drawback of a higher production unit cost. The materials choice introduces several key risks in the aircraft development with regards to project feasibility, however the benefits of a mostly composite structure are significant. Figure [35](#) displays the proposed solution, which uses a combination of composites and traditional metals:



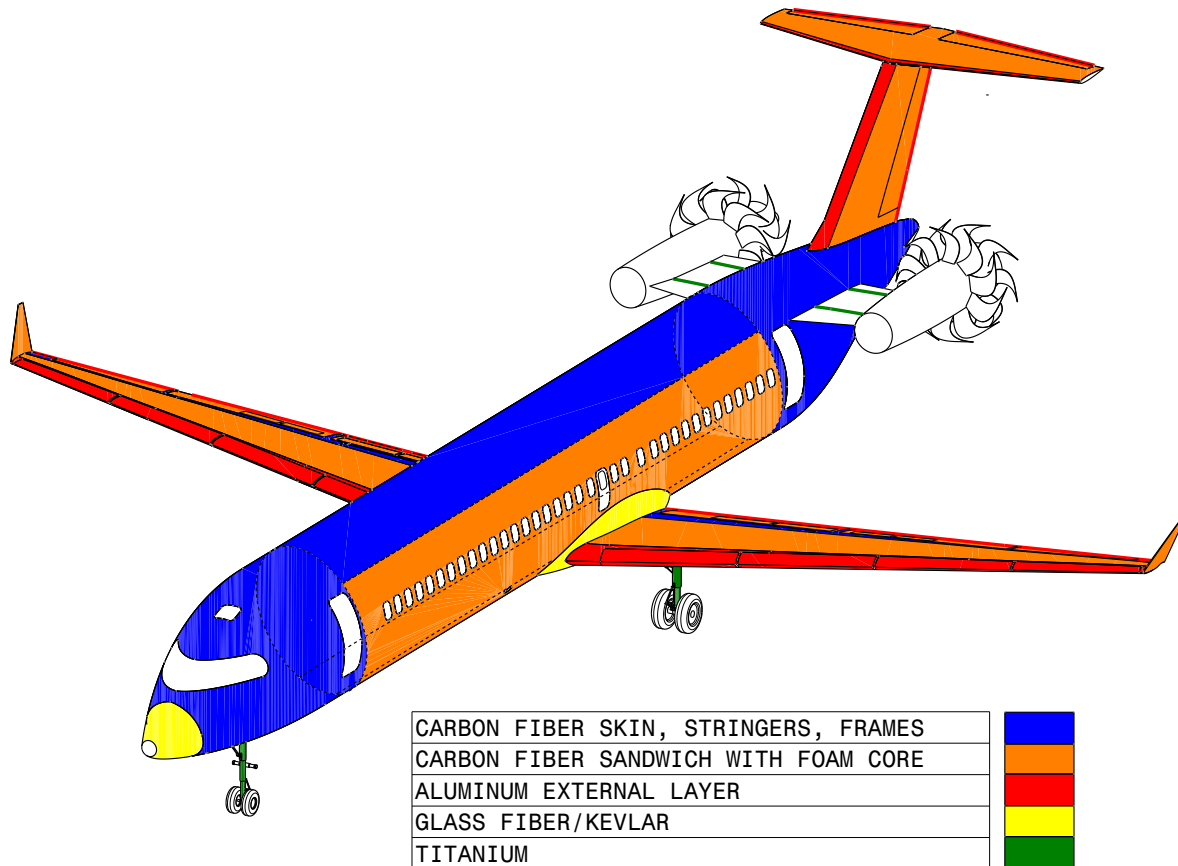


Figure 35: Aircraft Material

The material choices were made considering the various aspects developed earlier, but the variation of costs with time (raw materials, manufacturing & processes availability and feasibility) may present some critical points. The detailed structural design for the principal elements of the aircraft will be now presented.

6.2 Fuselage Structure

The fuselage is one of the most important and complex parts of the aircraft structure. With various restrictions coming from systems, the passengers and various structural junctions confer a certain challenge in the design. The Figure 36 shows all those interactions and the proposed solution.

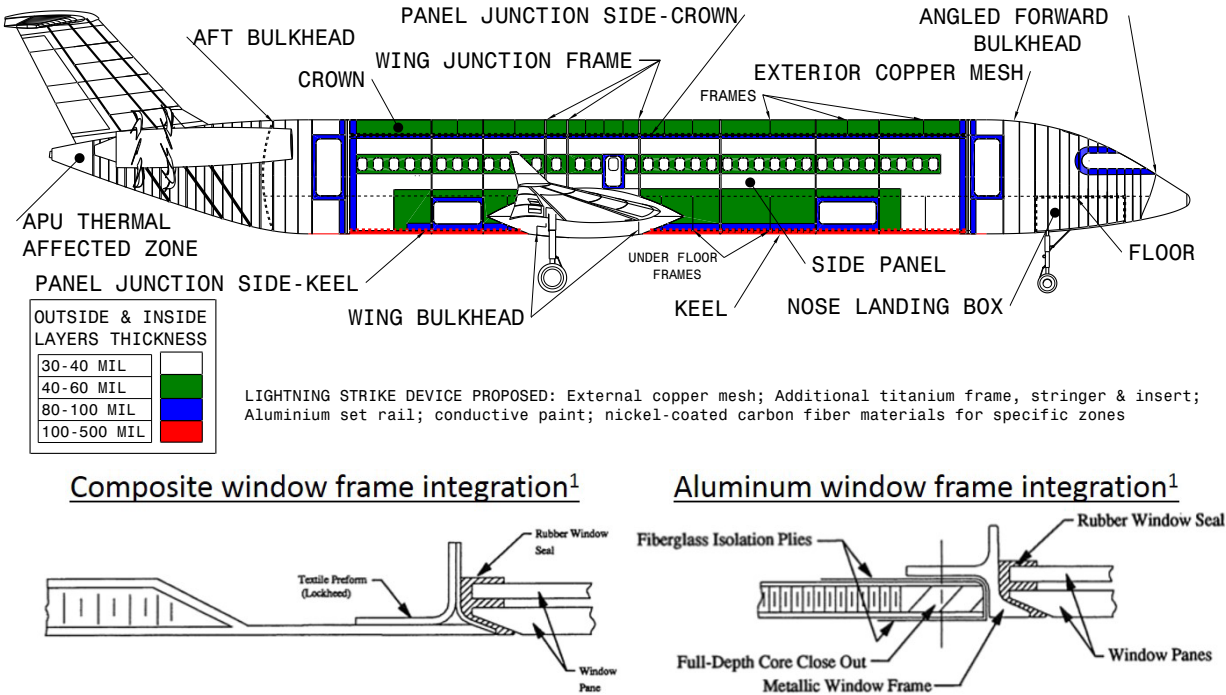


Figure 36: Fuselage Structure

First, the pressurization of the aircraft is maintained by the fuselage skin alongside four principal bulkheads: one in the fwd and aft as well as one on each side on the wing box under the floor. The Nose Landing Gear box acts as an underfloor bulkhead as well. The forward and the aft bulkhead are both dome-shaped to diminish the structural weight, and the forward is also angled to lower structural damage in the case of a nose crash. In the tail section, the APU is positioned at the aft of the tail cone and supported by titanium frames, which will resist to the high temperatures. The ducts and wiring that ensure fuel and electrical distribution are retained by clamps attached to the frames and floor structure.

All along the cabin, additional carbons fiber layers reinforce the windows and doors. The thicknesses presented here were estimated with values given in an analysis from NASA. Despite the low cost and conductivity of aluminum, composites were chosen for the window and door frame structures (at the bottom of Figure 36) due to the ease of integration, as presented in the two illustrations at the bottom of the slide. The dimensions of our windows were chosen to be slightly larger than our competition's average in order to increase passenger comfort.

Below the cockpit, the nose landing gear (NLG) is positioned to have a minimum load of 3 000 lb in order to ensure control on the ground. The NLG is surrounded by a landing gear box which is reinforced around the edges and reaches the floor under the cockpit.



Aside from various structural aspects, a key risk of our composite design is lightning strike cases. An electrical path must be planned throughout the aircraft to ensure safety of the passengers and crew. Our current preliminary design involves an exterior copper mesh with titanium inserts, aluminum seat rails, metallic window and door reinforcements, as well as additional metallic stringers and frames. A possible avenue for improvement is nickel-coated carbon fiber materials for specific zones. The paint and fasteners could pose an issue to the current design and later electrical analyses will be necessary to confirm the design. However, the coatings and paint are also used to protect the composites against UV damage and humidity.

The side walls are composed of a 3 inch foam-carbon fiber sandwich which confers to the fuselage strength, thermal and acoustic isolation and imperviousness. This design could allow for a smaller outer fuselage diameter, however it has not been benchmarked in any other aircraft; a normal thickness for the fuselage was considered in the aerodynamic calculations due to the risk of the new design. Figure 37 presents the detailed panel design and their junctions.



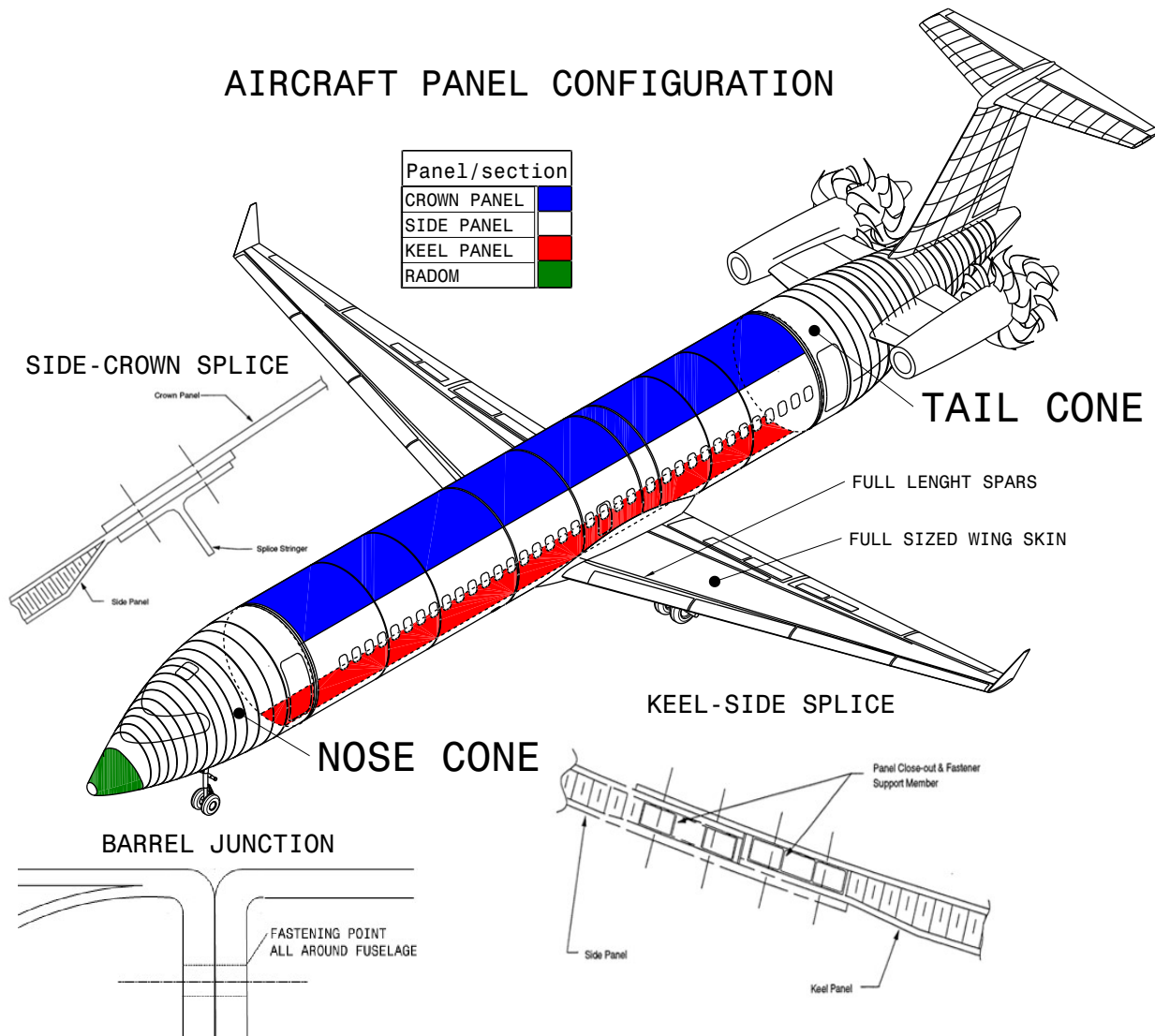


Figure 37: Fuselage Panel Configuration

Many composite configurations were analyzed in order to diminish the cost and weight of the fuselage. The barrel and panel designs both have great potential (see [A: Section A.3](#)), but a panel design was selected in order to diminish the number of parts and junctions. The ORCA family design consists of a radom, a single-piece nose cone, a cabin section made of four panels (full length sides, crown and keel), and a single-piece tail cone.

The four panels were chosen in order to facilitate the transportation before assembly as compared to barrel design. The tail and nose cones use a stringer and frame construction primarily in order to diminish weight and to facilitate systems attachments and integration. In the tail cone, the structural design in the high temperature section around the APU can be taken apart in case of a

major repairs. For manufacturing, no plugs are considered - the cabin section's panels are simply extended for the ORCA101. The composite junction solutions, presented beside the aircraft, were based upon a study from NASA. Additionally, the crown panels and under floor assembly may have co-cure frame - this solution requires further analysis before being fully implemented.

The main power supplier aside from the engines, the APU, is positioned at the rear of the tail cone and supported by titanium frames, which will resist to the high temperatures generated by the APU. Carbon fiber was chosen for the main aft fuselage for weight reasons, however an in-depth thermal analysis should be studied in order to ensure that this composite could be used for the whole tail cone. Finally, the elements ensuring fuel and electrical distribution (the various ducts and wires) are retained by clamps on the frames, floor and in exceptional cases to brackets.

As for the doors, many types were considered: side opening, upward or downward opening, and inside or outside opening. The main criterion for this choice is the functionality of the system. The chosen designs are shown in the Landing section of the Annex ([A.4](#)). Minimum dimensions were set using benchmarks in order to attain the cargo loading requirements discussed in the configuration section. In order to facilitate loading and decrease loading times, the cargo openings were enlarged as compared to the benchmarks. Further optimization could be performed considering the various constraints and the real impacts of cargo loading. In terms of positioning, the door was placed at a certain distance from the panel junctions in order to reduce unnecessary stress concentration.

The structural junctions with the wing, tail, landing gear and engines require special considerations, and will be presented in the following sections of the report.

6.3 Wing Junction

The different composite panels and their junctions are shown in Figure [38](#) alongside the wing-fuselage integration and the main landing gear integration. The crowns have five main stringers where the carbon fiber baggage bins are attached and six secondary stringers for additional rigidity. The keel beam consists of one beam and an integrated cargo floor which confers further rigidity to the structure. In order to ensure landing gear integration, a section is cut out while ensuring a minimum keel width of 18 inches. For side and keel panels, a foam core is used to increase rigidity. The thickness of the core panels on each side vary from 1 inch, along frame, to 3 inches to ensure rigidity in certain areas.



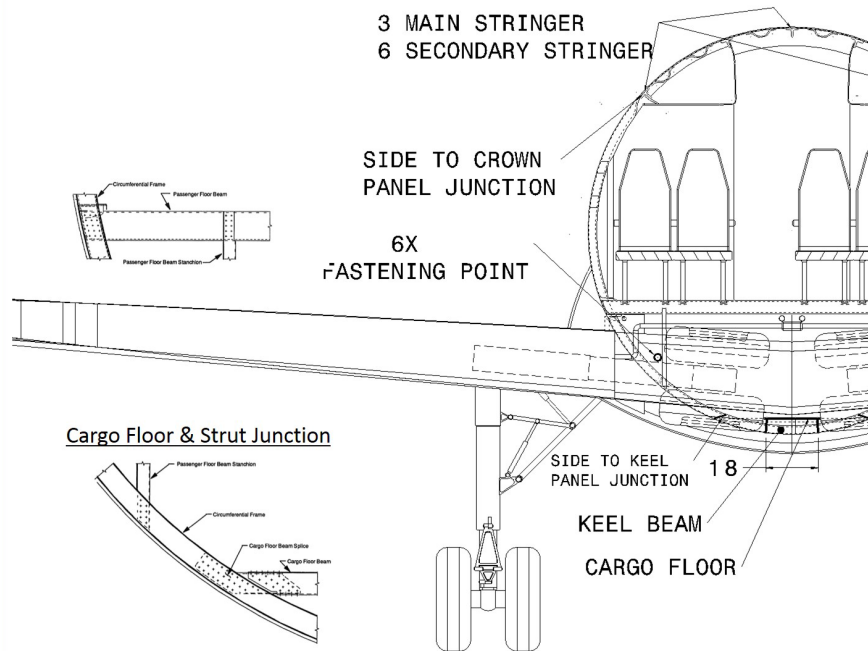


Figure 38: Wing Junction

The floor is glued with epoxy to the external reinforced layer and to the reinforced edge as shown in the diagram above. The three wing spars are attached with two titanium fastener points and inserts. The main landing gear box encases the landing gear and is also used to ensure rigidity and pressurization of the rear cargo area.

6.4 Wing Structure

The wing construction was modelled after a conventional wing with winglets and straight spars. However, one of our only benchmarks for a full composite wing is the Boeing 787 which has a far more complex wing structure; further analyses will be required to verify if a similar idea could be applied to our design. Figure 39 shows the ORCA wing structure.

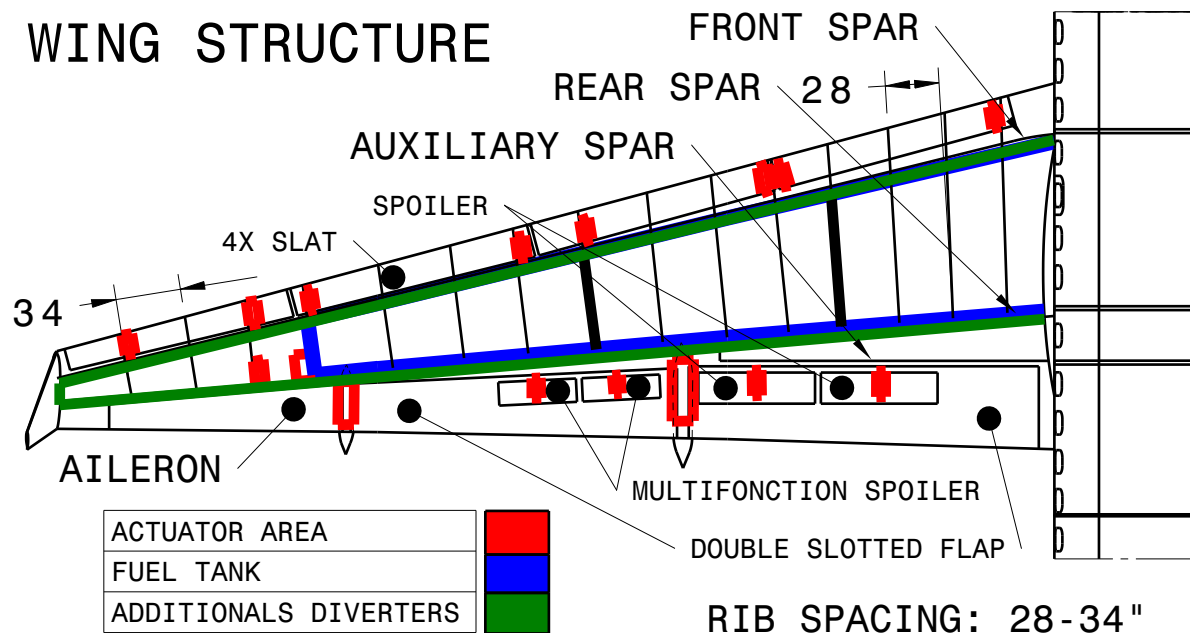


Figure 39: Wing Structure

As shown in the Figure 40, space for the control surface actuators was considered in all the wing sections; the actuators analysis is presented in Section 7.6. These actuators will be attached to the wing ribs or spars.

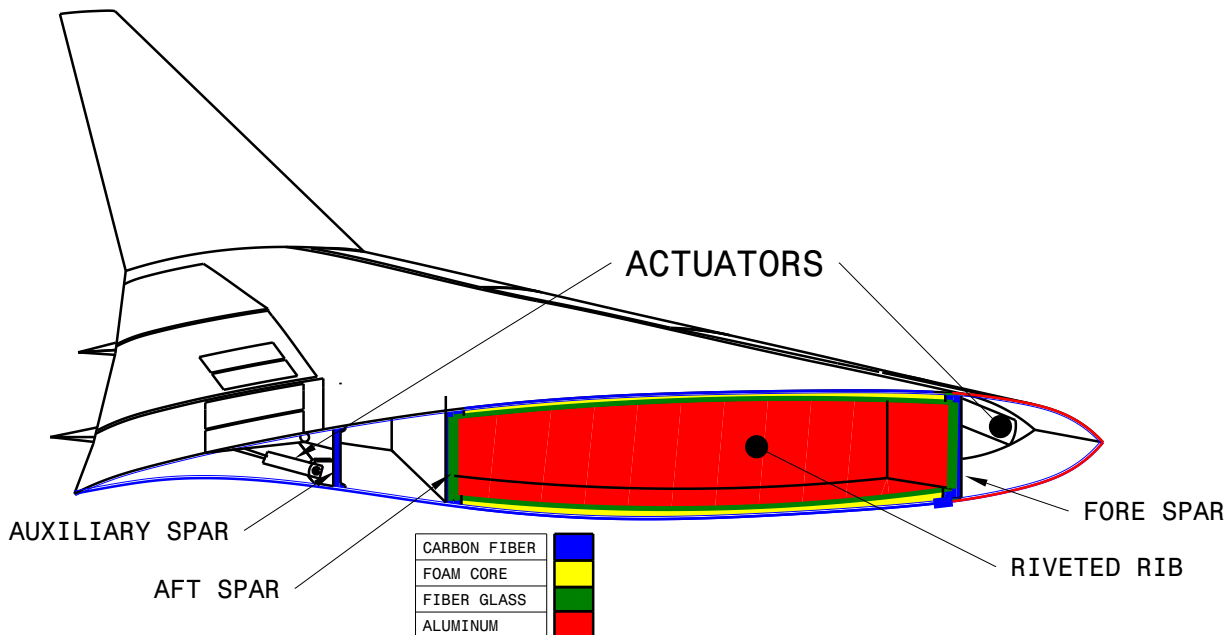


Figure 40: Wing Section Along with Baffle Rib

The principal wing structure consists of three full length carbon fiber spars. The front and the rear are glued to the fuel tank with epoxy and neutral fibers. The skin consists of a sandwich with carbon fiber exterior skin with a foam core, while carbon and glass fiber are used for the interior skin. This sandwich is glued with epoxy to the aluminum fuel tank which contains a riveted rib. Additional aluminum bar diverters could be added for lightning strike cases. The leading edge is composed of an exterior layer of aluminum reinforced with glass and carbon fiber to protect against bird strikes. A similar approach is considered for slats with an additional electric heating device. The spoilers are made of a carbon fiber sandwich with honeycomb. The other high lift devices have a similar construction with an additional aluminum trailing edge to discharge electricity from a lightning strike. An additional electrical analysis is required to confirm if an additional outside copper mesh, aluminum layer, or conductive paint is required to manage lightning strike cases. The empennage, which will be presented next, uses the same lightning strike management devices as the wing.

6.4.1 Wing & Fuselage

The empennage is mainly composed of a carbon fiber sandwich structure and ribs. To ensure more space for the actuators, the sandwich could be replaced by stringers. The rudder and elevator are made of a carbon fiber skin with a foam or honeycomb core, as well as an aluminum trailing edge for lightning strikes. Figure 41 & 42 show the empennage structure.

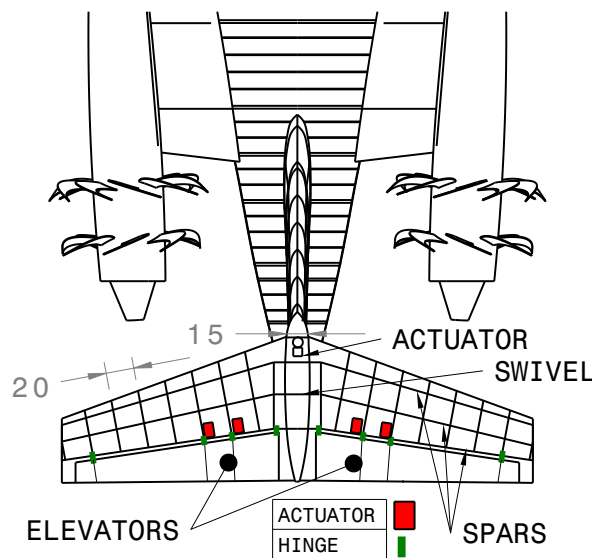


Figure 41: H-Tail Structure

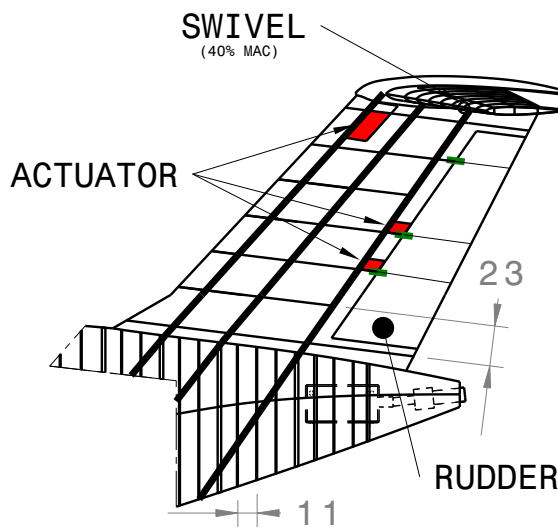


Figure 42: V-Tail Structure

For the vertical stabilizer, three oblique frames and continuous spars transfer loads to the

fuselage. The actuators for horizontal incidence control are attached to the first spar while the swivel is attached to the second spar at 40% of the horizontal stabilizer cord to minimize the load on the actuator during critical loadings. Subsequently, the rudder is attached to the third spar. The actuators for the rudder and elevator are attached to the ribs; the space allocated to these actuators may be critical. All rib spacings were benchmarked on similarly-sized regional jet cutaway drawings.

6.5 Landing Gear

Below the cockpit, the nose landing gear is integrated to minimize loading variation during servicing while ensuring a minimum loading of 3000 lbs for ground steering. The extreme loading case considered occurs during landing when the pilot begins braking, but then aborts the landing, thus causing maximum brake and engine momentum. Another limiting case to be considered for a normal landing is when the CG is forward while the brakes are applied. As shown previously, Table 10 presented landing gear dimensions in Section 5.1.5. Also, the integration of the landing gear is shown on Figures 19 & 20 and the structural integration is shown on Figures 21 & 22. An analysis (Figure 43 below) was performed to optimize the mechanism and to select the materials.

Design	Kinematic concept	Gear Weight (Lighter)	Wing weight ¹ (Lighter)	Simplicity	Land lateral stability
Actual design		+	-	+	+
Proposed design		-	+	-	-

¹Wing weight depends on the criticality of the landing gear load

Material	Weight (lbs)	Unit Production cost (\$)	Development Cost (\$)	Partial life cycle cost ² (\$) (weight=10 ³ ,1,10 ⁻³)
Forged & machined Steel	2900 lbs	70 000	12 000 000	2 982 000
Titanium	2500 lbs	100 000	20 000 000	2 620 000
Composite (Titanium-Boron or Carbon/high temperature thermostat)	2300lbs	150 000	35 000 000	2 485 000

²Landing Weight is the main driver for the life cycle cost

Figure 43: Material and Functional Analysis

An initial sizing calculation was accomplished in order to ensure design feasibility, which is



presented in Annex A along with a weight and cost estimate. This sizing demonstrates that the wheel dimensions are sufficient to fit carbon heat sinks. In parallel, as shown earlier, many landing gear mechanisms and materials were analyzed. The current design of the main landing gear was chosen for its simplicity and light structural weight, particularly considering our choice of titanium for the main landing gear structure. A lighter material could reduce the landing gear weight and therefore fuel consumption, however the overall structural weight may also increase due to a less rigid material - further analyses could refine the design and allow for such a material.

In conclusion, the proposed design using mainly composite materials and components induces higher development costs but lower weights and therefore a lower fuel consumption. Manufacturing costs may be lowered slightly due to the reduction of the number of parts as well their reduced complexity. The certification of new materials and new manufacturing methods, particularly for foam composite sandwiches, will be an issue. For systems integration, the APU positioning and structural design considered the engine rotor burst as well as the space necessary for the actuators of the ailerons, horizontal stabilizer, rudder and elevator.

For a company without composite knowledge heritage, a classic aluminum design would be preferable to reduce the risk associated with the structure. It will be necessary to closely manage the requirements conferred to the suppliers in order to ensure the proper integration of the structure with the rest of the aircraft, and particularly with the systems, which will be presented in Section 7.



7 Systems

The biggest challenge in creating a more efficient aircraft is to minimize the fuel burn while ensuring that the passengers enjoy their flight experience with a more comfortable environment. The proper development of systems is a key component in accomplishing this mandate; the developed systems are the brain of the aircraft as they activate and control the aircraft. The overall system architecture has been developed according to a More Electric Aircraft (MEA) technology. The main motivation behind this electrical systems choice is to improve fuel consumption by avoiding wasteful energy production and avoiding dumping spare power overboard as seen in conventional systems.

7.1 Overall System Architecture

The ORCA family is considered to have a More Electrical Aircraft (MEA) design. The More Electric Aircraft concept is more and more prevalent in the industry being adopted by companies such as Airbus and Boeing on their A380 and Dreamliner 787 respectively. These aircraft are used as benchmarks throughout the systems development for the ORCA design.

The objective of a more electrical aircraft is to minimize power withdrawals from the engines in hopes of achieving a higher efficiency. A bleed-less architecture will be more energy-efficient than a conventional architecture by producing exactly the energy required rather than taking energy elsewhere and modifying it to suit the aircraft's needs. Also, a bleed-less architecture will induce an electrical ice protection system. The ice protection system is assured by thermoelectric plates placed underneath the leading edge and slats which prevent accumulation of ice on the wing leading edges. Nevertheless, a more electrical architecture is more complex and expensive than a conventional system and not guaranteed to always be more efficient since the electric power is often generated with the engines.

Conventional architectures extract mechanical power directly on the engine shaft to power the hydraulic system. Conforming to the MEA concept, the ORCA family uses AC hydraulic pumps instead of using engine driven pump (EDP) to power hydraulic system. This technology with electrical flight control actuators reduce the complexity of hydraulic architecture.



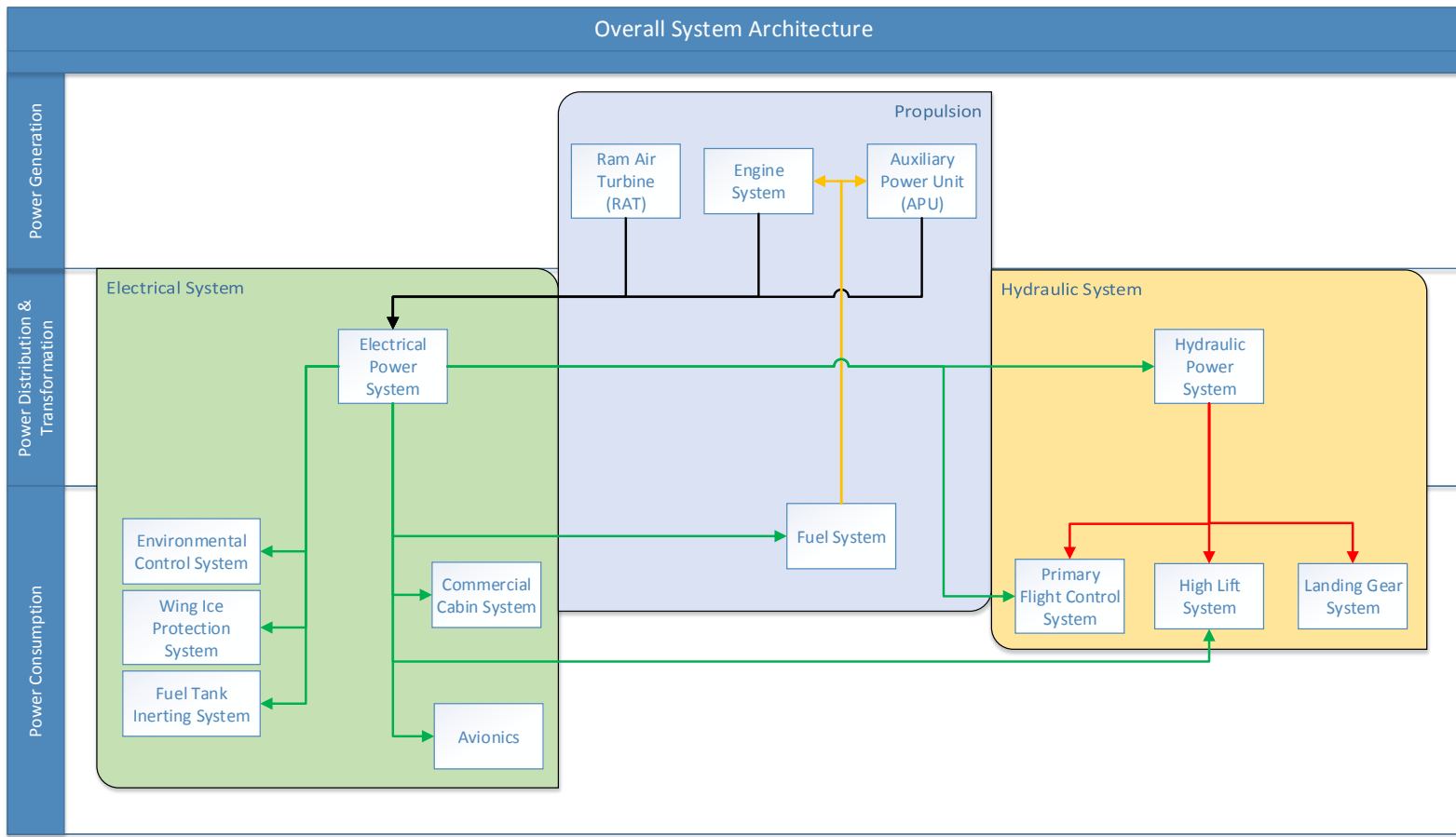


Figure 44: Overall System Architecture



7.2 Electrical System

The ORCA family pushes new boundaries with its MEA architecture. Indeed, the ice/rain protection system, as well as the environmental control system are powered electrically. However, with a bleed-less architecture, electrical demand in the aircraft will be higher compared to a conventional aircraft. The major electrical consumers in the ORCA family are the environmental control system compressors, avionics full integrated system, engine start system, hydraulic AC motor pump, cabin creature comfort systems (galleys, cabin entertainment and lights), cooling system and the fuel system. Figure 45 displays the electrical architecture.

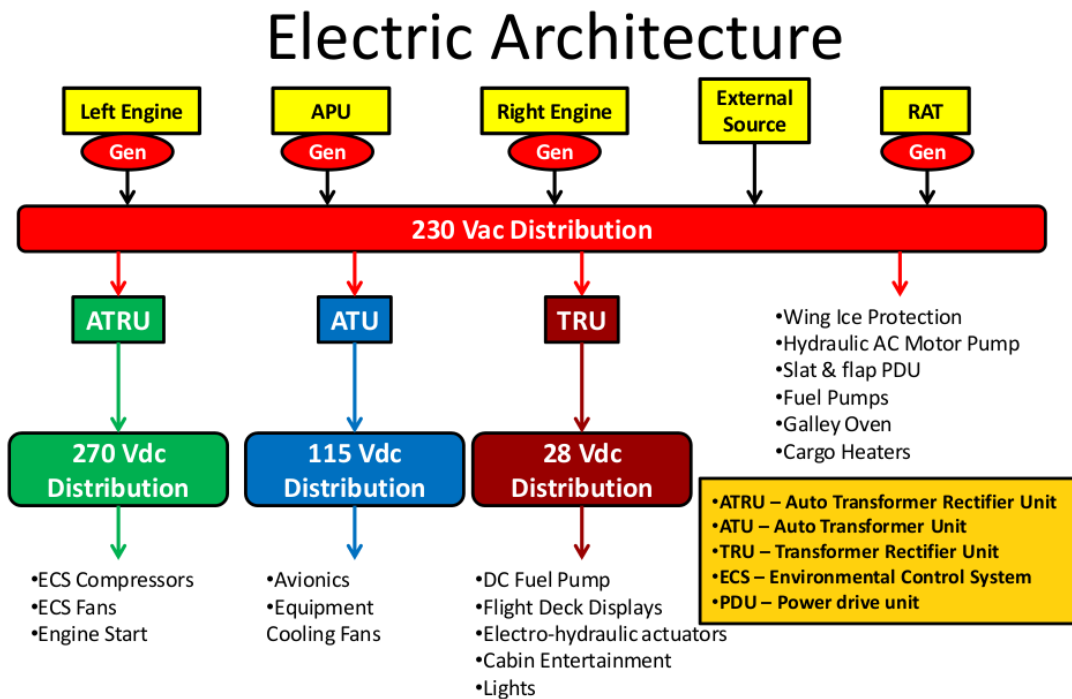


Figure 45: Electrical Architecture

The sizing of engine and APU generators is determined by the sum of each electrical components required on the most critical mission phase. This electrical load analysis has been baselined using scaled data from the DC-10 aircraft and the Boeing 787. Table 15 shows the total amount of VA on each mission phase.



	Ground	Takeoff	Climb	Cruise	Descent	Landing	Justification
Fuel System (VA)	0	1,200	1,200	1,200	600	600	Volume of fuel ratio w/ DC-10
ECS (VA)	40,000	100,000	185,000	185,000	185,000	40,000	PAX ratio w/ B787
Ice protection (VA)	0	0	50,000	0	50,000	0	Span ratio w/ B787
Galley (VA)	12,500	0	30,000	30,000	30,000	0	PAX ratio w/ DC-10
Entertainement + cabin lighting (VA)	150	10,000	10,000	10,000	10,000	150	Same as dc-10 plus 100 screens (40W) added
Avionics (VA)	7,950	11,250	11,250	11,250	11,250	11,250	Estimation 1.5 * DC-10
Hydraulic AC Motor pump + flight control actuators (VA)	0	59,000	60,000	30,000	60,000	60,000	Panel estimation feedback
Exterior lighting (VA)	3,000	3,000	3,000	200	3,000	3,000	Same as dc-10
Miscellaneous (VA)	0	200	250	250	250	200	Same as dc-10
Engine starter (VA)	50,000	0	0	0	0	0	Estimated to 1/3 of B787
Total (VA)	113600	184650	350700	267900	350100	115200	

Table 15: Electrical Load per Mission Phase

The most critical phase on electrical demand is the climbing phase, which consists of a total of approximately 350 kVA. Since the APU is usually inactive in climb, cruise and descent phases, the engine generators must produce at least this specified quantity of VA. This translates to an electric generation of 175 VA per engine. The ORCA engines will implement 2 generators per engine to the power of 90 kVA each. Figure 46 displays the electrical system layout and the major electrical consumers in the aircraft.



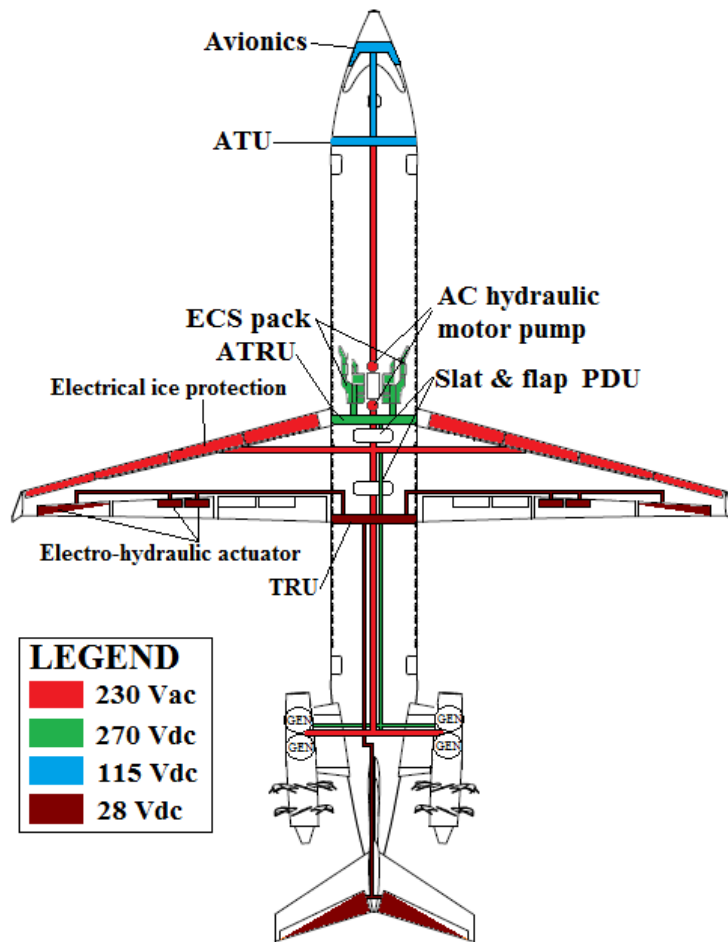


Figure 46: Electrical Layout

Also implemented on the ORCA aircraft is a battery which will be used as backup in emergency conditions, will assist in damping transient loads and also provide power in start-up situations. For the conceptual design phase, the size of the battery has not been determined.

7.3 Hydraulic System

A conventional hydraulic architecture presents three hydraulic channels to ensure a redundancy on important flight control surfaces. There are two channels that are powered by engine driven pumps - one EDP per engine. The third channel is powered by two electrical pumps in case of different failure scenarios like engine failures. The MEA concept leads to the replacement of hydraulic actuators with electro-hydraulic actuators (EHA) and mechanical-hydraulic actuators (MHA) that are controlled by an electrical signal. This replacement allows the removal of the two channels powered by EDPs in order to only have one channel that is powered by two hydraulic pumps



placed in parallel to increase flow rate. This hydraulic architecture saves hundreds of pounds with the removal of: two hydraulic reservoirs, two EDPs and meters of hydraulic ducts. This replacement do not affect the redundancy on flight control surfaces because there are alimented by two different sources: hydraulic and electric. The ORCA77 and the ORCA 101 present the same hydraulic architecture and layout since both aircrafts have the same flight control surfaces. This similitude respects the MR&O. Figure 47 showcases the ORCA's hydraulic architecture.

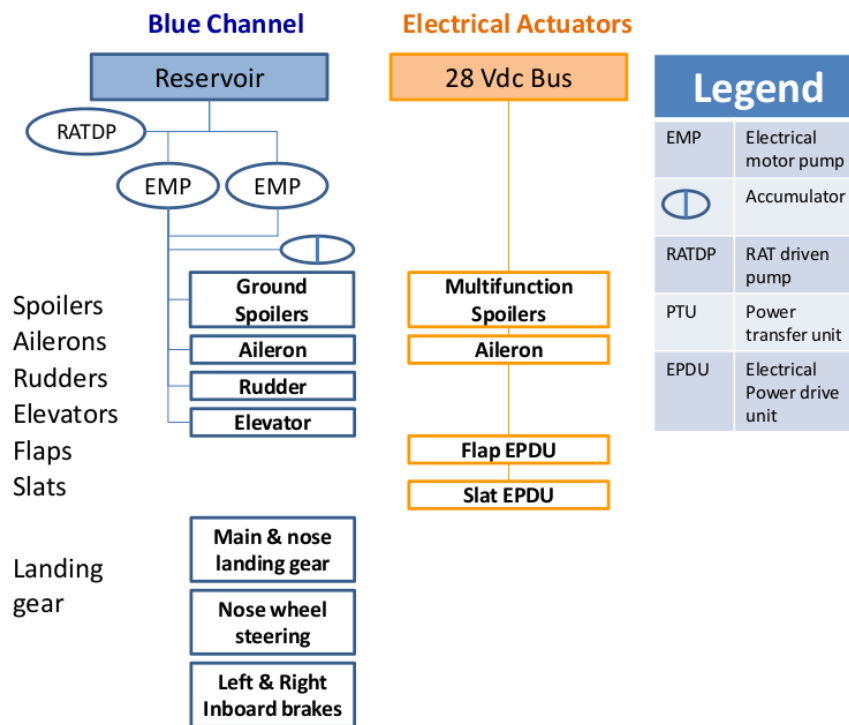


Figure 47: Hydraulic Architecture

The working pressure in the hydraulic actuators sets the whole system pressure at 3 000 psi. This is based on the maximum force required in the hydraulic actuator to activate flight control surfaces in extreme conditions. The MEA concept lead to a simplification of the hydraulic system and a better integration of this system in the ORCA's aircrafts. Figure 48 illustrates the hydraulic system layout in the aircraft.

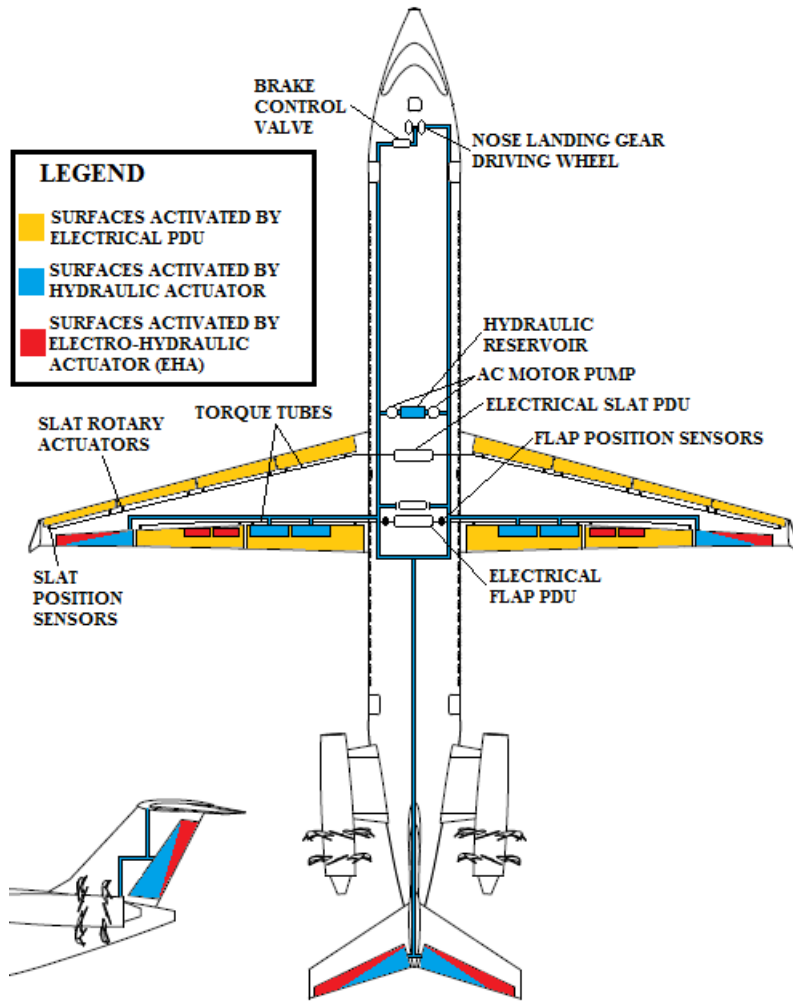


Figure 48: Hydraulic Layout

Figure 48 shows the simplification of the hydraulic integration with one hydraulic channel. The removal of EDPs allows better engine efficiency because there is no power extracted from the engines to supply other hydraulic channels. This configuration decreases the intensive maintenance for engines and minimizes chances of hydraulic leaks in flight with a less complicated hydraulic architecture.

7.4 Pneumatic System

A conventional pneumatic architecture requires the extraction of bleed air from low and high engine compressor stages to pressurize the cabin and heat the wing leading edges for the ice protection. The MEA concept aims to replace this extraction from the engines by compressing ram air electrically. An electrically-powered ECS has a better overall efficiency than a conventional



pneumatic architecture. In a conventional pneumatic architecture, bleed air taken from the engine is too hot (approximately 200°C) and is at a higher pressure than required (about 40 psi) to be directly used by ECS pack. Therefore the temperature and pressure must be reduced to the cabin requirements: 11.8 psi and a temperature of 23°C. The excess energy is dumped overboard resulting in significant losses. The most significant advantage of an electrical environmental control system is that the electrical compressors pressurize the ram air to the required pressure. Since the air is taken from the free stream air instead of the engine, the risk of contamination in the cabin air is reduced. Thus, an electrically powered ECS eliminates those risks and improves the quality of cabin air. Nevertheless, an electrical ECS consumes a lot of electricity that result in an important increase of the electrical load. This increase translates into the need for bigger generators in the engines to produce electrical power for compressors. A fully electrical ECS system is known to be heavier and larger than a conventional bleed ECS system. Also, electrical compressors must be protected by a noise dampener because those equipments are very noisy. Figure 49 illustrates all components in the ECS packs.

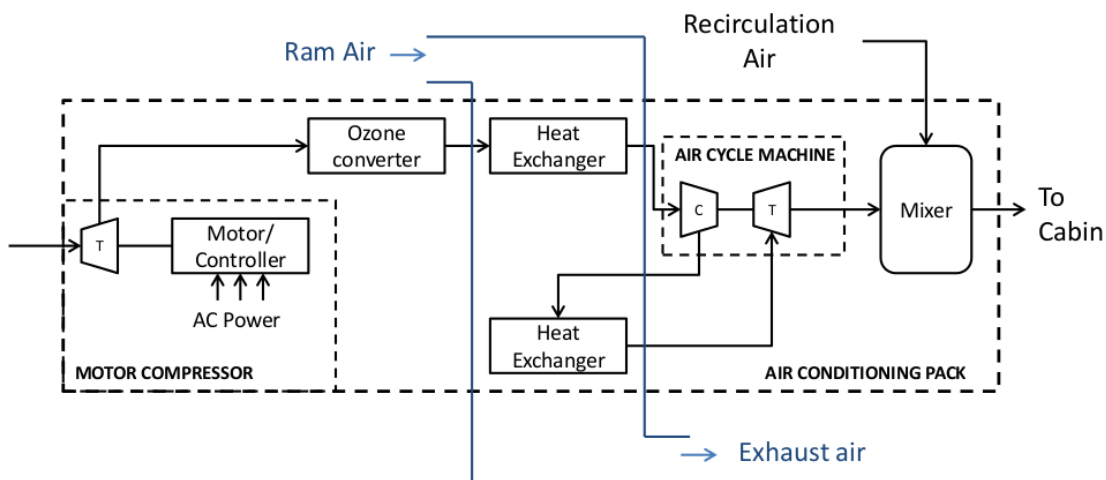


Figure 49: Pneumatic Architectures

An electrical ECS also requires the integration of air vents on the fuselage surface. According to FAR 25.831: "For normal operating conditions, the ventilation system must be designed to provide each occupant with an airflow containing at least 0,55 pounds of fresh air per minute".



	Total Fresh Air Flow Needed in the Cabin (ft ³ /s)	Total Fresh Air Flow Taken from Exterior (ft ³ /s)
ORCA77 (with flight crew)	1.2	31.8
ORCA101 (with flight crew)	1.5	41.1
ORCA 101 High Density (with flight crew)	1.7	47.4

Table 16: Fresh Air Flow Requirement

Those values were obtained with perfect gas relation. The total of fresh air flow taken from outside requires two ECS pack because one compressor cannot produce this volumetric flow and the required pressure of 11.8 psi at the same time.

Two different pipes supply the cabin in fresh air: one steady that is placed in the roof and one variable above passengers head. The variable one is a blast that each passenger has, which can be opened or closed at any time. The two air pipes in the cross view are shown on Figure 50.

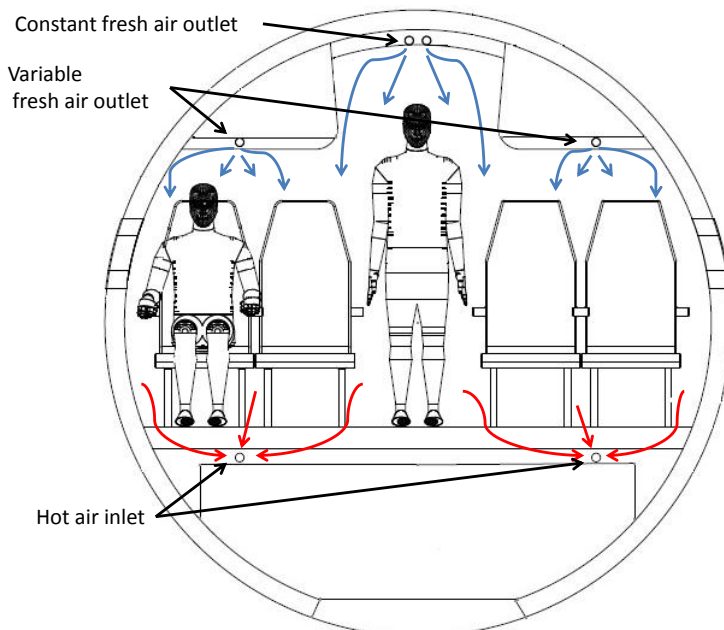


Figure 50: Air Distribution - Business Cross View

Figures 51 shows the air distribution in the aircraft. The compressed air form ECS packs outlet are transported, under the floor, to the rear of the aircraft.



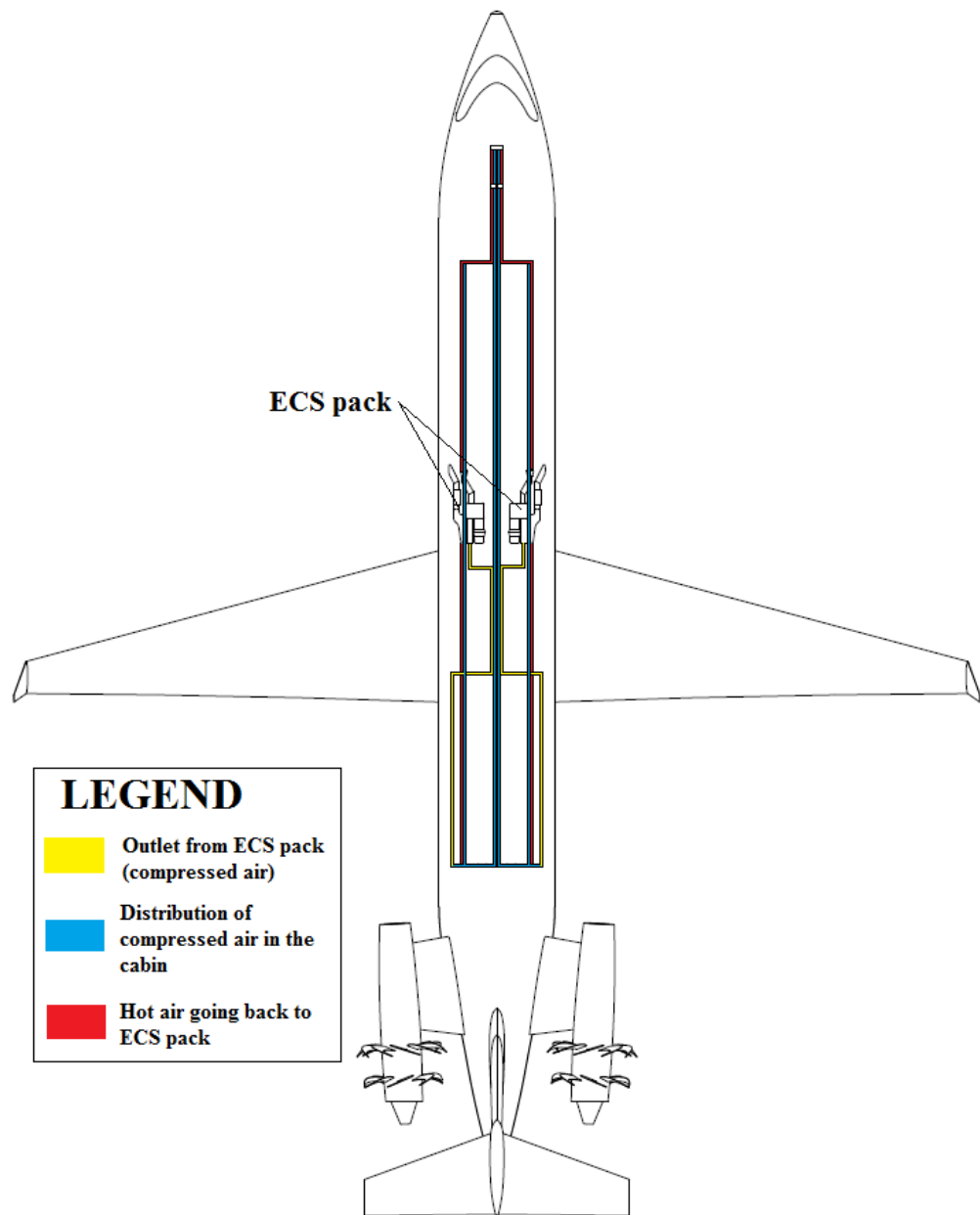


Figure 51: Pneumatic Layout

7.5 Fuel Reserve

The fuel system for the ORCA 77 and ORCA101 is the same. There will be two tanks on either side of the plane each containing two 230V AC motor pumps feeding the engines and another one for fuel jettison. The main architecture of the fuel system is based on the Bombardier Global Express [39] fuel system because it is mainly electrically powered and has a similar volume capacity as the



ORCA. This will ensure that no problems are encountered during the system certification. Figure 52 presents the architecture of the ORCA systems as well as the fuel arrangement. Note that the design is fully symmetrical and that only one side is shown here.

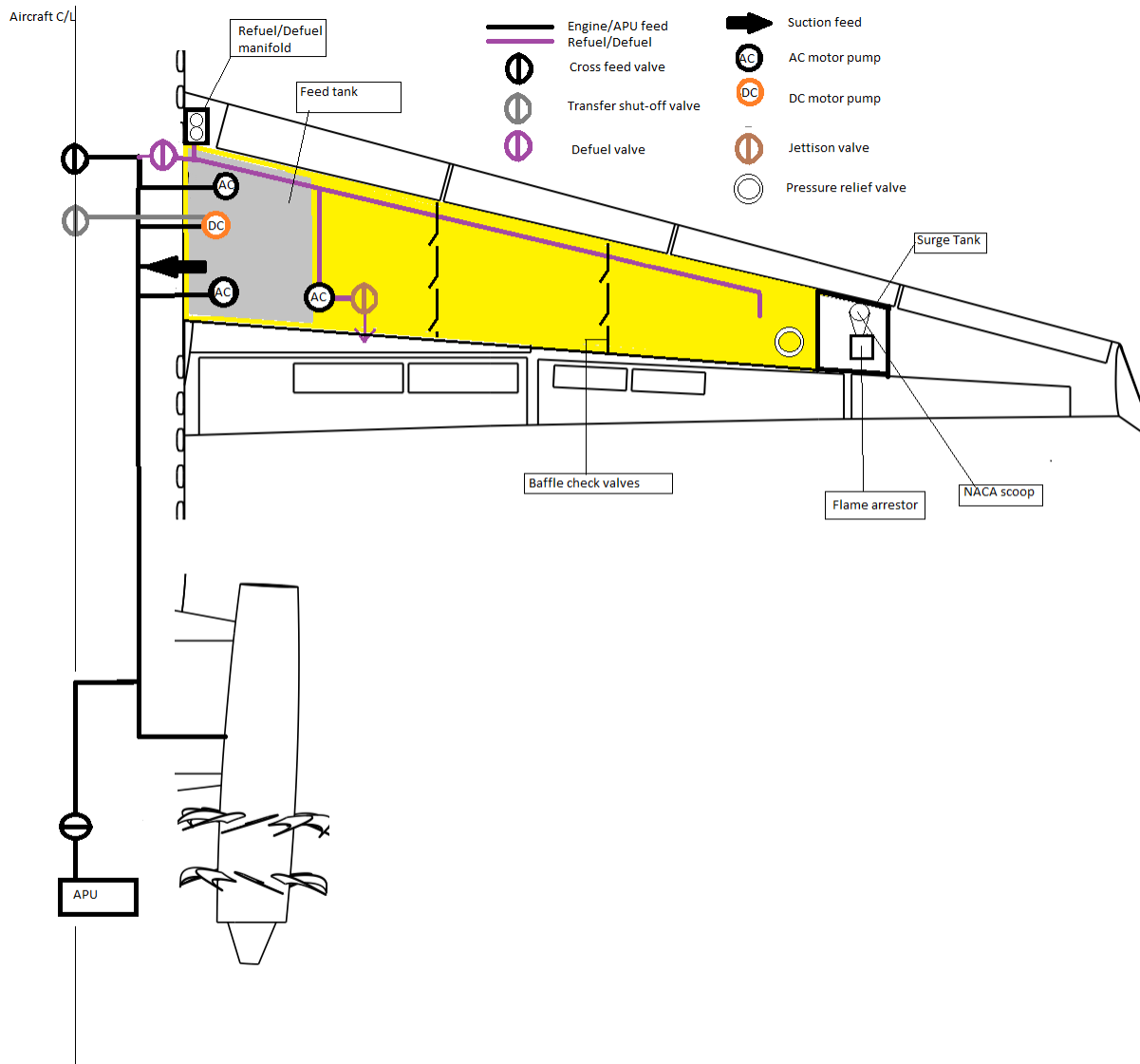


Figure 52: Fuel Storage and Venting System[29]

As seen in the previous figure the tanks are divided in four compartments separated by baffle check valves. They allow fuel to flow towards the feed tank but not outward and minimize CG variation. The feed tank is the compartment of the tank where the feed pumps are located. A surge tank is located at the edge of each tank and an open vent system is implemented as seen in Figure 53.



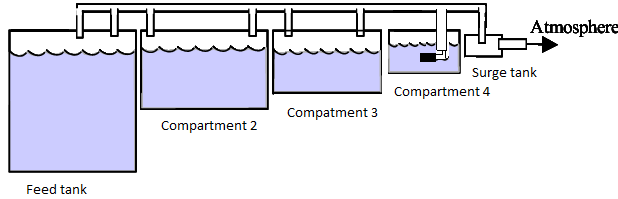


Figure 53: Surge Tank

A float activated valve allows air circulation between the surge tank and the last compartment during cruise and descent phases. For pressurisation purposes there is a NACA scoop inlet connected to the surge tank allowing to recover some of the total pressure from the airstream. They are connected to the surge tanks via flame arrester to prevent flame propagation into the vent system in the case of a lightning strike. In case of ice formation in the flame arrestors, a pressure release valve will be fitted to each tank (compartment 4) that operate automatically if the pressure exceeds a certain level.

7.5.1 Refuel and Defuel

Similar to the Global Express, the ORCA will use a refuel/defuel distribution manifold with two shut-off valves that can be actioned electrically or manually. Since only two main tanks are used, the refueling distribution is simple as the fuel is fed at the extremity of the wing and the baffle check valves help routing the fuel towards the feeding tanks. For the defueling process the feed AC motor pumps are used with the valves routing the fuel to the defuel manifold.

7.5.2 Engine and APU Feed

The engine is supplied with fuel with two (one forward and one aft) AC motor pumps in each feed tank. In case of pump failure there is a DC pump connected to engine feed line and will be used as a backup pump. The APU is fed by both tanks, each having their respective shut-off valve. In case of all pump failure, a suction feed valve is able to supply the engines up to an altitude of 24000 ft [39]. Also included is a cross feed valve to be able to supply fuel to the working engine in the case that one engine is inoperative.



7.5.3 Fuel Transfer and Jettison System

Fuel is transferred between the two tanks to ensure lateral balance. This is achieved with the two backup DC motor pumps and a lateral balance system that allows to keep fuel weight on either side within 500lbs from the other[39].

Inspired by the jettison system on the Boeing 777, our system only has one AC motor pump acting as a jettison pump connected to a jettison valve. Equipping the aircraft with a jettison system is required by the marketing objectives and should only be used in emergency situations to allow the aircraft to land safely. To activate the system, a two-step procedure is required.

7.5.4 Fuel Measurement and Management

Again, similar to the fuel system implemented on the Global Express, the fuel management computer is a LRM compatible with the avionics system. Named the fuel management and quantity gauging computer, the module handles all pumps, valves and in-tank sensors, fuel transfer and feed tasks, as well as displaying the information in the cockpit. The gauging system is AC powered and is designed to meet requirements of a class III system defined by MIL-G-26988C.

7.6 Flight Controls

A conventional flight control architecture use hydraulic power to activate flight control surfaces with hydraulic actuators. The MEA concept on flight control system lead to replace hydraulic power source by electrical source that activates electrical actuators. In this case, a DC powered variable speed pump is used to displace a local hydraulic system in the actuator. Table 17 points out some advantages and disadvantages present in this new actuator, compared to conventional actuators.



Advantages	Disadvantages
Weight saving in hydraulic architecture	Cooling is problematic
Low maintenance cost	Bigger size compare to hydraulic actuator
Power on demand	More expensive than hydraulic actuator
Minimise risk of leak	These new actuators will induce some risk

Table 17: Actuators Analysis

The main advantage of these actuators is the reduction of components in the hydraulic architecture (EDPs, reservoirs and tubing) which reduces the hydraulic weights. This type of actuator is known to be more efficient due to the fact that it uses power only on demand. The redundancy on these actuators is assured by using two independent electrical input wires. Since EHAs are usually larger in size than hydraulic actuators, it could make the integration with the other aircraft components harder. The ORCA's have just enough space near the ailerons to fit an EHA of the smallest volume. These new actuators will induce some risk and could present some issues with certifications. A further step is to ensure that these actuators can be certified without any problem.

As shown previously, Figure 48 shows each actuator used to activate every flight control surface. The slat and flap systems are powered by an electrical power drive unit (PDU), which controls torque tubes to make sure that slats and flaps are deployed simultaneously. There are sensors on torque tubes to give information to the pilots. Hydraulic channel powers flight control surfaces required in emergency scenarios: ailerons, ground spoilers, rudder and elevators. Table 18 shows the number of actuators for each flight control surface:

	Hydraulic actua- tor/surface	Total hydraulic actuators	Electrical actua- tor/surface	Total electrical actuators
Slat	0	0	2	16
Flap	0	0	2	8
Aileron	1	2	1	2
Ground spoiler	1	4	0	0
Multi-function spoiler	0	0	1	4
Rudder	1	1	1	1
Elevator	1	2	1	2
Total	–	9	–	33

Table 18: Number of Actuators per Control Surfaces

The required number of actuators for slats and flaps is determined by a benchmark of competitor aircraft. Also, the forces applied on each slat and flap surfaces required two actuators because a bigger actuator that are able to receive all that force applied on the flight control surface, will



result some integration issues in the wing. The primary flight control surfaces (ailerons, rudder and elevators) are powered by one hydraulic actuator and one electrical actuator each to improve efficiency and reliability with using two independent power sources. Spoilers require only one actuator per surface because they swivel around a pivoting point. Furthermore, the spoilers are relatively small compared to others flight control surfaces. Hydraulic actuators are used for ground spoilers instead of electrical actuators because forces applied on these surfaces are higher than multi-function spoilers.

7.7 Avionics

As seen with the Boeing 787 Dreamliner and the Airbus A380, an Integrated Modular Avionics (IMA) architecture was implemented for the following reasons [42]:

- volume, weight and maintenance savings
- sharing of resources, such as power supplies, across a number of functional modules
- standard module designs yielding a more unified approach to equipment design
- incremental certification of hardware and application software
- management of obsolescence

In light of those conclusions, it has been decided to implement our avionics system in a similar manner to that of the A380. Note that the architecture used is common to the two configurations and since this concept has previously been certified, there should be no problems in regards to having the ORCA planes certified. Figure 54 shows the avionics system disposition.



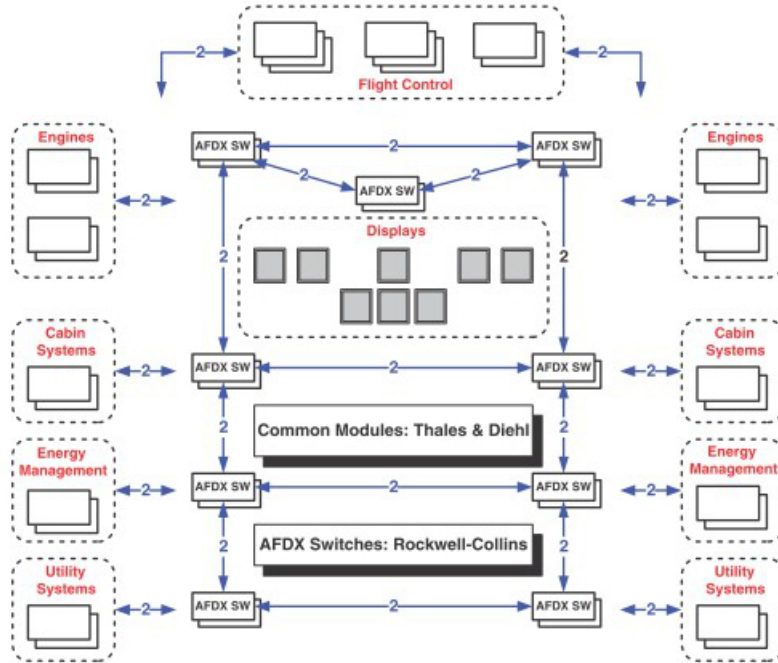


Figure 54: Avionics System Disposition [42]

It can be seen that there is a dual redundant AFDX switched network, also known as ARINC664 part 7, which is based on 10/100mbps Ethernet technology, MAC addressing, Internet and user datagram protocols. It has been decided to split the systems up in domains arranged with eight pairs of switches, as well as distributed them in left and right elements in the aircraft. Each domain is implemented in a set of CPIOMs, which in turn hosts end-system terminals. Within each domain, different end-systems communicate through the domain network switch, and between domains communication is done between domain switches. It is to be noted that the CPIOMS incorporate domain specific input/output functions to communicate with domain specific sensors using ARINC 429 and CANbus data buses. Also each end-system terminal has 2 independent pathways (2 channels) for redundancy purposes.



From these learnings, a simplified top level architecture of the avionics system was designed as seen in Figure 55.

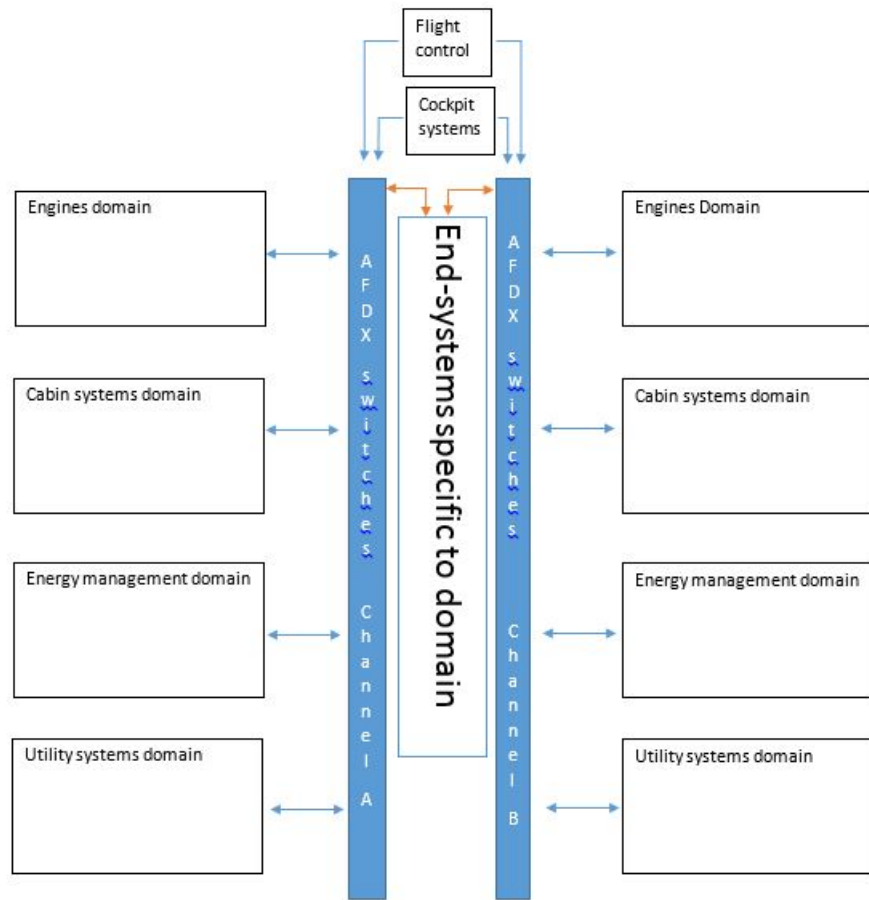


Figure 55: Top Level Architecture of the Avionics System



For example, in Figure 56 is what a domain would look like, in terms of sensors, CPIOMs, and AFDX redundant switches and network.

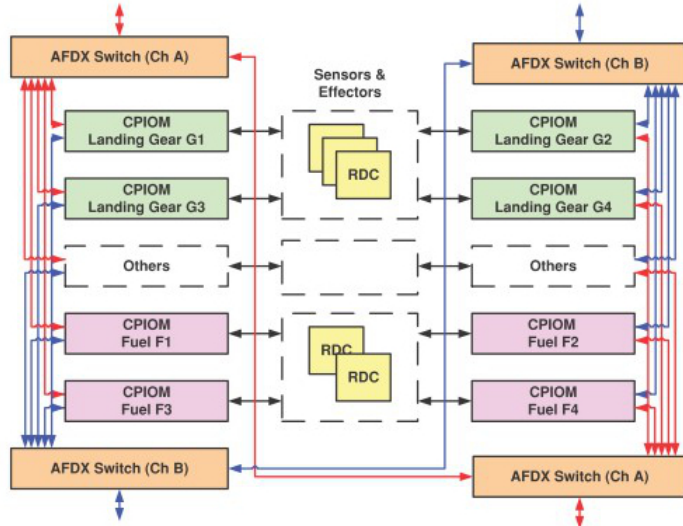


Figure 56: Avionics Domain [42]

Considering that the aircraft will require one cabinet per side per domain, it can be determined that the design will need roughly 10 cabinets to contain the CPIOMs. Considering that the information for the Airbus A380 cabinets is still unavailable, a Honeywell AIMS cabinet has been used for sizing purposes:

- Cabinet dimensions 9.8x47x19.5 in
- Weight per cabinet: 115 lbs

Based on those assumptions, it can be effectively calculated that our 10 cabinets would require approximately 90000 cubic inches and weigh about 1150 lbs. To be able to fit such large components, it was determined to install these cabinets under the cockpit behind the main landing gear. The avionics cabinet are shown in Figure 57.



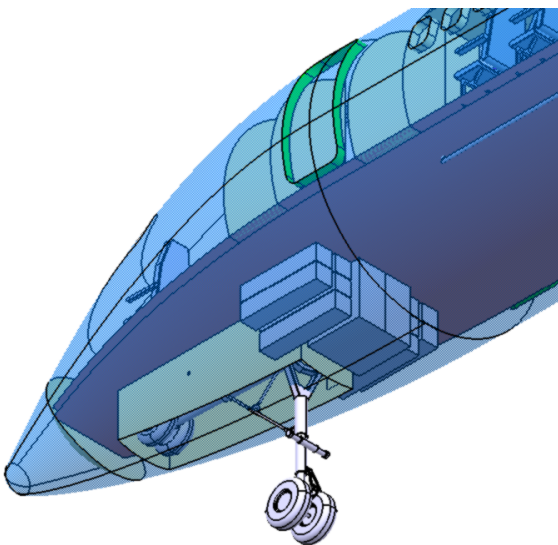


Figure 57: Avionics Cabinet

7.7.1 Auto Land Category IIIB

To ensure that the aircraft lands safely in poor conditions and also be at the fine point of technology, a CAT IIIB auto-land system is implemented. As defined by the FAA this system has a minimum decision height of 50 ft. and a minimum runway visibility of 150 ft. In order to implement this system, the following constraints must be met:

- 3 independent AC and DC power channels
- 3 independent flight control channels
- Auto-trim system

It should also be noted that a GPS augmentation system (LAAS: Local area augmentation system) will be integrated to provide improved guidance for the CATIIIB system.

7.7.2 Auto-Throttle

An automated throttle command system is implemented on the ORCA family. This system allows to keep a constant thrust provided from the engines or to maintain a constant airspeed without human input. This system can be used without the activation of the autopilot system. Having the auto-throttle could reduce fuel consumption and helps the pilot focus on other tasks[3]. Nonetheless, these systems must be used with caution because it could result in unexpected throttle variations if

flight conditions change.

7.7.3 Head-Up Display Visual Guidance System (HVGS)

An HVGS helps provide the pilots with necessary flight data while keeping his eyes on the exterior environment. It is comprised of a display guidance computer, an overhead projector, a combiner, a control panel and a message panel. These components are shown in Figure 58.

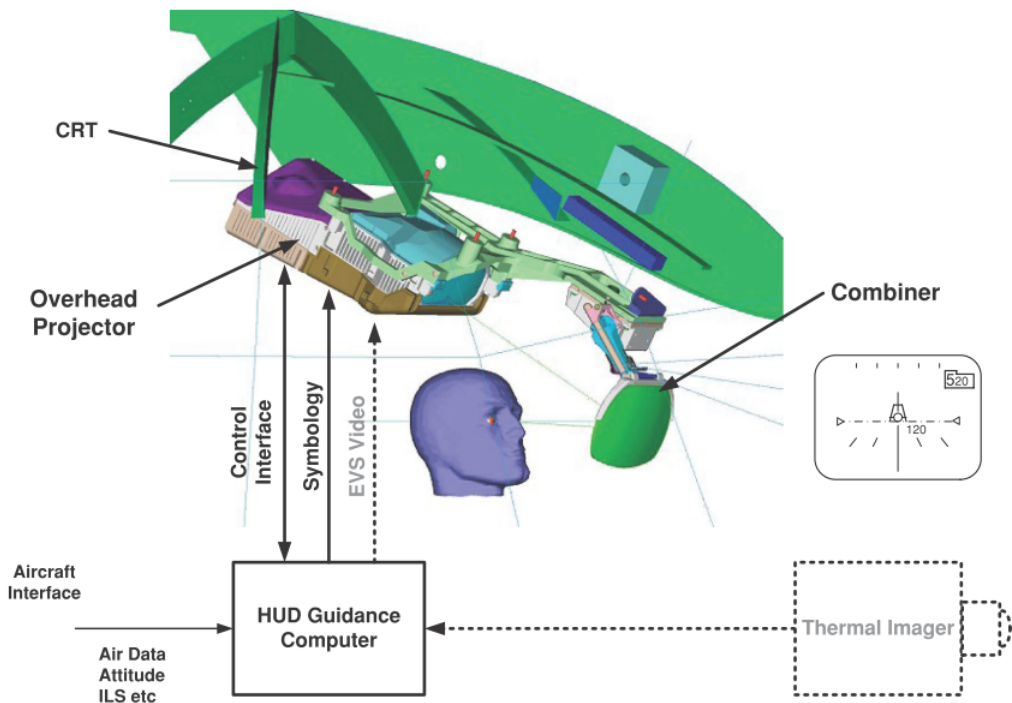


Figure 58: HVGS [12]

The information provided to the pilots is:

- Flight path vector
- Boresight symbol: indicator as to where the plane is physically pointed
- Horizon line
- Heading on the horizon line
- Current airspeed
- Desired approach speed
- Current altitude and altitude scale



In addition to the HVGS is an enhanced vision system (EVS). It uses forward-looking infra-red sensors, low light-level image intensifying devices and active imaging sensors to provide the pilots with a view of their exterior surroundings. This system is only used while manoeuvring the aircraft in reduced visibility weather conditions. This system's output is usually projected on a head-down display as we can see on Figure 59.

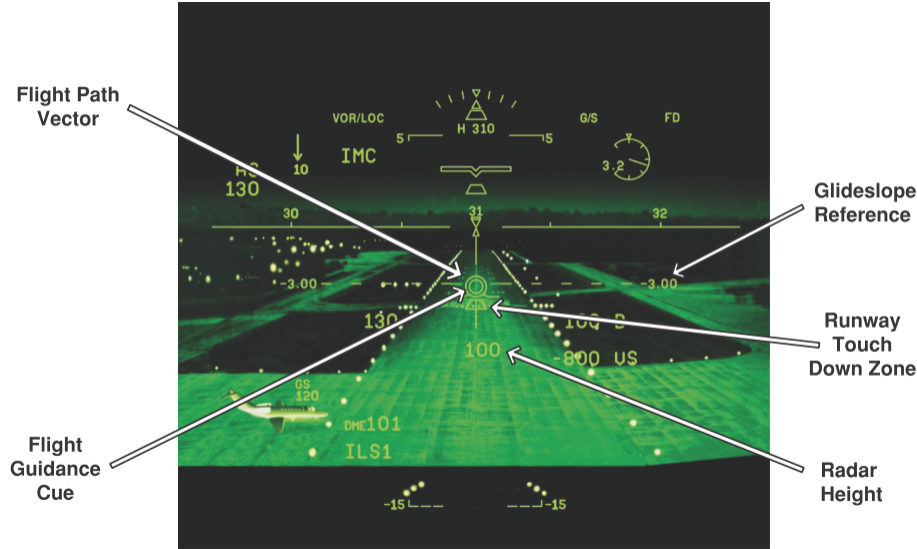


Figure 59: Enhanced Vision System (EVS) [12]

Rockwell Collins [12] offers a combination of the HVGS and EVS, calling it head-up vision system (HVS). A similar concept is what will be implemented on the ORCA family.

7.8 Ice Protection

The systems design philosophy dictates that there isn't any bleed air extracted from the engines, which increases fuel efficiency and minimizes weight of the components. This leads to the conclusion that a conventional piccolo solution is out of question to heat the wings. The ORCA ice protection system is benchmarked on the Boeing 787. The reason for that is that Boeing boasts that this system reduces drag and as much as 50% less energy is required compared to a conventional pneumatic system [55]. In fact, heat blankets will be implemented on the leading edges of the wings (including high lift devices) as well as heat elements on probes, sensors, water lines and the wind-shield. As for the engine inlet, the team will adopt a similar solution to the B787, which uses bleed air for that purpose. It's actually a very convenient solution because of the proximity of the compressors to the inlet. The strategy adopted towards ice protection is reactive. Basically, the



system will only be activated when needed and during specific flight phases such as climb and descent. Finally, materials provided by supplier Minco are to be used, which already has experience in the field [41] These are the components that will require heating:

- Wing leading edge
- Windshield
- Engine inlet
- Probes and sensors
- Drain water lines

7.9 APU

The APU and RAT are backup systems designed to provide electrical power during engine failure situations. To be able to size the generator on both these components, an engine failure analysis must be conducted. Presented in table form this analysis is seen in Table 19.



Extreme cases	Single engine fail	Electric load (VA)	All engines fail	Electric load (VA)	All engines fail and APU fail	Electric load (VA)
Fuel System	Remains active	1,200	Only APU feed	Estimated at 600	Inactive, if needed uses suction valves	0
ECS	Only pack will remain active to maintain cabin comfort for passengers. Temperature and pressure could be less than optimal.	92500	No ECS is active. Aircraft must descent to suitable altitude for passengers, oxygen masks must be used during descent.	0	No ECS is active. Aircraft must descent to suitable altitude for passengers, oxygen masks must be used during descent.	0
Ice protection	Assuming cruise conditions, Icing conditions are not probable but in case of need some ice protection is still available.	Estimated at 25,000	Assuming cruise conditions, Icing conditions are not probable but in case of need some ice protection is still available.	Estimated at 20,000	Inactive	0
Galley	Stays active	30,000	Inactive	0	Inactive	0
Entertainment + lighting	Remains active	10,000	Minimal cabin lighting	Estimated at 3000	Inactive	0
Avionics	Remains active	11,250	Remains active	11,250	Runs on battery	0
Hydraulic AC Motor pump + flight control actuators	Remains active	60,000	Reduced to only necessary control surfaces	30,000	Reduced to only necessary control surfaces	30,000
Exterior lighting	Remains active	3,000	Reduced but remains active	Estimated at 2000	Reduced but remains active	2,000
TOTAL		232,950		71850		32000
Conclusions	1 engine and APU provide the required power		APU provides the required power		RAT provides the requires power	

Table 19: Engine Failure Analysis [42]

In the previous table we have assessed 3 critical situations: one engine failure (OEF), all engines failure (AEF) and AEF with the APU failing as well. As seen here, the APU will need to provide 75 kVA and the RAT will need to provide 35kVA.

Sized with the failure analysis in mind, the APU used provides 75 kVA. Since a bleed-less approach is applied, an APU supplied by Hamilton Sundstrand APS2000 with slight modifications to delete the bleed air function and revamp the generator would be able to respond to our needs. Initially, the APU is able to supply 60 kVA and therefore is very close to the figure needed on each of the ORCA. It is for that reason that this auxiliary power unit was implemented to contribute to the electrical system of the aircraft. The following dimensions can be set to integrate it: 42.1"x20.9"x21.9" [42]. Also, this allows to estimate a weight of 300 lbm for the APU. The APS2000 will also be able to be started and operated at altitudes as high as 37000 ft. The APU is shown in Figure 60 will be located in the tail cone as shown in the Figure 61.





Figure 60: APU[2]

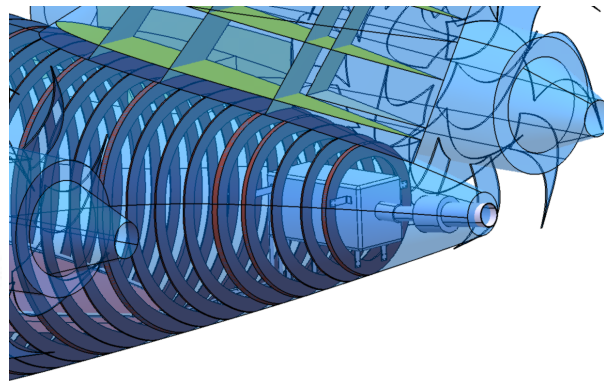


Figure 61: APU Location

Please note that the supports are there for illustrative purposes and not a finished or mature design.

Knowing that A380 has a RAT able to provide 70kVA and has a 5 feet diameter [42], the assumption is the the ORCA family will require a RAT with approximately 2.5 feet diameter since the required power generation is 35 kVA. It will be stowed on the forward fuselage, but an exact position isn't determined at this stage.

8 Engines

Societal needs are evolving towards greener transportation solutions, and air transport isn't an exception. Historically, the open rotor engine was developed during the 1980's, during an oil crisis when fuel prices were climbing significantly; manufacturers wanted to find ways to reduce their fuel consumption. Since the fuel crisis was short lived, the development of such engines was shelved in favor of the well-known turbofan engines solution. Nowadays the jet fuel prices are once again on the rise, and there are increasing demands to reduce aircraft pollution. In fact, the MR&O imposes a 20% CO₂ emissions reduction as compared to the competition and that NO_x emissions are 50% lower than CAEP6 requirements (also see Table 21). Since the mid 2000's engine manufacturers have quietly been going back to the drawing boards with the open-rotor concept. GE, being one of the pioneers of the technology, has developed the GE36. The engine implemented on the final ORCA family design is based on the GE36 engine one since a substantial amount of research documentation is available regarding this engine.

On top of its theoretical fuel-saving advantages, the open-rotor concept was chosen for being a unique and innovative solution to aircraft propulsion that has the potential to set the aircraft apart in a competitive market. The power plants are the same for both the ORCA77 and ORCA101 in order to respect the commonality requirement. The engine selection will be based on the criteria stated in Tables 20 and 21.

	Takeoff (@SL ISA+15)	Cruise (@36 000 ft, M0.68, ISA)
Thrust per Engine (lbf)	13 000	3 000
Targeted Specific Fuel Consumption (SFC lbm/lbf/hr)	0.215	0.42

Table 20: Engines Criteria

Exterior Noise Levels	20 EPNdB Lower than Ch4-Annexe16 Requirements
CO₂ emissions	20% Lower than Competition
NO_x emissions	50% Lower than CAEP6 Requirements

Table 21: Marketing Requirements and Objectives



Bombardier, acting as the engine supplier, provided an engine matching these requirements. The engine provided supplies 15 000 lbf. and is modifiable to our needs. A set of equations, shown below, was provided with the engine to be able to adapt it to the aircraft.

$$SF = \frac{Rqd_t hruast}{Current_t hruast} \quad (3)$$

$$dia = dia_{actuelle} SF^{0.5} \quad (4)$$

$$W = W_{current} SF^{0.75} \quad (5)$$

These equations will be used to modify the diameters and weight of the engines. This leads to the final configuration of the engine. Presented in Table 22 are the original specifications of the engine as well as the modifications used to adapt it to our needs.

	Original	Modified with Scale factor = 0.87
Sea Level, ISA, Static Max Takeoff Thrust (lbf.)	15 000	13 000
Flat Rating	ISA+15	ISA+15
Bypass Ratio (BPR)	30	30
Overall Pressure Ratio (OPR)	N/A	N/A
Powerplant Price	5 Million US\$ per engine	5 Million US\$ per engine
Geometry		
FWD Propeller Diameter (ft)	10.2	9.5
AFT Propeller Diameter (ft)	9.2	8.6
Nacelle Type	Long Cowl	Long Cowl
Nacelle Diameter (in)	47.6	44.3
Nacelle Length (in)	250 inches	250 inches
Distance from Nacelle Front to FWD Mount (in)	37.5 inches	37.5 inches
Distance from Nacelle Front to AFT Mount (in)	125 inches	125 inches
Distance from Nacelle Front to Powerplant CG (in)	125 inches	125 inches
Weights		
Powerplant Weight (engine + nacelle) (lb. per engine)	5850	5255

Table 22: General Characteristics

A decrease in weight and size is observed because of the reduction in thrust. The engine dimensions are illustrated in the Figure 62 below:



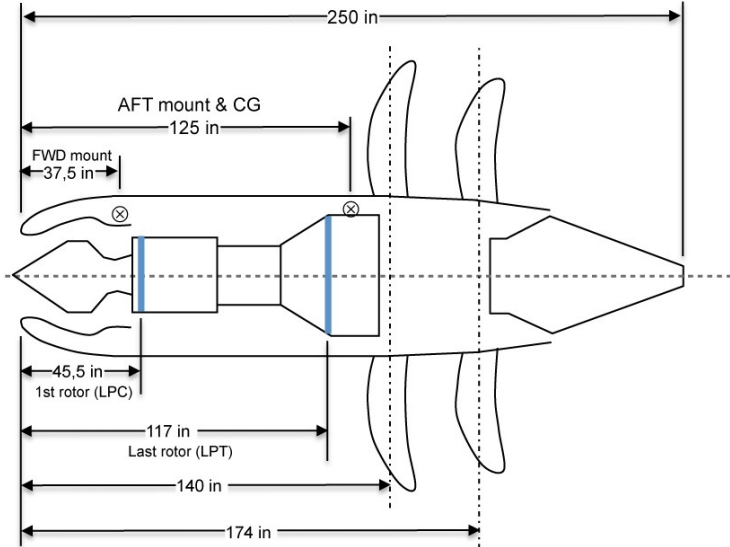


Figure 62: Engine Dimension

8.1 Noise and Emissions

According to a report for the FAA submitted by GE [37] further evolution of the propelling blades allow to confidently confirm that a 15 to 17 EPNdB margin to ICAO chapter 4 annex 16 is attainable. This margin does not meet the requirements in the MR&O, however it is satisfactory given the advantages offered by the engine. In addition the same document mentions a minimum of 26% fuel burn savings (and consequently at least 26% lower CO₂ emissions) compared to an older CFM56-7B engine. Considering the CFM56-7B engine has SFC's [23] equivalent to 0.36/0.58 lbm/lbf/hr (T-O/CR), this would result in an SFC of 0.26/0.43 lbm/lbf/hr. at higher speeds and a higher altitude than our plane. In regards to NOx emissions, they should be able to follow current turbofan technologies and bring further reductions to those emissions, however no estimations are offered. In addition, a secondary research article [31] further supports that research by estimating current SFC's of 0.158/0.44 lbm/lbf/hr while maintaining noise levels 13EPNdB lower than chapter 4 requirements for the open rotor engine. Hendricks estimates the NOx reductions to 50% lower to CAEP6 requirements by 2020 for these engines. In regards to dimensions, this research offers a dimensional estimation of 23 feet in length and 5.6 feet in nacelle diameter, while both research papers agree that the blade diameter is approximately 14 feet. Keeping in mind that both these documents have higher thrust ratings at takeoff than what is required by the ORCA family, this offered validation for the open rotor engine used on the ORCA family.

8.2 Position

As a safety precaution the engines are installed on the aft fuselage. This position will ensure that a rotor burst situation will not affect the pressurised area of the aircraft. Furthermore, an aft engine position reduces cabin noise and vibrations, thus increasing passenger comfort. Also, since the aircraft will be bleedless (except for cowl anti-icing, as explained in the anti-ice section 7.8) there isn't the concern of added weight and complexity for bleed air ducting.

The positioning of the engines with regards to the fuselage is done in same manner as a turboprop engine. The similarity of the concepts with the blades being in the airstream allows the turboprop approach to be applied to the ORCA engines. In the case of the ORCA open rotor engine, the clearance required is approximately 30 inches.

As for pylon design, a very simple representation is provided in Figure 63. Of course a detailed structural analysis is to be completed to ensure that the pylons are capable with dealing with extreme load cases as well as dissipate the high temperature of the engine while maintaining a light weight.

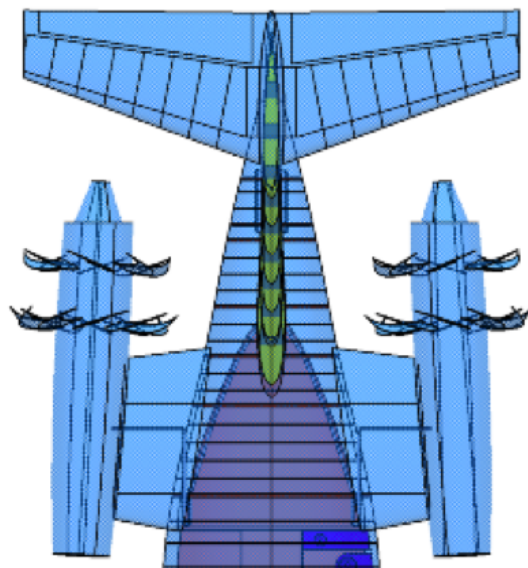


Figure 63: Pylon Design

8.3 Fuel Consumption

The expected fuel consumption, as described by Hendricks and Khalid [37][31], are an SFC similar to 0.16 to 0.26 lbm/lbf/hr. for Takeoff with 19 000 lbf. of thrust a (SL, +15 °C) and 0.43 to 0.44

lbm/lbf/hr. for cruise (35 000 ft/M0.78/ISA). Surely enough, the engine provided has similar values: The ORCA family engines have a static SFC of 0.1915 lbm/lbf/hr. at SL/ISA and a cruise SFC of 0.42 lbm/lbf/hr. for the ORCA77 (36 000 ft/M0.68/ISA) and a cruise SFC 0.41 lbm/lbf/hr. (36 000 ft/M0.66/ISA) for the ORCA101.

These values do vary with temperature variation and with different thrust requirements in cruise. Below we have a SFC vs Thrust curves (Figures 64, 65) provided by the manufacturer for the different cruise speeds of the two aircraft as well as a Thrust vs. Δ ISA curve:

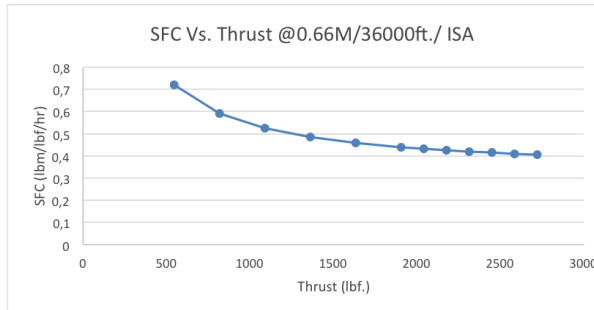


Figure 64: SFC vs Thrust @ M0.66

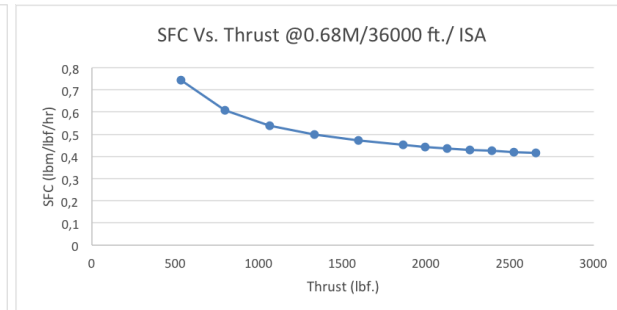


Figure 65: SFC vs Thrust @ M0.68

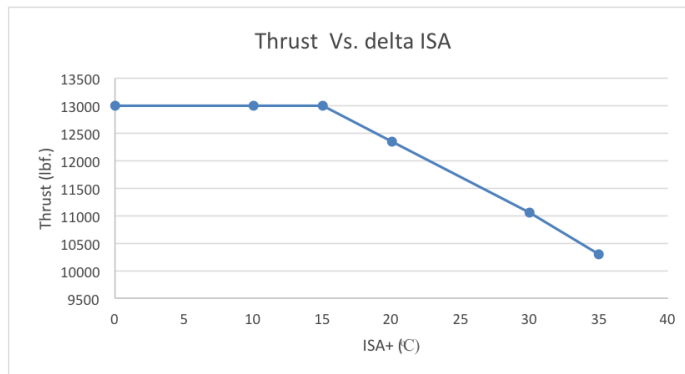


Figure 66: Thrust vs Delta in Takeoff

As seen in the previous graphs (Figures 64 and 65), the SFC is reduced while the thrust provided by the engine increases regardless of the cruise speed, which is an expected behaviour of a turbine engine. In Figure 66 the engines demonstrate a constant takeoff thrust until a temperature of 30°C at SL. after which a constant degradation of the available thrust is observed.

8.4 Thrust Reversers

For the concept of thrust reversers, it was chosen to not integrate such complex mechanisms on an engine concept that is in the process of reaching maturity. Thrust reversers may be considered in



the future of the aircraft development if there is a need to land or takeoff in shorter distances.

8.5 Electrical Generators

The electrical generators have been sized to provide 90 kVA. The configuration is two generators per engine to provide sufficient electric power for the climb, the aircraft's most demanding phase. The engines supplied do include a bleed off-take taken into account within its fuel consumption figures, but since the aircraft doesn't require bleed air, the assumption is that the removal of the bleed air will compensate for the added consumption of energy from the larger generators installed on the engine.



9 Aerodynamics

9.1 Airfoil

The airfoil selection was based on the design cruise lift, the value of which is around an average of 0.5. An optimal airfoil for this design lift should have its bucket drag concentrated at $C_l = 0.5$ to minimize the drag. In addition, the desired C_l of 0.5 should be obtained for an angle of attack close to 0 to allow the aircraft to fly at cruise condition with minimal angle of attack to minimize drag and also provide a comfortable flight for the passengers.

From these considerations, many airfoils with characteristics complying to the desired performance were identified and plotted in Figures 67-69 to analyzed the bucket drag (Figure 69) and C_{l_α} (Figure 68) (Data in Figures 67-69 are from reference [8] and at $Reynolds = 1E6$).

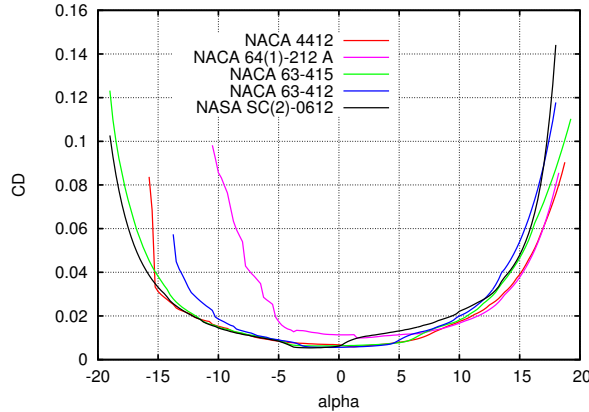


Figure 67: Airfoil Analysis - C_d vs α [8]

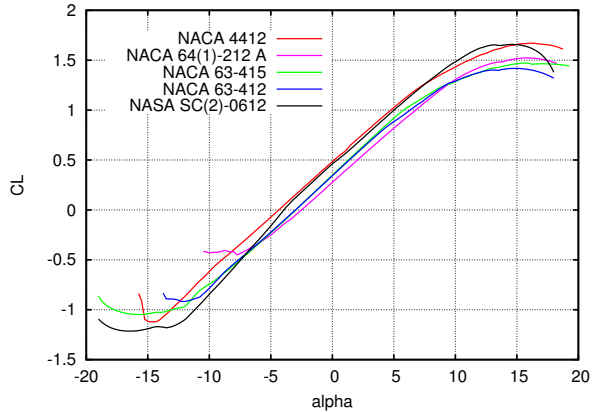


Figure 68: Airfoil Analysis - C_l vs α [8]

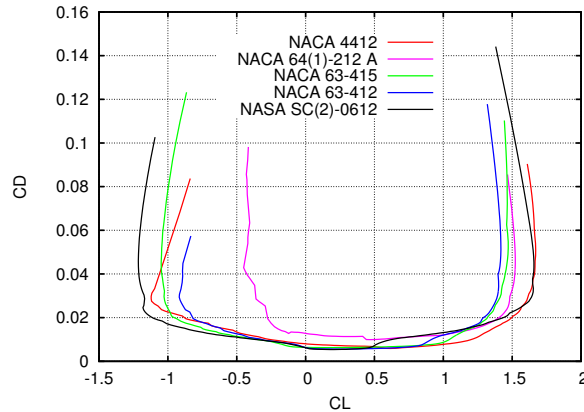


Figure 69: Airfoil Analysis - C_d vs C_l [8]



From the results of Figures 67-69, the best airfoil is clearly the supercritical SC(2)-0612. The bucket drag is not exactly at a $C_l = 0.5$, but it's very close and it's the airfoil with the best C_{l_α} and $C_{l_{max}}$. Supercritical airfoils are not only interesting for their performance in the transonic regime but also for high-lift considerations which is of great value here considering the limited takeoff length allowed. For those reasons, airfoil SC(2)-0612 was chosen and Table 23 presents its geometry and aerodynamics characteristics.

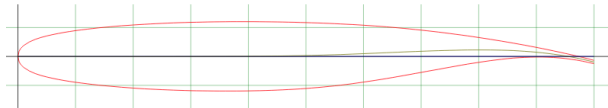


Figure 70: Airfoil SC(2)-0612

With a 12% thickness, the supercritical airfoil SC(2)-0612 poses no problem of integration for the fuel volume required to complete the 1200 nm and 1800 nm missions. Finally, the airfoil chosen for the vertical and horizontal stabilizer is a classic four digit NACA-0010. It's a symmetrical airfoil with 10% thickness to reduce the friction drag while allowing enough volume for the surface actuators.

These are the basis and the foundation from which the wing aerodynamic performance is calculated.

9.2 Wing Characteristics

9.2.1 Clean Wing

The wing surface area was established from an optimization based on the fuel weight, as showed in Section 4.2.3, while complying with the MR& O for takeoff and landing distances. Tables 24 & 25 present the wing's geometry and aerodynamic characteristics.

The wing aspect ratio of 9.5 was based on a competitor wing comparison presented in Table 26. The wing aspect ratio reduces the induced drag, but it also adds structural problem and as a

Airfoil Characteristics	
$C_{l_{max}}$	1.6
α_0	-4
Cm_0	-0.1118
Thickness	12%
Conditions	
Solver	Xfoil
Re	1E06
Source	Airfoil Tools[8]

Table 23: Airfoil Characteristics



consequence weight. A safe value of 9.5 was chosen to be realistic with competitors' aspect ratio trending.

A low taper ratio (typically under 0.5) allows a lower induced drag by having a geometry closer to an elliptical wing which confers the lowest induced drag possible. A low taper ratio also reduces the weight of the wing. Therefore, the lowest taper ratio is desired. Considering the integration of the various wing components, the lowest taper ratio possible is 0.190. Typical values for transport aircraft are around 0.240 (Table 26), but the 0.190 value is calculated from the Apex Wing chord. So, the actual wing taper ratio should be around 0.240 which is in the competitors ballpark.

Finally, the leading edge sweep was set to 15° . The ORCA family has a design cruise Mach number of 0.68 and 0.66 for the ORCA77 and ORCA101 respectively. These cruise speeds do not require a sweep angle, because there's no wave drag since the airflow is not transonic over the wing. Nevertheless, open rotor aircraft could achieve transonic speeds and as a preliminary design, the sweep was set to 15° to account for the eventual possibility of a higher cruise speed without adding considerable weight and affecting the takeoff/landing performance. Further analysis with more precise tools should be done in the next step of the design in order to validate this choice. The current tools could not provide an optimal value and a competition analysis did not provide data seeing as there are no aircraft currently flying with open rotor engines.

Wing Geometry	
Wing Area (m²)	92.90
Span (m)	29.71
MAC (m)	3.6
Aspect Ratio	9.5
Taper Ratio	0.190
Average (t/c)%	12
LE Sweep(°)	15

Table 24: Wing Geometry

Wing Aerodynamic's Characteristics	
α_0	-3.4
α_{\max}	13.13
CL_{\max}	1.4
CL_α	4.85

Table 25: Wing Aerodynamic's Characteristics at Mach=0.66



Competitors Wing Comparison								
	Airbus		Boeing			Polytechnique		
Type	A319	A320	727	737	737	737	ORCA	ORCA
Model	100	200	200Adv	300	400	600	77	101
Wing Area(m ²)	122.40	122.40	157.90	91.04	91.04	124.60	92.90	92.90
Span(m)	33.91	33.91	32.92	28.90	28.90	34.30	29.71	29.71
MAC(m)	4.29	4.29	5.46	3.73	3.73	4.17	3.6	3.6
Aspect Ratio	9.39	9.39	6.86	9.17	9.17	9.44	9.5	9.5
Taper Ratio	0.340	0.240	0.309	0.240	0.240	0.278	0.190	0.190
Average (t/c)%	–	–	11.00	12.89	12.89	–	12	12
Flap Span/Wing Span	0.780	0.780	0.740	0.720	0.720	0.599	0.7	0.7
C _{Lmax} (Takeoff)	2.58	2.56	1.90	2.47	2.49	–	2.6	2.6
C _{Lmax} (Landing)	2.97	3.00	2.51	3.28	3.32	–	2.9	2.9

Table 26: Competitors Wing Comparison[62]

9.2.2 High Lift Devices

The aerodynamic calculation of the wing is based entirely on the equations provided by Roskam [53]. Consequently, no optimization with a certain precision was possible to assess the high-lift devices' geometry. Therefore, the geometry was sized from competitors data from Table 26 and articles detailing high-lift design [62][22][51][18][26].

The leading edge device is essential to achieve a higher $C_{L_{max}}$ which dictates the takeoff and landing speed. From Table 27, the majority of civil transport aircraft uses a 3 position slats. As shown by Figure 71, a 3-position slat allows optimal and separate configurations for takeoff and landing which yields a lower C_D .

Boeing		Douglas			Airbus	
B707-320	2 position slats	DC8		Slots	A300	3 position slats
B727	2 position slats	DC9-10		None	A310	3 position slats
B737	3 positions slats	DC9-20/30/40/50	2 positions slats		A320	3 position slats
B747	Kruger	DC10		3 position slats	A321	3 position slats
B757	3 position slats	MD80/90		3 position slats	A330	3 position slats
B767	3 position slats	MD11		2 position slats	A340	3 position slats
B777	3 position slats					

Table 27: Slat Competitor Comparison[62]



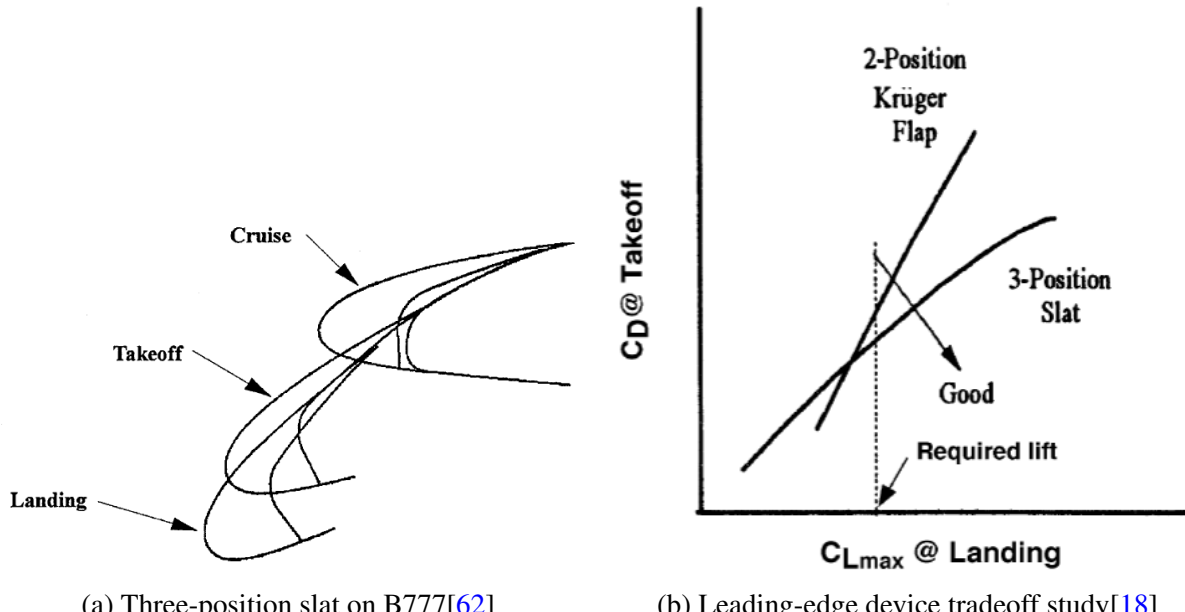
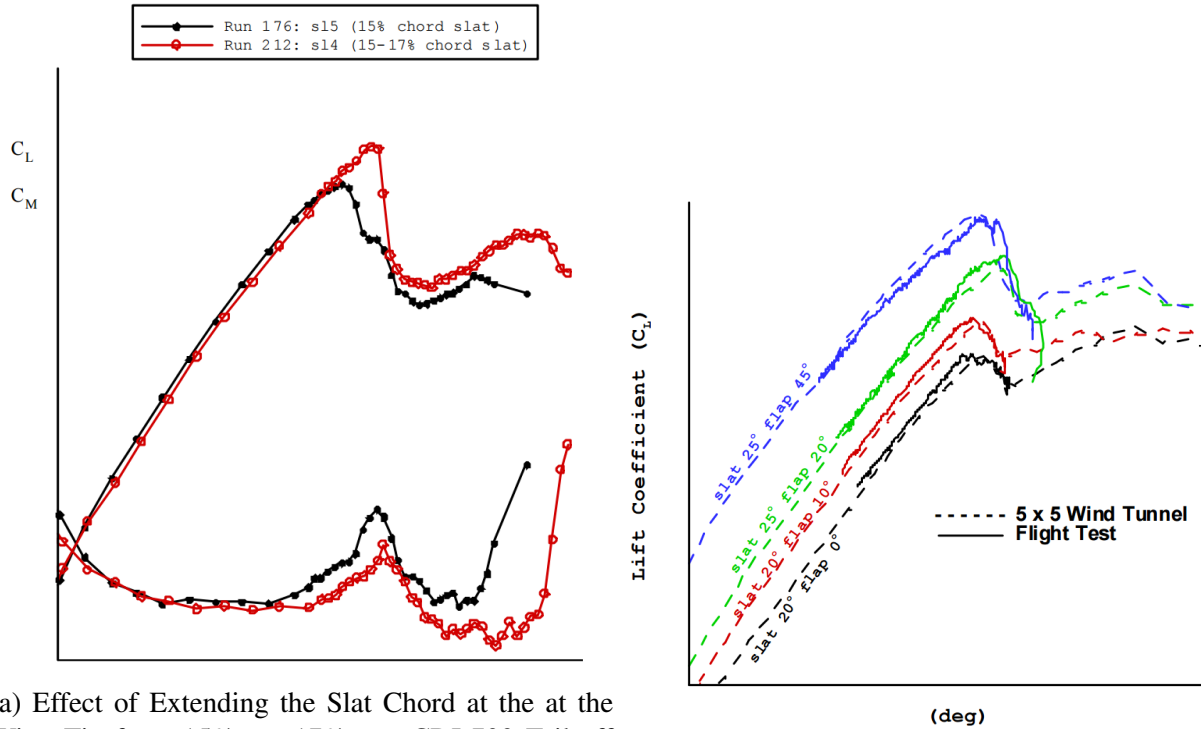


Figure 71: Leading Edge Device

The leading edge device will therefore be a 3-position slat. Subsequently, the deflection and chord of the slats were based on the high-lift design of the Bombardier CRJ-700 presented in the ICAS congress paper [26]. After CFD and wind tunnel testing, the optimal slat deflection was found to be 25 degrees landing slats and 20 to 22 degrees takeoff. Figure 72 shows the effect of flap/slat deflection and slat chord on the lift. On account of those results for the CRJ-700, the slat deflection will be the same for the ORCA aircraft family, 20 degrees and 25 degrees for takeoff and landing respectively. For flap deflection, 20 degrees and 45 degrees is taken for takeoff and landing respectively, which are the same for the CRJ-700.

Moreover, since no appropriate tool is available to analyze the chord size of flap and slat, these will be the same as the CRJ-700, 24% chord and 15% chord for flap and slat respectively until further analysis is accomplished in a subsequent design phase.



(a) Effect of Extending the Slat Chord at the Wing Tip from 15% c to 17% c on CRJ-700 Tail-off Configuration; Mach 0.20 Rec=6.5 Million, Flaps 45 degrees, Slats 25 degrees

(b) Comparison of trimmed lift curves from the IAR 5-ft wind tunnel test with flight test data

Figure 72: Bombardier CRJ-700 High-Lift design (ICAS Congress[26])

Table 28 and Figure 73 present a competitor comparison on flap devices and a flap gap analysis on the lift coefficient of a two-element airfoil.

Most commercial aircraft from Table 28 use double or triple slotted flaps. Triple slotted devices are more complex and heavier than double slotted flaps. Consequently, double slotted flaps were chosen since the BFL & LFL requirement are met as it will be discuss in Section 10. Thus, there's no need for triple slotted flaps.

Finally, the flap gap was based on wind tunnel test presented in Figure 73. From the wind tunnel test results, the optimal gap is between 1.5% and 2% of the wing chord.



Boeing		Douglas		Airbus	
B707	Fixed vane/main double	DC8	Fixed vane/main double	A300	Main/aft double
B727	Triple slotted	DC9	Fixed vane/main double	A300-600	Single slotted
B737 Classic	Triple slotted	DC10	Articulated vane/main double	A310	Articulated vane/main double inbd, single slotted outbd
B737 NG	Main/aft double	MD80/90	Fixed vane/main double	A320	Single slotted
B747	Triple slotted	MD11	Articulated vane/main double	A321	Main/aft double
B757	Main/aft double			A340	Single slotted
B777	Main/aft double inbd, single slotted outbd				

Table 28: Trailing-edge High-lift Devices on Several Civil Transport Airplanes[51]

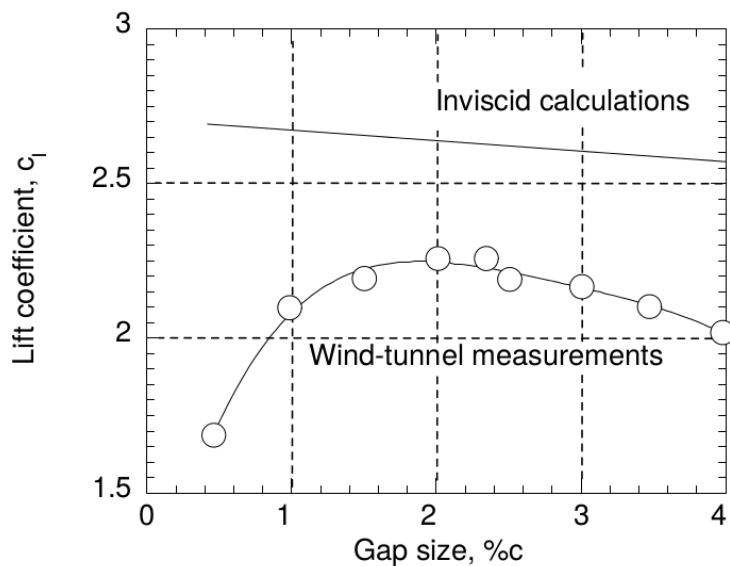
Figure 73: Effect of Flap Gap on Lift Coefficient of a Two-element Airfoil at $\alpha = 0^\circ$, $Re = 3.7\text{million}$, $M_\infty = 0.2$ [22]

Table 29 summarizes the high-lift geometry for the ORCA family based on the previous analyses of competitors and high-lift design articles according to the geometrical definitions provided by Figure 74.

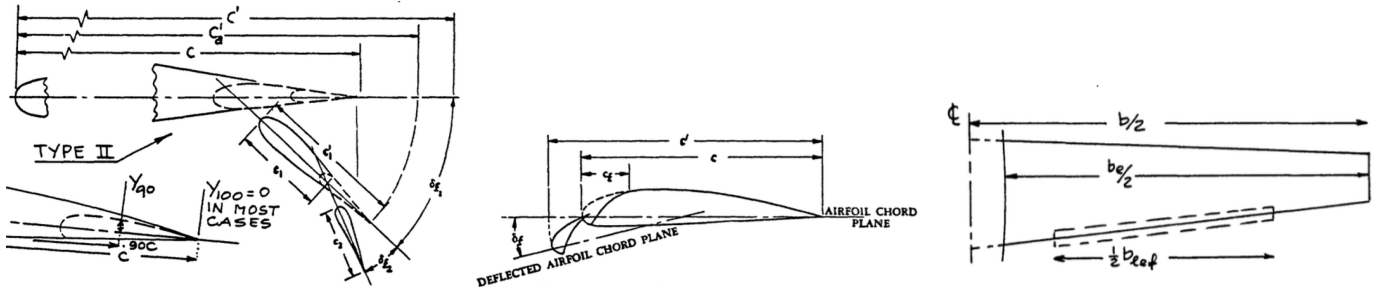


Figure 74: High-Lift Geometry Definitions

	Takeoff		Landing	
	Slat	Flap	Slat	Flap
δ_f	20°	20°	25°	45°
c'/c	1.1	1.15	1.4	1.45
c_f/c	0.15	0.24	0.15	0.24
b_f/b	0.9	0.7	0.9	0.7
ΔC_L	—	0.66	—	0.99
$\Delta C_{L_{max}}$	0.6569	0.59	0.66	0.84
$C_{L_{max}}$	2.6		2.9	

Table 29: High Lift Devices Characteristics

9.3 Drag Breakdown

This section presents the total drag breakdown and the profile drag breakdown for both aircraft at takeoff, cruise and landing conditions. The drag is calculated according to the Roskam [53] methodology and the flow is assumed to be fully turbulent except on the horizontal and vertical stabilizer where 10% laminar flow is assumed.

9.3.1 Takeoff

Table 30 and 31 present the total drag breakdown and the profile drag breakdown respectively in drag counts at takeoff conditions. The takeoff speed is taken as $1.13V_s$, where V_s is the stall speed calculated with $C_{L_{max}} = 2.6$.

Figure 75 and 76 presents the contribution of each drag component and induced drag is the most important with 80% of the total drag.

	ORCA77	ORCA101
CD_o	303	311
CD_i	1718	1718
CD_{int}	56	56
CD_{trim}	13	12
CD_{excre}	26	27
CD_{wave}	0	0
CD_{tot}	2116	2125
Conditions		
L/D	9.8	9.8
C_L	2.08	2.08
Speed (kts)	103.7	107.1
Altitude (ft)	0	0
Trim δ_f	-1.9°	-1.6°

Table 30: Total Drag Breakdown - Takeoff

	ORCA77	ORCA101
Wing	69	69
Nacelle	11	11
Pylon	4	4
Vtail	9	9
Htail	12	12
Fuselage	67	76
Flap	79	79
Slat	52	52
$CD_{o_{tot}}$	303	311

Table 31: Profile Drag Breakdown - Takeoff



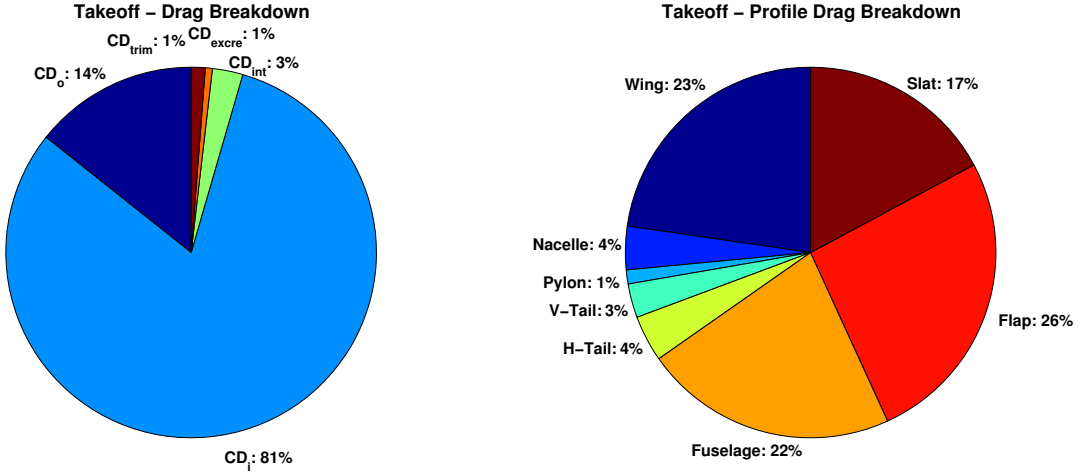


Figure 75: Drag Breakdown - Takeoff ORCA77

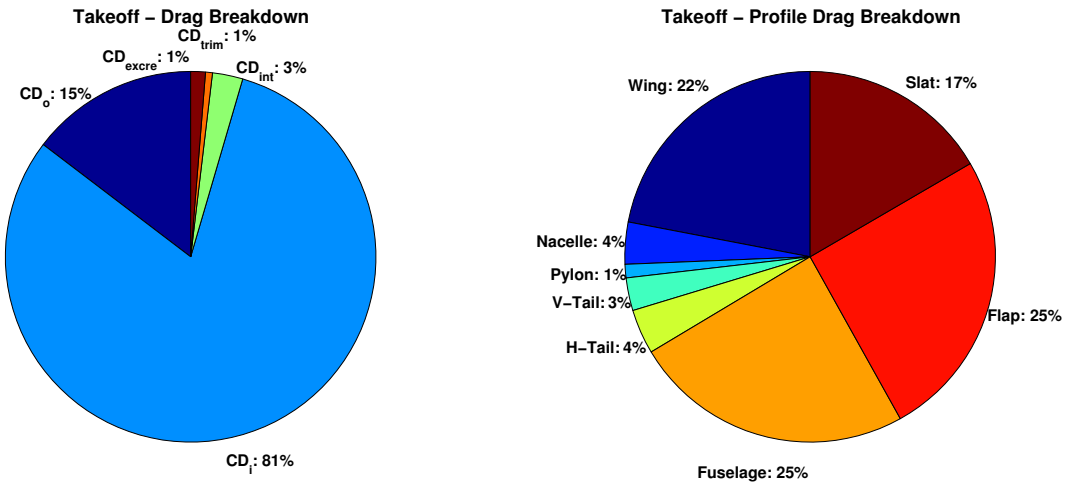


Figure 76: Drag Breakdown - Takeoff ORCA101

9.3.2 Cruise

Table 32 and 33 presents the drag breakdown of both aircraft at cruise conditions. ORCA77 and ORCA101 are cruising at the same altitude of 36 000 ft, but at different Mach numbers, 0.68 and 0.66 respectively for the 77 passengers and 101 passengers. This is the reason why ORCA77 has a total drag count of 288 and ORCA101 has 325 total drag count. The major difference is due to induced drag. Since the ORCA101 is heavier and its cruise Mach number is lower, a higher lift coefficient is required to maintain a level flight. Thus, more induced drag is created.



Figure 77 and 78 shows that induced drag account for about 30% of the total drag, as profile drag represents about 55% of the total drag. Since the cruise Mach number is not transonic, no wave drag is experienced.

	ORCA77	ORCA101
CD_o	158	168
CD_i	81	108
CD_{int}	12	12
CD_{trim}	13	13
CD_{excre}	24	25
CD_{wave}	0	0
CD_{tot}	288	325
Conditions		
L/D	15.9	16.2
C_L	0.46	0.53
Mach	0.68	0.66
Altitude (ft)	36000	36000
Trim δ_f	-1.1°	-0.9°

Table 32: Total Drag Breakdown - Cruise

	ORCA77	ORCA101
Wing	63	63
Nacelle	11	11
Pylon	3	3
Vtail	8	8
Htail	11	11
Fuselage	62	71
$CD_{o_{tot}}$	158	168

Table 33: Profile Drag Breakdown - Cruise

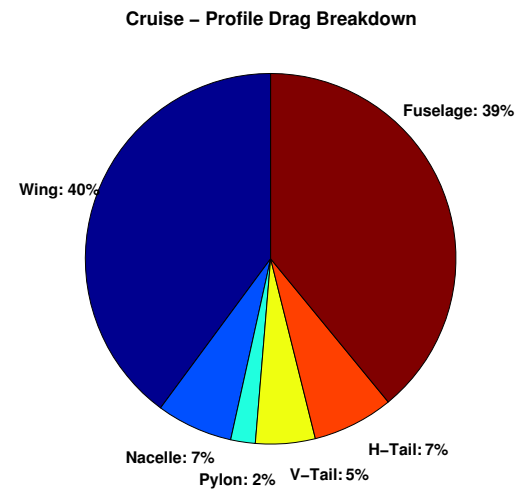
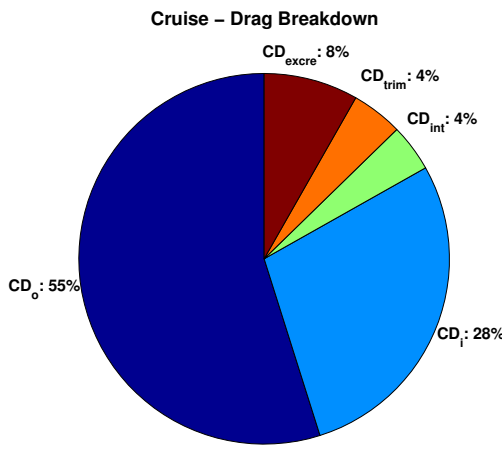


Figure 77: Drag Breakdown - Cruise ORCA77



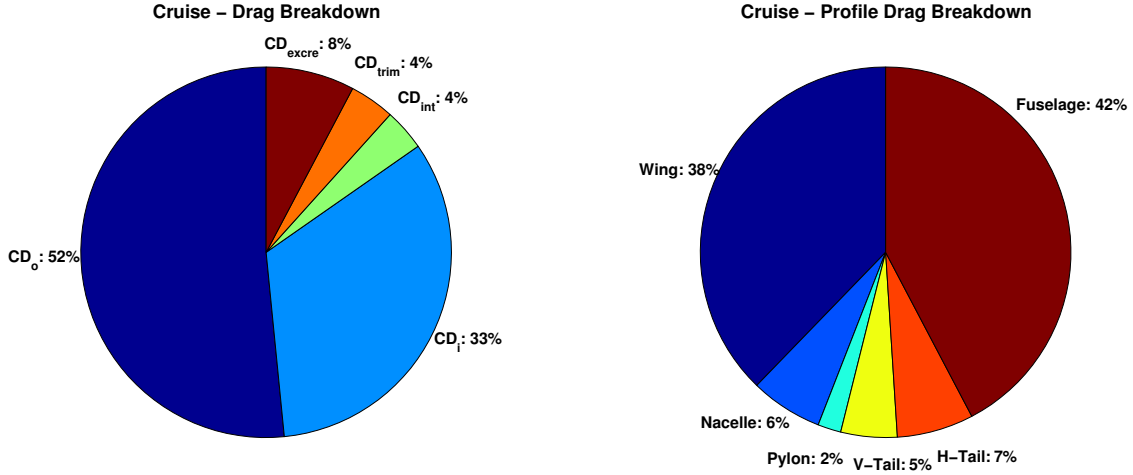


Figure 78: Drag Breakdown - Cruise ORCA101

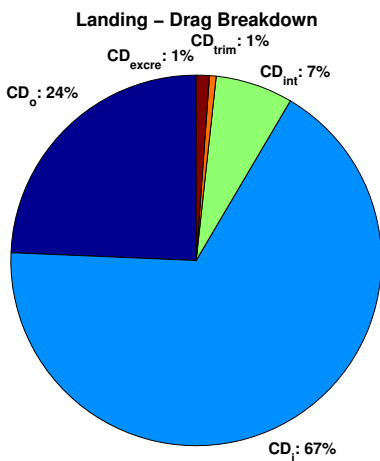
9.3.3 Landing

Landing speed is taken as $1.23V_s$, where V_s is the stall speed calculated with $C_{L_{max}} = 2.9$. As it can be seen in Table 34 and 35, profile drag is much more important in landing conditions than takeoff conditions, because in the former situation the high-lift system is fully deployed with 25° deflection for slat and 45° deflection for flap. Figure 79 and 80 shows that the double-slotted flaps are responsible for almost 60% of the total profile drag. Therefore, both aircraft have a low lift-to-drag ratio of around 8.5, which is realistic.



	ORCA77	ORCA101
CD_o	552	559
CD_i	1523	1523
CD_{int}	153	153
CD_{trim}	12	12
CD_{excre}	26	27
CD_{wave}	0	0
CD_{tot}	2266	2275
Conditions		
L/D	8.5	8.4
C_L	1.92	1.92
Speed (kts)	100.1	105.4
Altitude (ft)	0	0
Trim δ_f	-2.2°	-1.9°

Table 34: Total Drag Breakdown - Landing



	ORCA77	ORCA101
Wing	69	69
Nacelle	12	11
Pylon	4	4
Vtail	9	9
Htail	12	12
Fuselage	67	76
Flap	312	312
Slat	67	66
$CD_{o_{tot}}$	552	559

Table 35: Profile Drag Breakdown - Landing

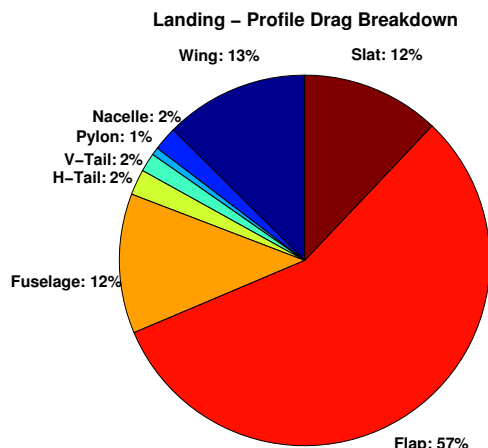


Figure 79: Drag Breakdown - Landing ORCA77



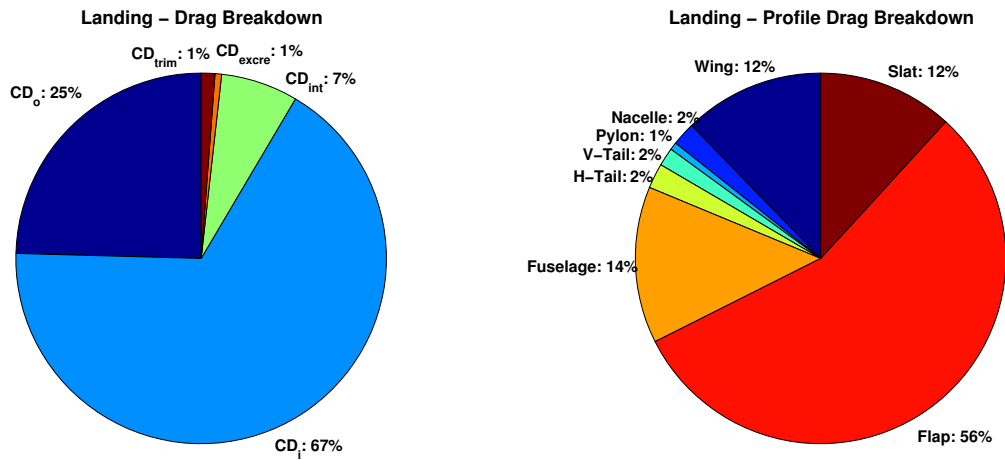


Figure 80: Drag Breakdown - Landing ORCA101



10 Performance

Aircraft performance calculations are accomplished using iterative techniques written in MaTLab code. The method used to simulate aircraft performance is outlined in AER4855: Aircraft Performance class from Polytechnique de Montréal. Several requirements and constraints were given by the MR&O. The evaluation of the aircraft performance will be described in the following manner: takeoff along with the BFL vs. TOW chart, landing, climb and cruise. Then, results of the calculations will be summarized with a mission profile table and a payload-range chart. Finally, a study on the impacts of high density aircraft will be presented.

10.1 Takeoff

According to FAR-25 commercial requirements, the ORCA family must be able to takeoff within a balanced field length of 4 500 ft. / 5000 ft. (ORCA77 / ORCA101) by clearing a 35 feet obstacle and achieving a V2 speed of $1.13 V_{stall}$. Knowing that there are commercial airports at the altitude pressure of 5 000ft, the BFL calculations were calculated for two conditions: (MTOW, SL, ISA) and (MTOW, 5 000 ft., ISA=25). It is noted that both calculations assumed no wind and a dry/straight runway. Takeoff performance requirements for each aircraft variant is shown in Table 36.

	MR&O	ORCA77	ORCA101
Takeoff Thrust Per Engine	–	13 000 lbf	
BFL (MTOW,SL,ISA)	$\leq 4\ 500 \text{ ft} / 5\ 000 \text{ ft}$	4 108 ft	4 681 ft
BFL (MTOW, 5000 ft, ISA+25)	$\leq 6\ 000 \text{ ft} / 6\ 500 \text{ ft}$	5 060 ft	5 779 ft
Flap Deflections	–	20 degrees	
Slat Deflections	–	20 degrees	

Table 36: Takeoff Performance

The aircraft does not always take off at MTOW because of the fuel weight and payload weight variations. Therefore, a BFL vs. TOW chart (Figure 81, 82) is useful to predict take off distance based on actual takeoff weight.



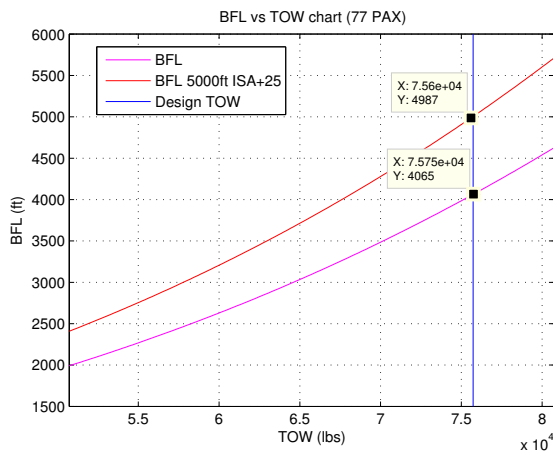


Figure 81: BFL vs TOW - ORCA77

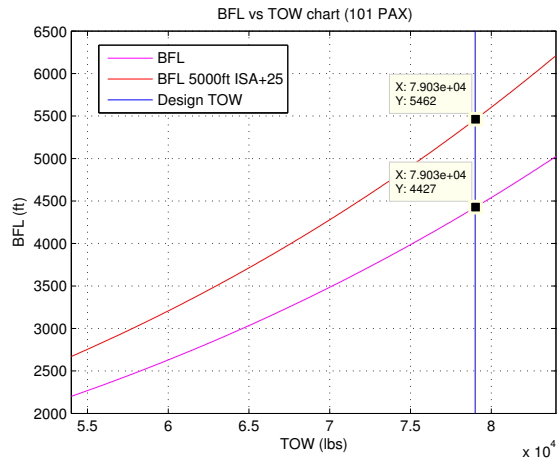


Figure 82: BFL vs TOW - ORCA101

10.2 Landing

According to FAR Part 25 commercial requirements, both ORCA variants must be able to land within a landing field length of 4 500 ft while clearing a 50 foot obstacle and achieving a approach of speed (V_{REF}) of $1.23V_{stall}$. The total landing field length is broken down into three distinct segments: approach, roll and braking. It is noted that the landing is evaluated at (MLW, SL, ISA) on a wet runway. Therefore, the rolling friction coefficient with brakes applied was selected to be 0.4 for a wet concrete surface. Landing performance requirements for each aircraft variant are given in Table 37.

	MR&O	ORCA77	ORCA101
LFL (MTOW,SL,ISA)	$\leq 4\ 500 \text{ ft}$	4 203 ft	4 441 ft
LFL Approach Speed	$\leq 120 \text{ KCAS}$	100 KCAS	105 KCAS
Flap Deflections	—	45°	
Slat Deflections	—	—	25°

Table 37: Landing Performance

10.3 Climb

According to FAR 25, commercial airplanes must not exceed indicated speeds of 250 knots during the first 10 000 ft climb. However, based on the climb speed optimization results as described in design process, the ORCA variants will not be able to reach climb speeds higher than 210



KCAS. Table 38 shows the initial cruise altitude for the all-engine-operating condition as well as the maximum OEI altitude for the one-engine-inoperative condition.

	MR&O	ORCA77	ORCA101
Initial Cruise Altitude	$\geq 25\ 000 \text{ ft}$	36 000 ft	36 000 ft
Specific Excess Power (MTOW, ICA, } M_{cruise})	$\geq 300 \text{ fpm}$	454 fpm	329 fpm
Maximum OEI Altitude (95% MTOW, ISA)	$\geq 300 \text{ fpm} @ 17\ 000 \text{ ft}$	20 000 ft	17 000 ft

Table 38: Climb Performance

10.4 Cruise

The contributing factors in defining the cruise speed, presented in Table 39, were described in the cruise altitude-mach optimization in the Design Process Section. In fact, the results were highly sensitive to the value of the assumed cost index (CI). As a future improvement, it is recommended to identify a precise method of evaluating the CI.

	MR&O	ORCA77	ORCA101
Cruise Speed	$\geq M0.60$	M0.68	M0.66

Table 39: Cruise Mach Number

10.5 Mission Profile

The aircraft mission profile is completed by the performance-weight convergence loop as described in the design process. Firstly, Table 40 illustrates the mission profile along with performance details pertaining to fuel burn, flight time and distance travelled.



Mission Profile		ORCA77	ORCA101
Range	Distance (nm)	1800	1200
Taxi-out	Fuel (lb)	148	148
	Time (min)	10	10
Takeoff and Climb to 1500 ft	Fuel (lb)	150	150
	Time (min)	2	2
	Distance (nm)	-	-
Climb (1500 ft to ICA)	Fuel (lb)	1420	1637
	Time (min)	26	30
	Distance (nm)	136	153
Cruise (ICA)	Fuel (lb)	6806	4445
	Time (min)	245	155
	Distance (nm)	1593	978
Descent (ICA to 1500 ft)	Fuel (lb)	128	136
	Time (min)	21	22
	Distance (nm)	96	99
Approach and Landing	Fuel (lb)	24	24
	Time (min)	3	3
	Distance (nm)	-	-
Taxi-in	Fuel (lb)	90	90
	Time (min)	5	5
Reserve	Fuel (lb)	2097	2042
Block Fuel	Fuel (lb)	8766	6629
Block Time	Time (min)	311	227

Table 40: Mission Profile

Secondly, Table 41 illustrates the results of the reserve fuel requirements optimization where the LRC profile is optimized for maximum specific air range and where the VMD profile is optimized for minimum drag.

	ORCA77		ORCA101	
	LRC Reserve	VMD Reserve	LRC Reserve	VMD Reserve
Optimization Criteria	$SAR_{max} = 0.141 \text{ nm/lb}$	$Drag_{min} = 3044 \text{ lbf}$	$SAR_{max} = 0.134 \text{ nm/lb}$	$Drag_{min} = 2885 \text{ lbf}$
Altitude (ft)	24 000	15 000	24 000	15 000
Range (nm)	100	154	100	151
Time (min)	33	45	34	45
Mach	0.29	0.29	0.47	0.29
Fuel required (lbs)	739	1303	739	1358

Table 41: Reserve Fuel Requirements Optimization

The LRC Reserve calculations uses a MatLab fminsearch function that loops through two variables: initial cruise altitude and cruise Mach in order to maximize SAR (minimize 1/SAR). The



VMD reserve also uses an fminsearch that loops through cruise speed in order to minimize the calculated drag.

10.6 Payload Range

The aircraft payload and range are limited by three possible aircraft loadings: Max Payload Limit, MTOW Limit and Max Fuel Limit. First, in order to generate the horizontal line, the Max Payload Limit defines the fuel loading until design MTOW. Then, the first diagonal defines the trade-off between the decrease of payload and the increase of fuel until wing fuel tank is completely filled. Lastly, with a complete wing fuel tank, payload is removed until it reaches zero. Figures 83 & 84 illustrates the payload-range charts for both aircraft variants.

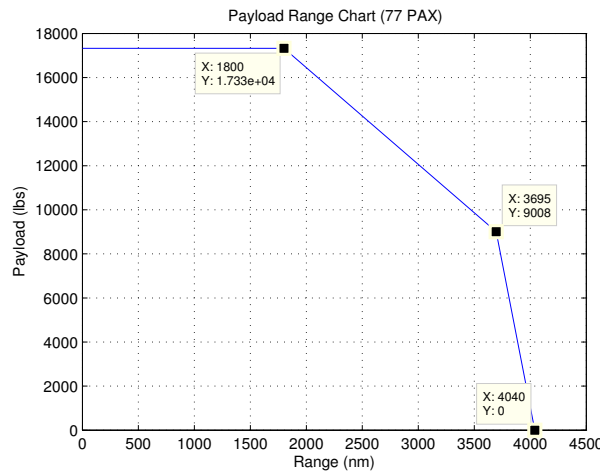


Figure 83: Payload Range - ORCA77

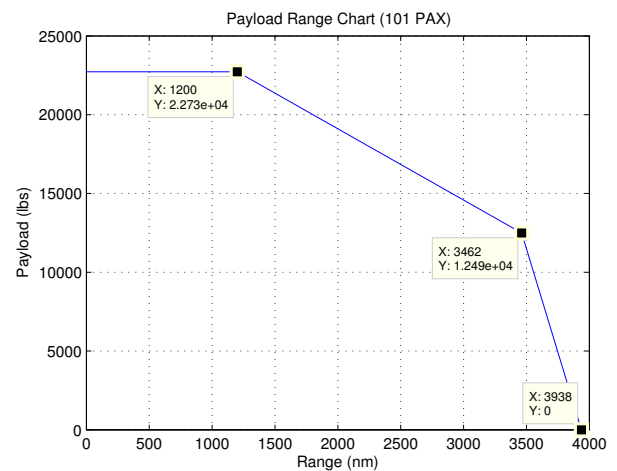


Figure 84: Payload Range - ORCA101

10.7 High Density Configuration

Table 42 and Table 43 shows the effect of applying high density configuration in both aircraft variants. It can be seen that the MR&O is respected for the ORCA77 HD. However, for the ORCA101 HD, many requirements are not attained such as the Specific Excess Power, the maximum OEI altitude and the LFL.



	ORCA77	ORCA77 HD	Variation
BFL (MTOW,SL,ISA)	4 108 ft	4 306 ft	+ 198 ft (+4.8%)
BFL (MTOW, 5000 ft, ISA+25)	5 060 ft	5 309 ft	+249 ft (+4.9%)
LFL (MLW, SL, ISA, Wet Runway)	-4 203 ft	4 287 ft	+84 ft (+2.1%)
LFL Approach Speed	100 KCAS	101 KCAS	+1 KCAS (+0.9%)
Specific Excess Power (MTOW, ICA, M_{cruise})	454 fpm	408 fpm	-46 fpm (-10.1%)
Maximum OEI Altitude (95% MTOW, ISA)	20 000 ft	19 000 ft	- 1 000 ft (- 5.0%)
Block Fuel	8766 lbs	8 910 lbs	+144 lbs (+1.6%)
Block Time	311 mins	313 mins	+2 mins (+0.6%)

Table 42: High Density Impact on Performance - ORCA77

	ORCA101	ORCA101 HD	Variation
BFL (MTOW,SL,ISA)	4 681 ft	4 915 ft	+ 234 ft (+5%)
BFL (MTOW, 5000 ft, ISA+25)	5 779 ft	6 070 ft	+291 ft (+5%)
LFL (MLW, SL, ISA, Wet Runway)	4 441 ft	4 601 ft	+160 ft (+4%)
LFL Approach Speed	105 KCAS	111 KCAS	+6 KCAS (+5%)
Specific Excess Power (MTOW, ICA, M_{cruise})	329 fpm	154 fpm	-175 fpm (-53%)
Maximum OEI Altitude (95% MTOW, ISA)	17 000 ft	8 000 ft	- 9 000 ft (-53%)
Block Fuel	6 629 lbs	7 009	+380 lbs (+6%)
Block Time	227 mins	227 mins	+0 mins (+0%)

Table 43: High Density Impact on Performance - ORCA101



11 Weights and CG Envelope

In an aircraft preliminary design, weight estimation and CG evaluation is a critical step. This section will consist of the weight breakdown for both aircraft followed by their corresponding CG envelopes and details about the wing positions and plug sizes. The section will be concluded by a brief evaluation of the impacts on the weights and balance of the ORCA77 and ORCA101 in the case of a high density configuration.

11.1 Weight Breakdown

At first, the weights of the different components of an aircraft must be evaluated using empirical equations. Many authors define their own equations in order to achieve that, and two were compared in order to make an informed choice. Table 44 presents estimation of weights for ORCA101 from Kroo's and Raymer's equations.

ORCA101	Raymer	Kroo	Technology factor
Wing	5 000 lb	6 050 lb	0.85
H-tail	575 lb	1 525 lb	0.83
V-tail	625 lb	475 lb	0.83
Fuselage	5 075 lb	10 000 lb	0.90
Landing Gears	2 750 lb	3 050 lb	0.95
Fuel System	125 lb	—	
Flight Controls	1 200 lb	1 125 lb	
APU	525 lb	1 700 lb	
Avionics & Instruments	2 450 lb	1 700 lb	
Hydraulic System	275 lb	650 lb	
Electric System	1 675 lb	3 150 lb	
De-ice & ECS	225 lb	3 650 lb	
Outfitting	6 075 lb	6 075 lb	
Propulsion System	11 275 lb	11 275 lb	
Operational Weights	3 500 lb	3 500 lb	
OWE	41 400 lb	53 900 lb	

Table 44: Author Comparison for Weights Estimation

By inspection of both these breakdowns, the necessity for a compromise had to be made based on benchmarks. A brief competitor analysis guides the team in this evaluation, and is presented in Table 45.



	N_{PAX}	Range	OWE	MZFW	MLW
MRJ70 LR	78	1 820 nm	47 800 lb	N/A	79 807 lb
SSJ 100-75 STD	68-88	1 566 nm	51 809 lb	71 900 lb	77 000 lb
BAe 146-100	70	1 000 nm	51 368 lb	68 500 lb	77 500 lb
CRJ700	66-78	1 092 nm	44 245 lb	62 300 lb	67 000 lb
MRJ90 ER	92	1 290 nm	49 800 lb	N/A	83 776 lb
SSJ 100-95 STD	86-108	1 590 nm	55 300 lb	82 200 lb	85 800 lb
BAe 146-300	100	1 000 nm	54 675 lb	80 500 lb	84 500 lb
CRJ1000	93-104	971 nm	51 120 lb	77 500 lb	81 500 lb

Table 45: Competitor Weight Analysis

Based on the evaluation of these aircrafts and a further look in both authors' equations, it seemed more accurate to use Kroo's estimations for the structure (wing, tail, fuselage and landing gears) and Raymer's for the remaining systems. Moreover, the technology factors that were applied are suggested by Raymer, and are realistic with the intense use of advanced composite throughout the structure.

While empirical equations are realistic approximations for conventionally designed aircrafts, new estimations were needed to account for the weights of the innovative components of the ORCA family. Bearing that in mind, precise more-electric aircraft benchmarks had to be found to account for the APU, hydraulic, electric environment control, flight control and de-ice systems. A scaling from these benchmarks permitted to adjust systems weights to the current configuration, allowing for realistic estimation. The resulting breakdown is shown in Table 46.



	ORCA77	ORCA101
Wing	6 050 lb	6 050 lb
H-Tail	1 525 lb	1 525 lb
V-Tail	475 lb	475 lb
Fuselage	8 750 lb	10 000 lb
Landing Gears	3 050 lb	3 050 lb
Fuel Systems	125 lb	125 lb
Flight Controls	1 225 lb	1 225 lb
APU	300 lb	300 lb
Avionics & Instruments	1 600 lb	1 600 lb
Hydraulic System	300 lb	300 lb
Electric System	3 500 lb	3 500 lb
De-Ice	100 lb	100 lb
ECS	300 lb	300 lb
Outfitting	5 450 lb	6 075 lb
Propulsion System	11 275 lb	11 275 lb
Operational Weights	3 200 lb	3 500 lb
OWE	47 300 lb	49 400 lb

Table 46: Weight breakdown for ORCA77 and ORCA101

We can see that the only weights that differ from one aircraft to the other are the fuselage and outfitting weights, which reflects the high commonality between the two. The remaining weights have been estimated to be the same, even though ORCA 77 might have slightly lower values than its counterpart due to reduced distances between the modules. The conservative estimates used ensure that the real weights may be lighter, but not much heavier than the current calculation. An overview of the design weights is presented in Table 47.

	ORCA77	ORCA101
MWE	44 100 lb	45 900 lb
OWE	47 300 lb	49 400 lb
MZFW	64 600 lb	72 100 lb
MLW	69 100 lb	76 600 lb
MTOW	75 500 lb	80 600 lb
MRW	76 000 lb	81 100 lb
$W_{maxpayload}$	17 300 lb	22 700 lb
$W_{maxfuel}$	19 200 lb	19 200 lb

Table 47: Design Weights Summary

Since the aircraft is designed to be optimal at conditions defined in the MR&O, the $W_{maxpayload}$ is set to be equal to the standard 2-class configuration instead of the high density configuration. The MZFW is then defined as the sum of OWE and $W_{maxpayload}$. Moreover, referring to Table 45,



the difference between the MZFW and the MLW was found to be between 3 600 lb and 9 000 lb; a value of 4 500 lb was selected by the team to allow landing with acceptable fuel weight in the tank.

The structure weight breakdown is presented for both aircrafts in Figure 85. The only difference in commonality between both is in the fuselage weight, with the ORCA 101 having a slightly higher weight percentage dedicated to this component.

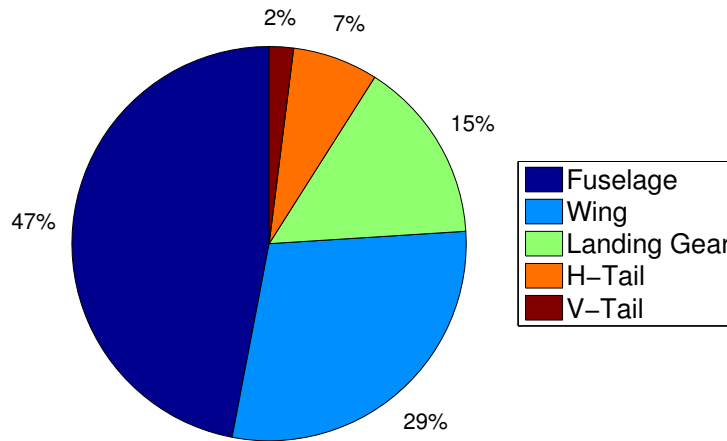


Figure 85: Structure Weight Breakdown

The systems weight breakdown for both aircraft is equal in percentages, and reflects the design strategy of going more electric: the electric system accounts for a third of the systems weight, with the hydraulic system far behind at 3%. The breakdown is presented in Figure 86.

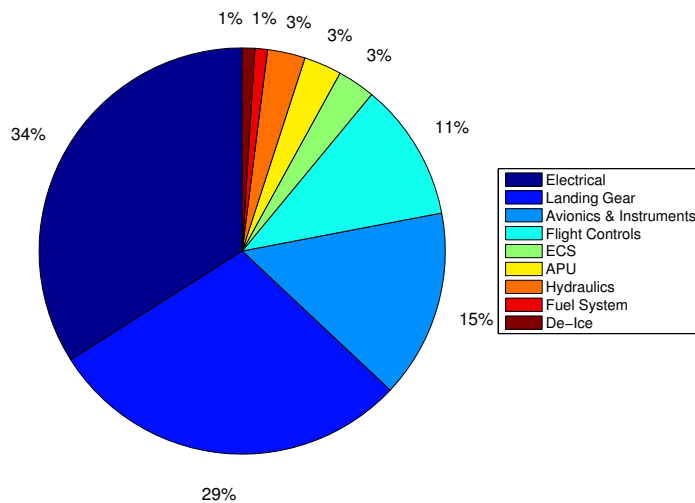


Figure 86: Systems Weight Breakdown

Finally, structure and systems weights add up with furnishing and operational weights to OWE. The breakdown is presented in Figure 87.

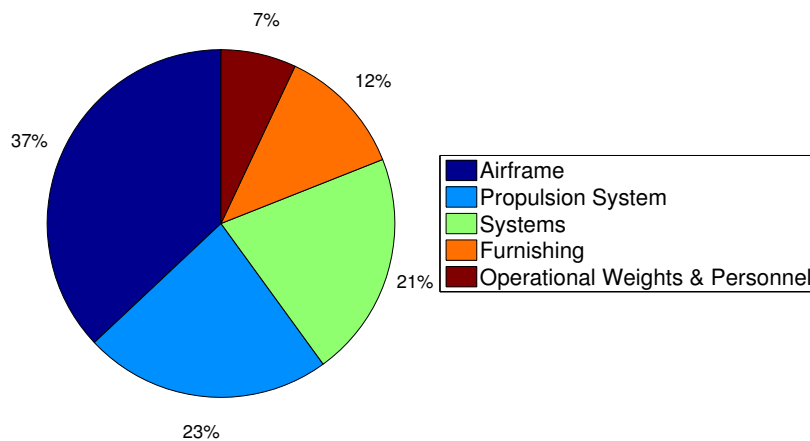


Figure 87: Operating Weight Empty Breakdown



11.2 CG Envelope

In order to evaluate the CG envelope, the weight associated with each component is located in the aircraft as a single point. This exercise greatly impacts balance of the aircraft. Aside certain details pertaining to system locations, Kroo's estimations have been used to place the weights. The positions of the different weights are detailed in Table 48 and Figure 88 according to ORCA101.

Wing	30% MAC (E)	APU	Actual Position (I)
H-Tail	30% Chord @ 35% Span (J)	Avionics & Instruments	40% Nose Length (A)
V-Tail	30% @ 35% Span (H)	Hydraulic System	75% @ (E) and 25% @ (J)
Fuselage	45% Fuselage Length (C)	Electric System	75% @ (D) and 25% @ (G)
Landing Gears	Actual Positions (B & F)	De-Ice	50% Fuselage Length (D)
Fuel Systems	30% MAC (E)	ECS	50% Fuselage Length (D)
Flight Controls	40% MAC	Propulsion System	Center of engine (G)
Outfitting	From Layout	Operational Weights	From Layout

Table 48: CG Location for Individual Components

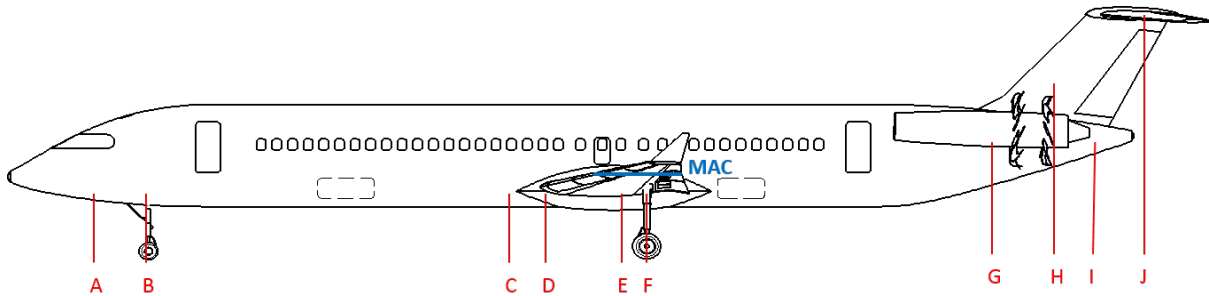


Figure 88: CG Location for Individual Components

The CG envelope analysis ensures a stable flight pattern and a sufficient control on the ground. Limits used here for forward and aft possible CG locations will be detailed in Section ???. The main limiting criteria are avoiding tip-over while on the ground, and maintaining a 5% static margin in flight. The CG envelopes for the ORCA 77 and ORCA 101 are presented in Figure 89 and Figure 90.

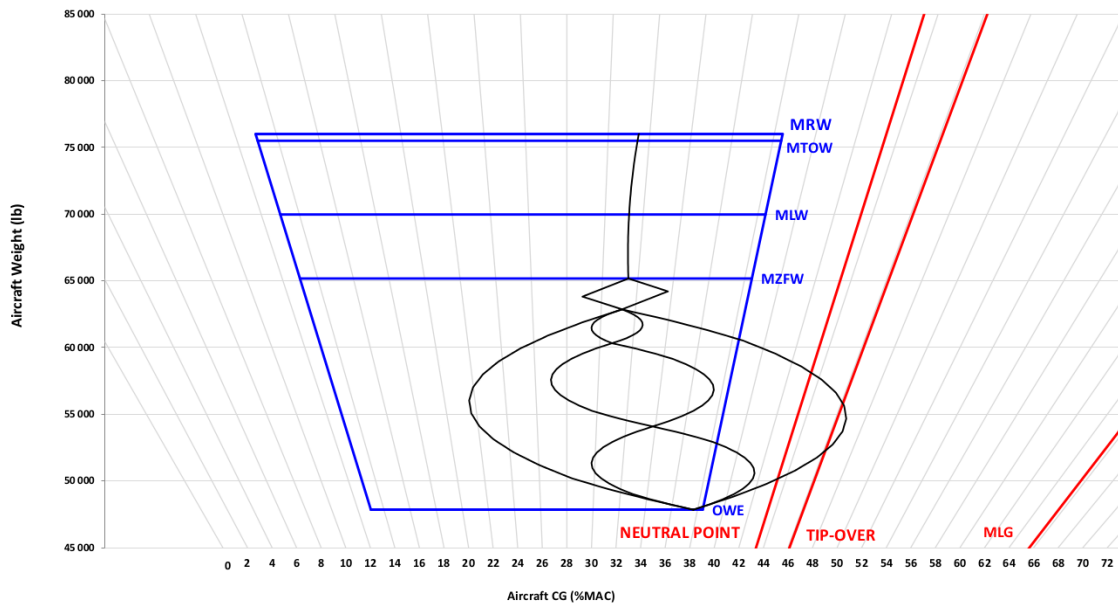


Figure 89: CG Envelope - ORCA 77

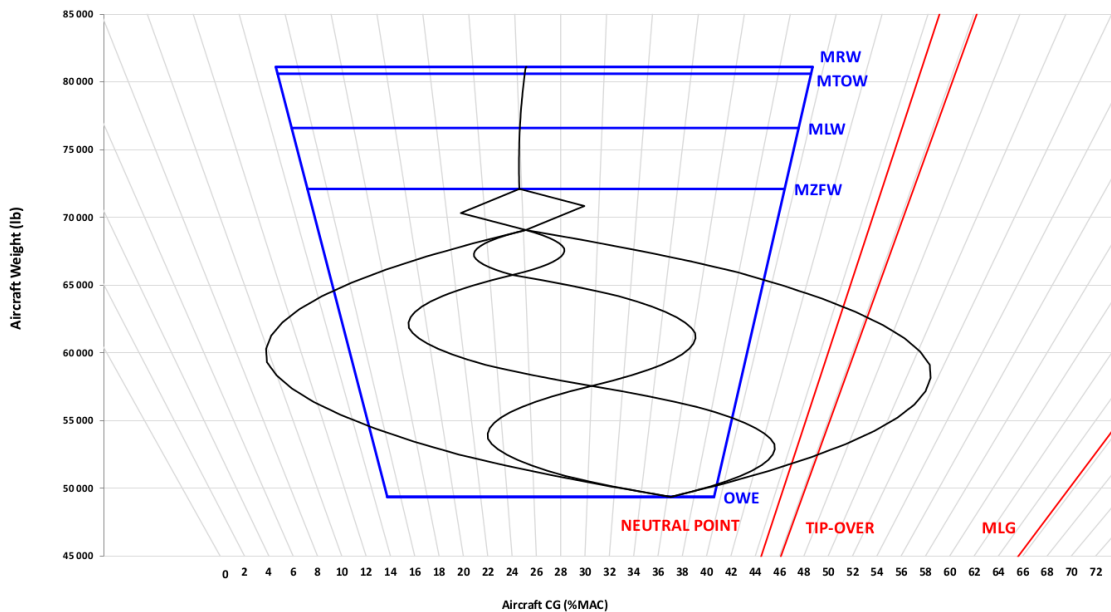


Figure 90: CG Envelope - ORCA 101

As can be seen in these figures, the current configuration limits certain loading patterns: it does not allow the loading of all passengers neither from the front back nor the opposite, due to the tip-over and nose gear collapse limitations. This also brings the necessity, in a partially loaded aircraft, to carefully consider the placement of passengers. Although it introduces a few complications, the current envelope allows for minimized in-flight trim drag with all load configurations.



11.3 Wing Position & Plugs

With the fuselage being made as four full-length pieces without regularly spaced frames, the length of each plug would not influence the manufacturing costs in a significative manner. The wing positions of the ORCA77 and ORCA101 combined with the added fuselage lengths fore and aft of the wing were then set to have 5% static margin at the most critical flight configuration, which in this case is $OWE + W_{maxfuel}$. As previously shown in Section 5.2.1, the added lengths are depicted in Figure 24.

11.4 High Density Configuration

Most aircraft are sold to accommodate a high density configuration, and fly below MTOW when more comfort is offered by the airliner in a lower-density configuration. However, in the present case, MTOW was not considered to accommodate high density configuration. When increasing seat pitch to 29 in economy class through the whole aircraft, 85 passengers can be fit in ORCA 77 and 120 in ORCA 101. A payload value of 175 lb/pax was required to account for all added passengers above regular configuration. In addition, most components individual weight would evolve to allow MTOW to increase and to accommodate the increased number of passengers. For example, by replacing Business Class seats with Economy Class, 35 lb/seat were saved to put elsewhere, but the Landing Gears weight increased by approximately 175 lb. An overview of High Density configuration impacts on the weights is presented in Tables 49 and 50.

	ORCA77	ORCA77HD	Variation
MWE	44 100 lb	44 400 lb	+300 lb (+1%)
OWE	47 300 lb	47 600 lb	+300 lb (+1%)
MZFW	64 600 lb	66 300 lb	+1 700 lb (+3%)
MLW	69 100 lb	70 800 lb	+1 700 lb (+2%)
MTOW	75 500 lb	77 400 lb	+1 900 lb (+3%)
MRW	76 000 lb	77 900 lb	+1 900 lb (+3%)
$W_{maxpayload}$	17 300 lb	18 700 lb	+1 400 lb (+8%)

Table 49: High Density configuration weight impact for ORCA77



	ORCA101	ORCA101HD	Variation
MWE	45 900 lb	46 500 lb	+600 lb (+1%)
OWE	49 400 lb	50 000 lb	+600 lb (+1%)
MZFW	72 100 lb	76 000 lb	+3 900 lb (+5%)
MLW	76 600 lb	80 500 lb	+3 900 lb (+5%)
MTOW	80 600 lb	84 900 lb	+4 300 lb (+5%)
MRW	81 100 lb	85 400 lb	+4 300 lb (+5%)
$W_{maxpayload}$	22 700 lb	26 100 lb	+3 300 lb (+15%)

Table 50: High Density configuration weight impact for ORCA101



12 Stability & Control

The goal of the stability and control study is to ensure static longitudinal and directional stability. In order to accomplish this, an initial sizing of the tail was completed based on volume coefficients. S&C derivatives, tail sizing verification through x-plots, neutral point location, aft and forward CG location were determined using Roskam's [53] and Raymer's [52] methodologies. Lastly, the control surfaces were sized based on historical data.

12.1 Initial Tail Sizing

ORCA was designed with a T-Tail empennage to provide propeller clearance. Initially, the tail was sized based on historical data provided by Raymer. Table 51 shows the historical data and the value chosen for the aircraft. The ORCA configuration is compared with two fuse-mounted engines and T-Tail aircraft namely the Tu-134 and DC-9-30. The data for the comparison was available from Morichon's "Selected Statistics in Aircraft Design" project [7].

Max Seats	ORCA	Tu-134	B717-200
	101	84	110
Horizontal Stabilizer			
Area (ft²)	170	330.2	260.5
Span (ft)	27.5	38.7	35.4
Aspect Ratio	4.4	4.54	4.82
Taper Ratio	0.4	0.396	0.380
Quarter Chord Sweep (°)	29.8	35	30
Vertical Stabilizer			
Area (ft²)	152	228.7	209.9
Height (ft)	12.1	17.2	14.27
Aspect Ratio	0.9	1.30	0.97
Taper Ratio	0.5	0.560	0.780
Quarter Shord Sweep (°)	47.8	40	45

Table 51: Tail Comparison

A quick comparison of the ORCA tail sizing shows that the stabilizers are significantly smaller than both reference aircrafts. An X-plot analysis will be required to identify the required adjustments.



12.2 Stability Coefficients

Empirical stability and control equations were used to determine S&C derivatives. Given the neutral point and CG locations, the stability derivatives can be calculated. Table 52 summarizes the evaluation of the stability coefficients.

	ORCA 77	ORCA 101
Xcg (% MAC)	30	23
Neutral Point (% MAC)	43.4	44.6
Cm _{alpha}	-0.67	-0.58
Cn _{beta}	0.23	0.26
Cl _{beta}	-0.23	-0.26

Table 52: Stability Derivatives

Even though both variants share the same stabilizers, their coefficients are different since they have different tail arm lengths. Due to the difficulty in evaluating the static lateral stability, this coefficient was assumed to be equal to the negative of the static directional stability.

For an Xcg of 25-30% MAC, the typical range of values for CM_{α} is (-1.6,-0.6). Table 52 confirms that both variants respect the requirements. Further analysis will be required to validate the breakdown of the CM_{α} calculations.

Furthermore, for an Xcg of 25-30% MAC, the typical range of values for Cn_{β} is (0.15, 0.25). The results also confirm that both ORCA variants meet the positive directional stability requirement.

12.3 Longitudinal Stability - AFT/FWD CG Limit

In terms of S&C, CG position limits are determined by several factors. First for stability, a static margin of 5% must be observed at all time to ensure static stability. Second, in terms of control, the main criterion is to be able to trim the aircraft for all possible CG travel. Using fixed values of +/- 6 degrees for the horizontal stabilizer, the limits at which trim is possible are plotted in Figures 91 and 92.



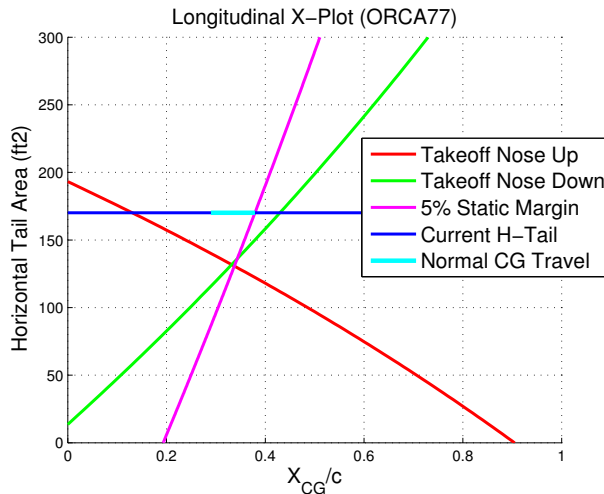


Figure 91: X-plot Longitudinal Stability - ORCA 77

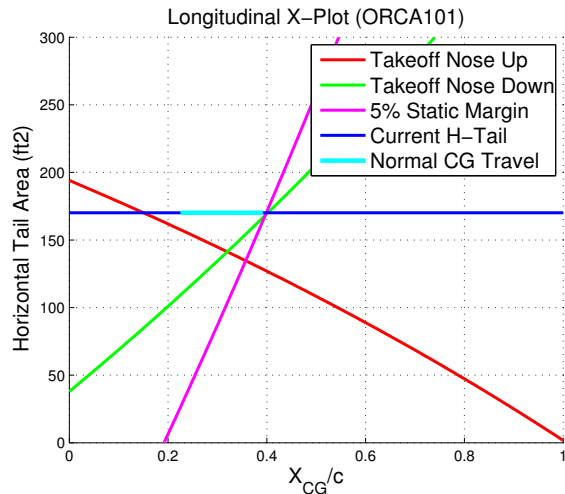


Figure 92: X-plot Longitudinal Stability - ORCA 101

In the above figures, it can be observed that with longer moment arm, ORCA101 is more stable (Neutral Point more aft) and less maneuverable (more limited with same H-Tail deflection). The cyan line represents normal CG travel between OWE and MTOW, as shown in Figures 89 and 90. Fore and aft limits for maximum in-flight CG travel are then 13.2% and 38.4% of MAC for ORCA77, and 15% and 39.6% of MAC for ORCA101.

12.4 Directional Stability

Figure 93 & 94 illustrates the evaluation of the $C_{n\beta}$ criteria for different V_{tail} areas. The evaluated C_{nb} falls within the lower and upper limit requirement. Consequently, the current V_{tail} area provides a good initial sizing value for the design of the ORCA.



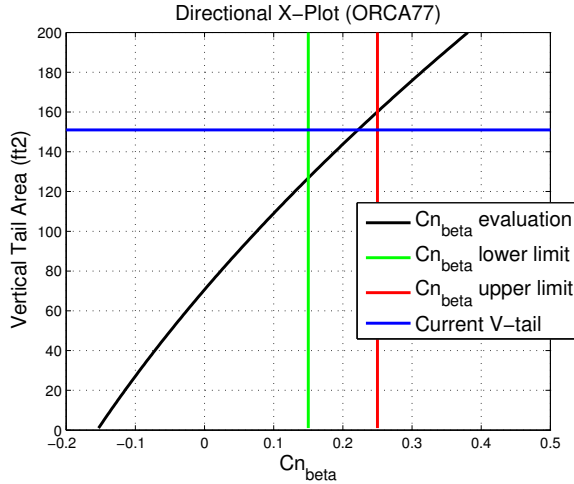


Figure 93: X-plot Directional Stability - ORCA 77

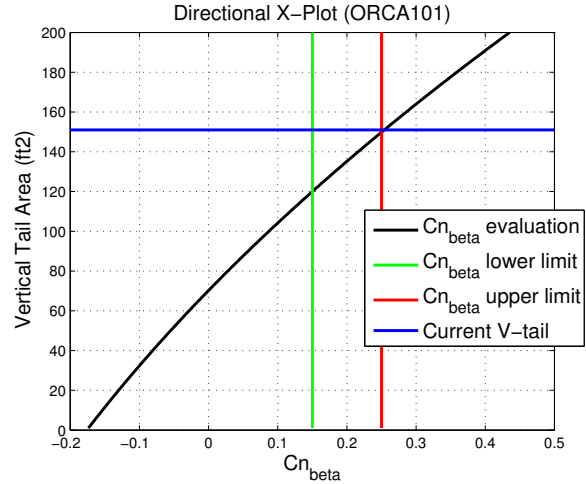


Figure 94: X-plot Directional Stability - ORCA 101

12.5 Control Surfaces

Table 53 illustrates the dimensions of the control surfaces. The ORCA configuration is compared with two T-Tail fuse-mounted engine aircrafts namely Tu-154 and DC-9-50. Data is available from Roskam Jet Transport data.

		ORCA	Tu-154	DC-9-50
Max Seats		101	180	139
Elevator	% chord	30	26	44
	% hstab span	90	-	-
Rudder	% chord	20	37	44
	% vstab span	95	-	-
Aileron	% chord	15	22	17
	% wing span	75 to 98	76 to 98	78 to 95

Table 53: Control Surfaces Dimensions

Initial sizing and disposition of the control surfaces are validated with existing aircrafts. However, more analyses will be required in this section, such as:

- Rudder deflection during engine out :

Under FAR 25.149, the yawing moment coefficient required to maintain a steady flight at a speed of $1.2V_{stall}$ with OEI. The other engine must maintain a maximum thrust and the bank angle cannot exceed 5 degrees.



- Elevator deflection during takeoff and landing:

Since takeoff and landing creates high nose down pitching moments, it is required to validate the stabilizer deflections necessary to trim the aircraft.

- Aileron roll speed :

Under MIL-F8785B, the aircraft must be able to achieve 30 degrees bank angle in 1.5 seconds in order to meet Class III (heavy transport) level 1 standard.

Figure 95 illustrates the aircraft with the control surfaces dimensioning.



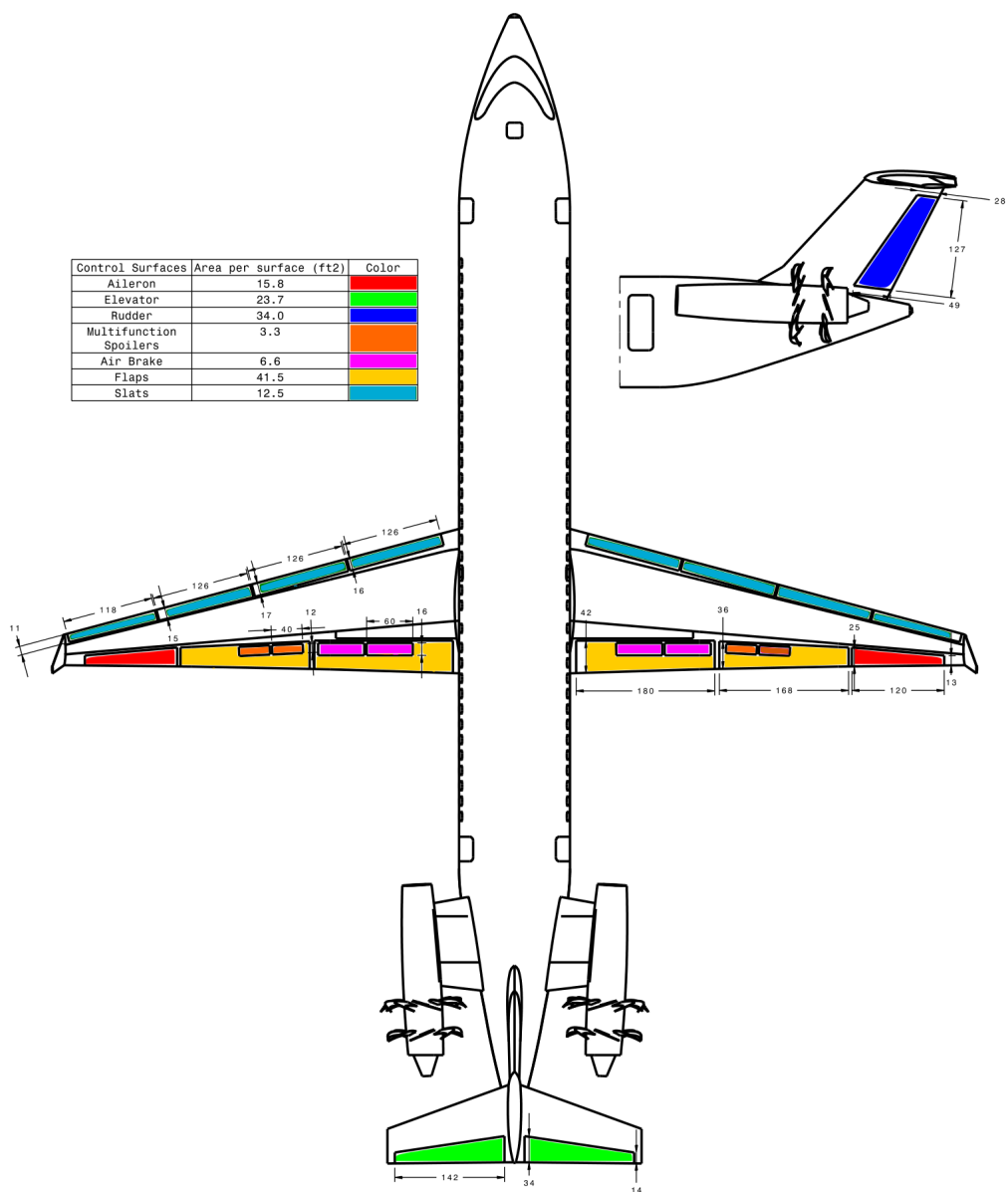


Figure 95: Control Surfaces Dimensions



13 Economics

In order to determine the profitability of a family of aircraft, it is necessary to understand the various sources that influence the aircraft cost. The following sections will explain the factors and hypotheses used to calculate the preliminary cost estimates, based upon Dr. Jan Roskam's aircraft design equations [53]. These equations were used to calculate the Cash Operating Costs as well as the Fixed and Variable Costs related to an aircraft development program, which in turn allow the evaluation of key marketing values such as the Unit Price per Aircraft. Using this information combined with the Market Analysis presented in Section 2 of this report, a break-even analysis is performed in order to determine the profitability of the aircraft program.

Following the cost evaluations, the current program's Preliminary Design Engineering Budget will be presented.

13.1 Cash Operating Cost Evaluation

Cash Operating Costs are costs incurred during the Operational phase of aircraft development which vary according to multiple factors such as aircraft performances and mission profile. Maintaining a low Cash Operating Cost is an essential selling point in the marketing of aircraft to clients. Evaluation of the Cash Operating Costs for a 500nm mission for the aircraft family in development was accomplished using certain Direct Operational Cost equations from Roskam's Airplane Design, Part VIII. In these equations, the COC calculation is subdivided into five parts: Crew Costs (C_{crew}), Fuel and Oil Costs (C_{pol}), Maintenance Costs (C_{maint}), Landing, Navigation and Registry Costs (C_{lnr}), and Depreciation Costs (C_{depr}), all in USD/nm. However, it was determined that the Depreciation Cost would be constant throughout the industry, and is therefore left out of this calculation. Each of these costs shall be explained in the following sections before presenting the COC calculation results.

$$C_{crew}$$

The Crew Costs are a function of the amount crew members onboard are paid, as well as the aircraft block speed determined by the Performance department. It was determined that for both aircraft a single captain and co-pilot each would be sufficient, and that 2 and 3 cabin crew members would be required for the 77 and 101 passenger planes respectively. The yearly salaries for each of these were set to be 100k USD, 85k USD and 37k USD per year. A crew bonus factor and travel



expense factor were both established based upon Roskam's recommendations, and factored up to current-day dollars.

C_{pol}

Fuel and Oil Costs are a function of current fuel and oil prices, as well as the fuel burned by the aircraft in a 500nm mission. The fuel price was established to be 2.55 USD/gal, based upon a price of 107 USD/barrel. The oil price was assumed to be equal to the fuel price. Based upon Roskam's recommendations, the fuel and oil densities were respectively 6 and 7.6 lbs/gal.

C_{maint}

The Maintenance Costs are subdivided into Airframe and Systems Maintenance, Engine Maintenance (both of which have costs for materials and labor), and an Applied Maintenance Burden Factor. These values are a function of various hypotheses and the block speed and time calculated for a 500nm mission. The Airframe and Systems Maintenance Cost were established using the MR&O values of 0.9 and 50 USD/h for the Maintenance Manhours per Flight Hour and Airplane Maintenance Labor Rate respectively. Furthermore, the MR&O values for Airframe and Systems Materials Cost per Flight Hour (65 USD) and Materials Cost per Flight (75 USD) were applied. The Engine Maintenance Cost calculation combines the labor and materials cost by using the MR&O values for the Engine Maintenance and Materials Cost per Flight Hour (45 USD) and Engine Maintenance and Materials Cost per Flight (130 USD). Finally, the Applied Maintenance Burden Factor was determined using 1.2 as the Labor Overhead Distribution Factor and 0.55 for the Materials Overhead Distribution Factor, as recommended by Roskam.

C_{lnr}

The Landing, Navigation and Registry Costs are primarily a function of the aircraft MTOW, as well as a Navigation Fee per Airplane per Flight Factor which was established as 10 following Roskam's recommendations.



13.2 COC Presentation

Table 54 and Figure 96, 97 below presents the calculated values for the ORCA77 and ORCA101 COC for a standard 500nm mission, followed by two graphs showing the distribution of the various COC factors:

	ORCA77	ORCA101
C_crew	1.65\$	1.94\$
C_pol	2.82\$	2.97\$
C_maint	2.29\$	2.36\$
C_lnr	0.34\$	0.36\$
COC per nm	7.11\$	7.62\$
COC per 500nm	3 552.80\$	3 810.28\$
500nm COC per PAX	46.14\$	41.23\$

Table 54: COC Breakdown

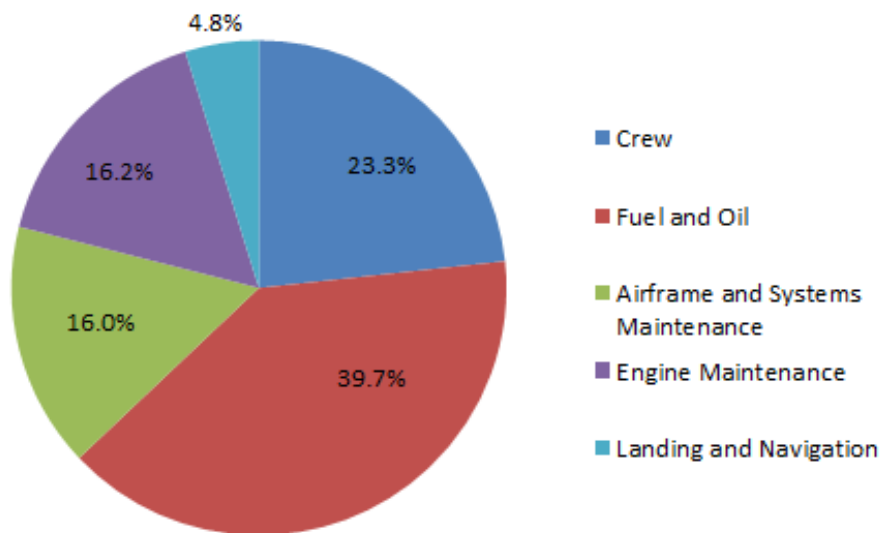


Figure 96: ORCA77 COC Distribution



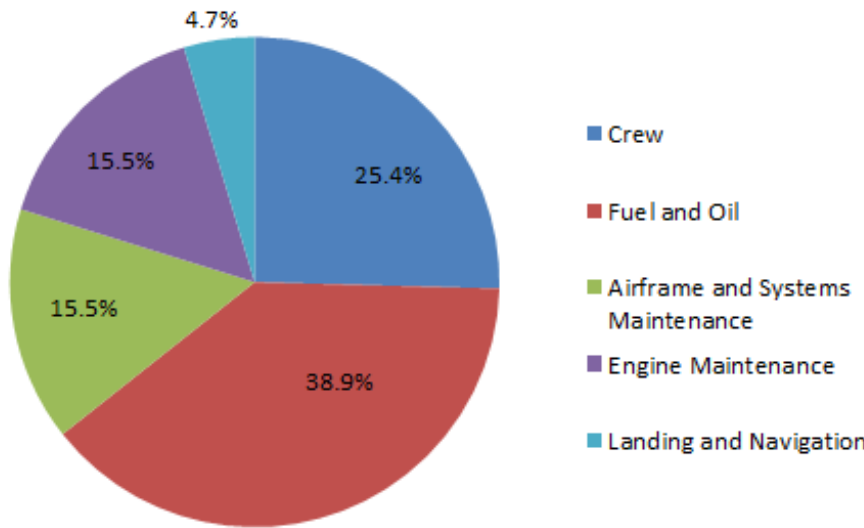


Figure 97: ORCA101 COC Distribution

13.2.1 Competitor Comparison

Once the Cash Operating Cost has been evaluated, it is important from a marketing standpoint to compare the obtained values to that of the competition – in fact the MR&O requires a 15% drop in COC as compared to the competition. The Figures 98 and 99 below show where the ORCA77 and ORCA101 compare to the competitors’ values.

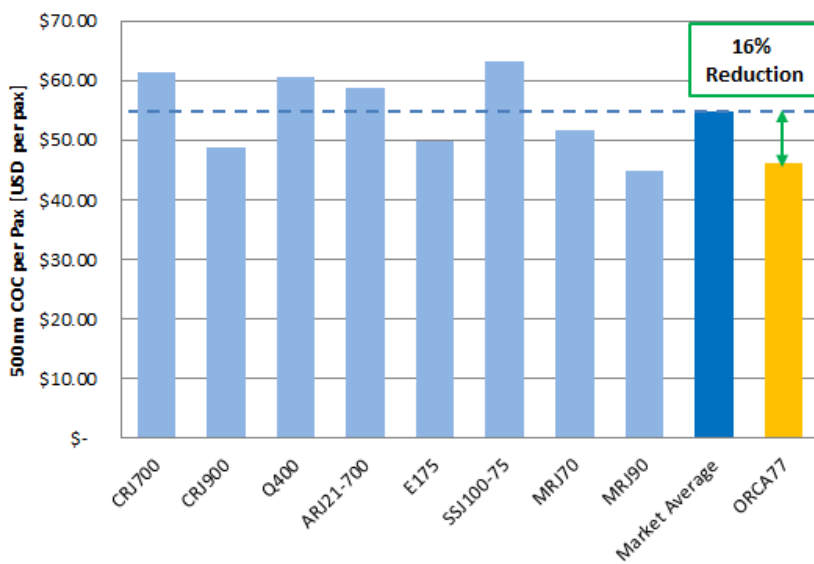


Figure 98: ORCA77 COC Competition Comparison



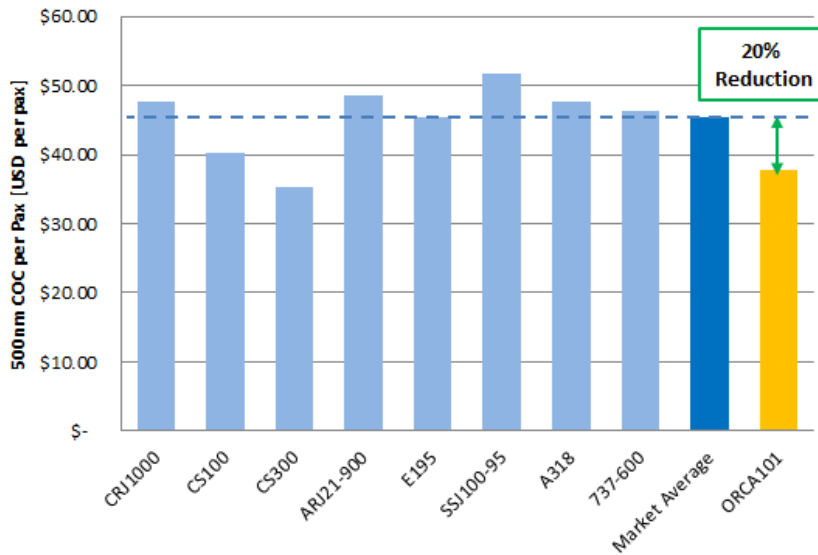


Figure 99: ORCA101 COC Competition Comparison

As can be observed, the current aircraft performances provide significant COC-saving advantages in both the 70-90 and 100-120 passenger ranges; both aircraft respect the 15% decrease required by the MR&O by having a 16% and 20% decrease for the ORCA77 and ORCA101 respectively. However, the calculated COC savings are not as significant as first expected, especially considering the large fuel savings the Open Rotor engines provide. This disparity may be due to the lower flight speed of the aircraft, which in turn increases the maintenance and crew costs in the Roskam method of COC evaluation. It is proposed that the Roskam preliminary calculation equations may require some refinement in order to determine the true cost savings of the ORCA family, but the current calculation does provide insight on the significant cost reductions that are possible with the combination of advanced technologies that come together in the ORCA family.

13.3 Fixed Costs: Research, Development, Test and Evaluation Cost

The RDTE Cost is calculated using Roskam's equations. As such, the RDTE Cost is divided into seven parts: Airframe Engineering and Design Cost (C_{aed_r}), Development Support and Testing Cost (C_{dst_r}), Flight Test Airplanes Cost (C_{fta_r}), Flight Test Operations Cost (C_{fto_r}), Test and Simulation Facilities Cost (C_{tsf_r}), RDTE Profit (C_{pro_r}) and Financing Cost (C_{fin_r}). Each of these values will be investigated in the following sections. The cost evaluation completed for both the ORCA77 and ORCA101 aircraft. In order to account for a high level of commonality between the two planes, certain factors were applied to the calculations which simplified the cost calculations; these factors, too, shall be presented in each section. However, unless otherwise indicated, the



ORCA77 and ORCA101 calculations standalone from each other.

$$C_{aed_r}$$

The Airframe Engineering and Design Cost is primarily a function of the Engineering Dollar Rate per Hour (established at 65\$/hr), and an estimate for the number of engineering man hours. This estimate is a function of the maximum cruise speed, the takeoff weight and a number of factors such as the Number of Airplanes Produced in RDTE (5 test aircraft), a Program Difficulty Factor (1.5, for moderately aggressive advanced tech) and a CAD knowledge factor (0.8, as recommended by Roskam). After comparing to market R&D costs, both the ORCA77's and ORCA101's Airframe Engineering and Design Cost were multiplied by a factor of 2.5 in order to account for the extensive use of advanced technologies for structure, systems and engines.

$$C_{dst_r}$$

The Development Support and Testing Cost is a function of the factors calculated and imposed in the C_{aed_r} calculation, multiplied by a certain Cost Escalation Factor (CEF). This factor corresponds to the ratio between the Consumer Price Index of a certain “then-year” over that of the current year. The CEF thus allows for the interpolation of “then-year” dollars to the current value. The CEF is used throughout the various cost calculations to do these value updates. Similarly to the C_{aed_r} calculation, the C_{dst_r} was first calculated for the ORCA101, then adjusted with a 35% factor for the ORCA77.

$$C_{fta_r}$$

The Flight Test Airplane Cost is the largest single contributor to the total RDTE Cost due to the production costs of these aircraft. It can be decomposed into multiple sub-categories: Avionics Cost from Vendor, Engine Cost from Vendor, Manufacturing Labor Cost, Manufacturing Materials Cost, Tooling Cost and Quality Control Cost. For lack of more exact data, the avionics cost was estimated to be 15% of the total C_{fta_r} , as suggested by Roskam. The Engine Cost was directly given by the engine supplier. The Manufacturing Labor Cost was calculated based on values previously defined in the C_{aed_r} calculation, as well as the manufacturing labor rate which was fixed to 35 USD/man hour (in accordance with Roskam's figures). Similarly, the Materials Cost Estimation was based on the same C_{aed_r} calculation values with a material type correction factor, which



was fixed at 2.5 to account for the widespread use of composite materials throughout the aircraft. In order to account for the common materials between the two, the ORCA77 was calculated to have 50% of the ORCA101's Materials Cost. The Tooling Cost Estimation was also based on values from the C_{aed_r} , with a tooling manhour calculation that involved the tooling labor rate (48 USD/manhour) and the RDTE production rate (0.33 units/month, as suggested by Roskam). This cost was estimated for the ORCA77 as being 35% of the ORCA101's Tooling Cost. Finally, the Quality Control Cost is assumed to be 13% of the Manufacturing Labor Cost.

$$C_{fto_r}$$

The Flight Test Operations Cost depends solely on the values established in the C_{aed_r} calculation, along with an Observables Factor (equal to 1), which accounts for a program secrecy requirement.

$$C_{tsf_r}$$

The Flight Test Facilities Cost was estimated to be equal to 10% for the ORCA77 and 15% for the ORCA101 in terms of percentage of their respective total RDTE costs. It is assumed that various testing facilities will be required in order to validate and certify the various advanced technologies that compose the ORCA family. The facility costs were distributed between the ORCA77 and ORCA101 approximately in proportion to their production quantities (about 30% more ORCA101's will be produced than ORCA77's).

$$C_{pro_r}$$

The Profit Cost is due to profits that may have incurred during the RDTE phase and accounts for a certain profit margin within the cost calculation. This value was assumed to be zero in order to determine the true cost of the program; a profit margin shall be considered further in this report during the Break-Even Analysis.

$$C_{fin_r}$$

The Financing Cost is based upon the theoretical interest rates for the loans required to accomplish the RDTE phase. This factor was estimated as 15% of the total RDTE Cost.



13.4 Variable Costs: Acquisition Costs

The Acquisition Costs consist of the sum of the Manufacturing Cost and the Profit Cost. These costs are considered Variable Costs since they are dependent on the number of units manufactured to production standard, whereas the RDTE Costs were not. We shall immediately establish that the Profit Cost is considered to be 0% of the Manufacturing Cost, since, as previously mentioned in the RDTE Cost Section, a profit margin shall not be considered at this stage of the analysis. The Manufacturing Cost is split very similarly to the RDTE Costs: Airframe Engineering and Design Cost (C_{aed_m}), Airplane Program Production Cost (C_{apc_m}), Production Flight Test Operations Cost (C_{fto_m}) and Financing Cost (C_{fin_m}).

$$C_{aed_m}$$

The Airframe Engineering and Design Cost for Manufacturing resembles the equivalent calculation for the RDTE phase. However, in the Manufacturing phase we impose the number of aircraft that will be manufactured to production standard for each aircraft type: 474 ORCA77's and 663 ORCA101's over the course of 20 years, as determined during the Market Share Analysis.

$$C_{apc_m}$$

The cost calculation of the aircrafts produced is split similarly to the Flight Test Aircrafts in the RDTE phase, except with the addition of a cost for interior furnishings: Avionics Cost, Engines Cost, Interior Cost, Manufacturing Labor Cost, Manufacturing Material Cost, Tooling Cost and Quality Control Cost. Each of these factors is calculated like its counterpart in the RDTE phase, except for the interior which involves an Interior Cost Factor of 1000 (a standard value for regional aircraft according to Roskam). In order to account for the similarity in manufacturing the ORCA101 and the ORCA77 due to commonality, the ORCA77 value for all these Costs was estimated to be 80% of the original calculated value, with the exception of the Tooling Cost, which was estimated at 35% of the ORCA101's.

$$C_{fto_m}$$

The Production Flight Test Calculation is primarily based upon the Operating Cost of the aircraft, which will be elaborated later in this report.



$$C_{fin_m}$$

As in the RDTE section, the Financing Cost is evaluated by a factor of the total Manufacturing Cost. In this case, the factor was supposed as 10%.

13.5 ORCA77 and ORCA101 RDTE and Acquisition Costs Overview

The RDTE costs elaborated above are presented in Table 55 and Figure 100, 101 below for both the ORCA77 and ORCA101 aircraft:

RDTE Cost Breakdown		ORCA77 - [M of USD]	ORCA101 - [M of USD]
Airframe Engineering and Design Cost		222.8	364.9
Development, Support and Testing Cost		17.0	48.6
Flight Test Airplanes	Avionics Cost	127.4	306.9
	Engine Cost	40	60
	Manufacturing Labor Cost	215.6	244.8
	Manufacturing Materials Cost	67.1	134.3
	Tooling Cost	73.9	211.0
	Quality Control Cost	28.0	31.8
	FTA Cost Total	552.0	988.8
Flight Test Operations Cost		11.9	20.0
Flight Test Facilities Cost		107.2	304.8
Financing Cost		160.8	304.8
Total RDTE Cost		1 071.7	2 031.9

Table 55: RDTE Cost Breakdown



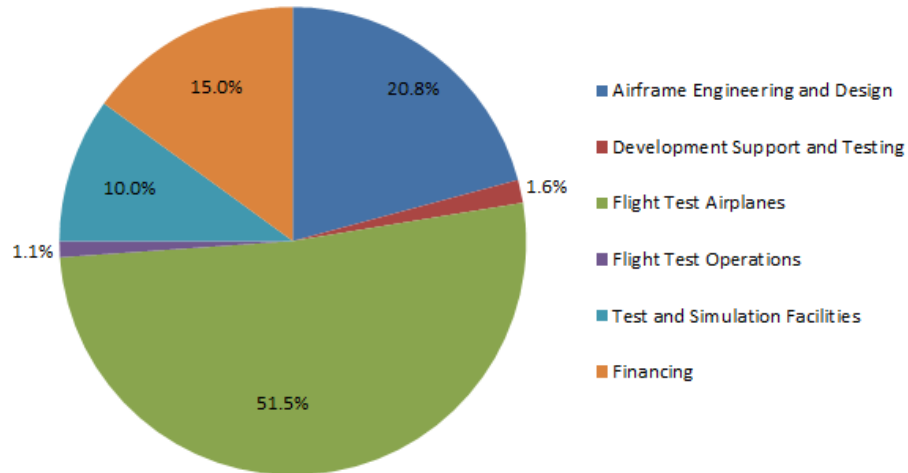


Figure 100: ORCA77 RDTE Cost Distribution

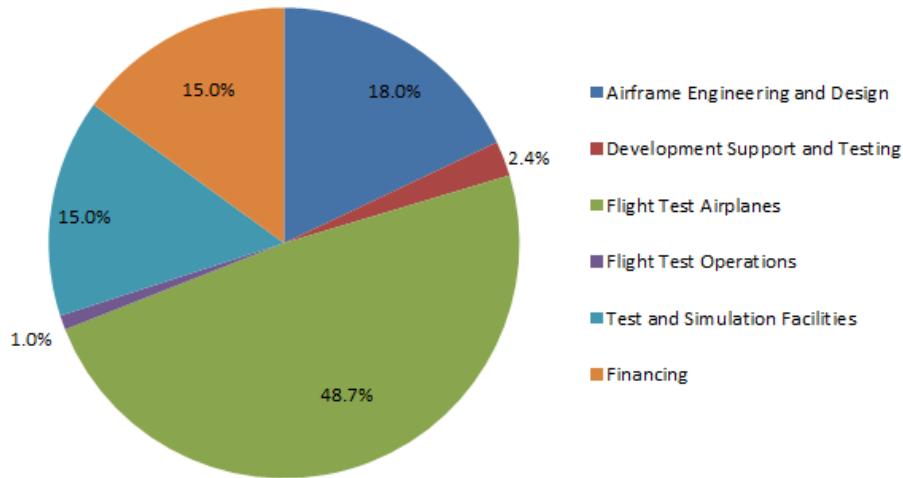


Figure 101: ORCA101 RDTE Cost Distribution

The Acquisition Costs elaborated in the previous section are presented in Table 56 and the Manufacturing Cost Breakdown in Figure 102, 103 for both the ORCA77 and ORCA101 aircraft:



Manufacturing Cost Breakdown		ORCA77 - [M of USD]	ORCA101 - [M of USD]
Airframe Engineering and Design Cost		269.1	137.8
Airplane Program Production Cost	Avionics Cost	1 104.2	2 343.8
	Engine Cost	3 792.0	6 630.0
	Interior Cost	47.7	109.3
	Manufacturing Labor Cost	971.4	1 468.7
	Manufacturing Materials Cost	1 938.4	3 173.4
	Tooling Cost	51.3	146.7
	Quality Control Cost	101.0	190.9
	Airplane Program Cost Total	8 006.1	14 062.8
Production Flight Test Operations Cost		14.2	33.2
Financing Cost		828.9	1 423.4
Total Manufacturing Cost		9 118.3	15 657.2

Table 56: Manufacturing Cost Breakdown

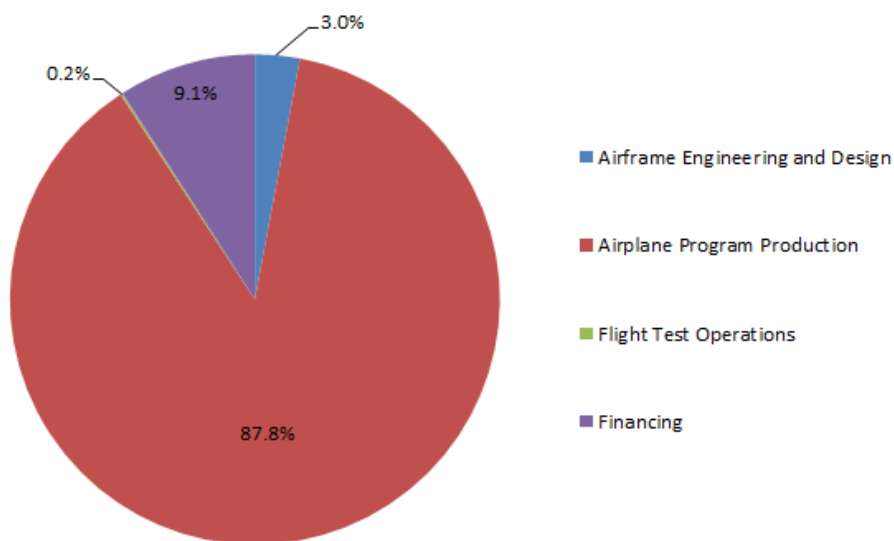


Figure 102: ORCA77 Manufacturing Cost Distribution



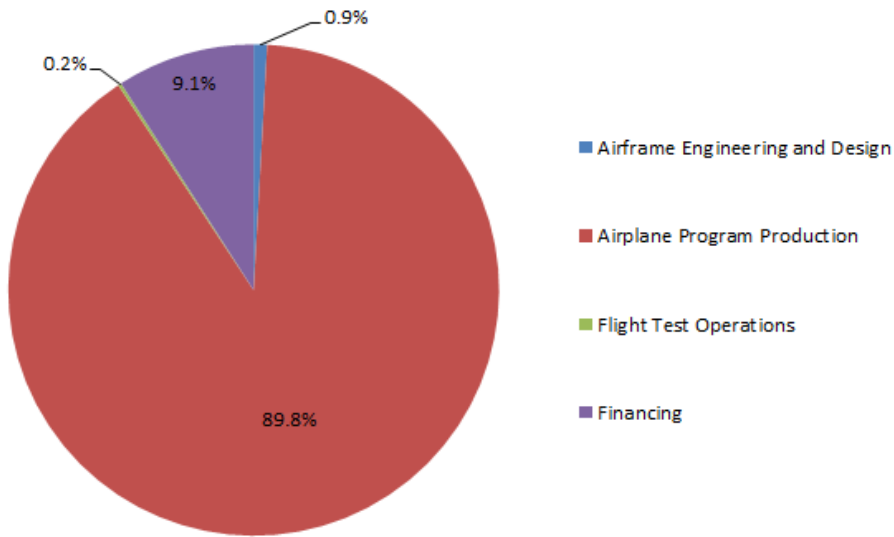


Figure 103: ORCA101 Manufacturing Cost Distribution

13.6 Unit Price per Aircraft and Competitor Comparison

Once the costs have been calculated, it is possible to determine a Unit Selling Price per Aircraft. It was established that the ORCA77 would be sold at 30M USD, and the ORCA101 at 36M USD by completing a survey of competitor's selling prices. These prices were also chosen with the mindset that the two aircraft would be sold as a family, and thus it would be advantageous to keep the selling prices as similar as possible. The Tables 57 and 58 below display the ORCA family selling values as compared to the competition values:

Company	Aircraft	Number of Pax	Unit Price (M of 2015 USD)	Difference Percentage
Polytechnique	ORCA77	77	30	[REFERENCE VALUE]
Bombardier	CRJ700	66	24	-20.0%
Bombardier	CRJ900	79	38.9	+29.67
Bombardier	Q400	68	27	-10.0%
Comac	ARJ21-700	78	20	-33.3%
Embraer	E-175	86	28	-6.67%
Mitsubishi	MRJ70	78	34	+13.3%
Sukhoi	SSJ100-75	68	30	+0.0%
Sukhoi	SSJ100-95	86	32	+6.67%
Market Average		76	29.24	-2.54%

Table 57: Unit Price - ORCA77



Company	Aircraft	Number of Pax	Unit Price (M of 2015 USD)	Difference Percentage
Polytechnique	ORCA101	101	36	[REFERENCE VALUE]
Airbus	A318	107	74	+105.56%
Boeing	737-600	110	59	+63.89%
Bombardier	CRJ1000	93	46	+27.78%
Bombardier	CS100	108	62	+72.22%
Embraer	E-190	94	32	-11.11%
Embraer	E-195	106	47	+30.56%
Mitsubishi	MRJ90	92	42	+16.67%
Market Average		101	51.71	+43.65%

Table 58: Unit Price - ORCA101

As can be observed in the tables above, the ORCA77's pricing is slightly above the competition's. However, the ORCA101 is significantly cheaper than the aircraft of the same passenger category. Therefore, as a family the ORCAs are largely advantaged from a selling price perspective, especially considering there would be more demand for the ORCA101 than the ORCA77. It is worth noting, nonetheless, that there may exist a difference in pricing between the competition's researched prices and those they currently offer to their clients. This disparity could skew the results of this analysis, however we consider that the ORCA's pricing is currently very competitive and advantageous from a marketing point of view.

Using these selling prices as compared to the costs detailed in the previous sections, we obtain a unit profit margin of 11.8M per ORCA77 sold, and 14.2M per ORCA101 sold. In order to determine the success or failure of the program using these selling prices, it is necessary to undertake Break-Even Analyses. These shall be presented in the following section.

13.7 Break-Even Analyses

The profitability of the ORCA program is studied in the following graphs. Figure 104 below presents the Break-Even Point in terms of units sold. It is to be noted that the Costs and Revenue used in this figure are weighted values in order to account for sales of both ORCA77's and ORCA101's. Afterwards, Figure 105 presents the Payback Period in terms of years until the Break-Even Point is attained. This figure uses the yearly sales of each respective aircraft determined during the Market Share Analysis in Section 2.3 of this report, and takes into account a constant 2% rate of inflation per year.



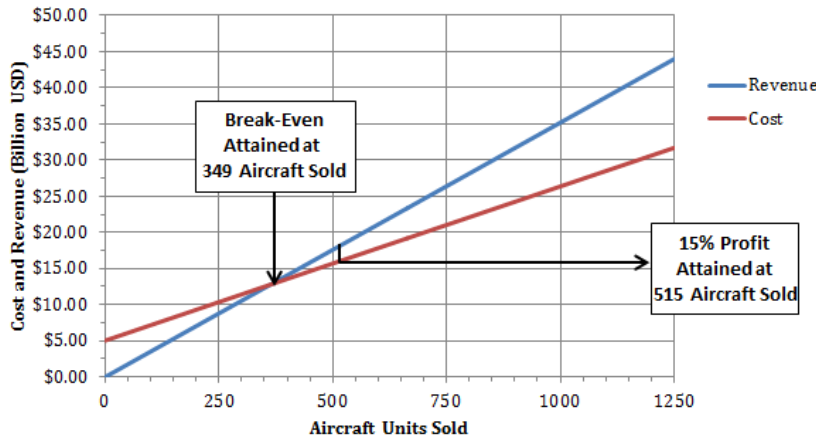


Figure 104: ORCA Family Weighted Break Even Analysis

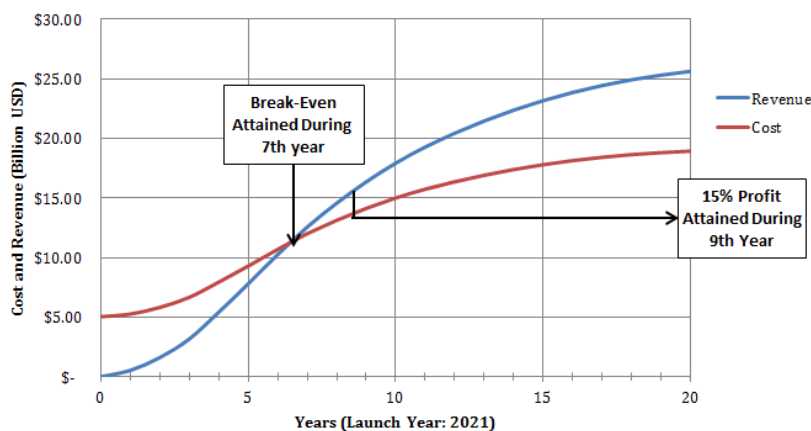


Figure 105: ORCA Family Payback Period Analysis

It can be observed from the two previous charts that the program will break even after approximately 350 aircraft sales, which will occur during the 7th year after the launch year of 2021. These are very respectable values for an aircraft program, and confirm the choice of unit pricing for the ORCA family; despite their low prices as compared to the competition, the ORCA77 and ORCA101 generate enough revenue per sale to eliminate the heavy initial costs within a reasonable amount of time. At the end of the 20-year program, it is estimated that the ORCA family will generate approximately 7B USD of net revenue.



13.8 Virtual Budget Evaluation

A virtual budget of 100 000\$ was initially provided to the engineering design team in order to accomplish the various preliminary design tasks. Following a budget re-evaluation at the mid-point of the project, this budget was raised to 130 000\$. The following graphs present the final standing and distribution of the budget throughout the various subgroups. The following bar graph (Figure 106) presents the total hours worked by the design team per week. It can be observed that works hours have remained relatively consistent throughout the semester, except in the weeks preceding the mid-term and final reports where a large spike of hours can be observed.

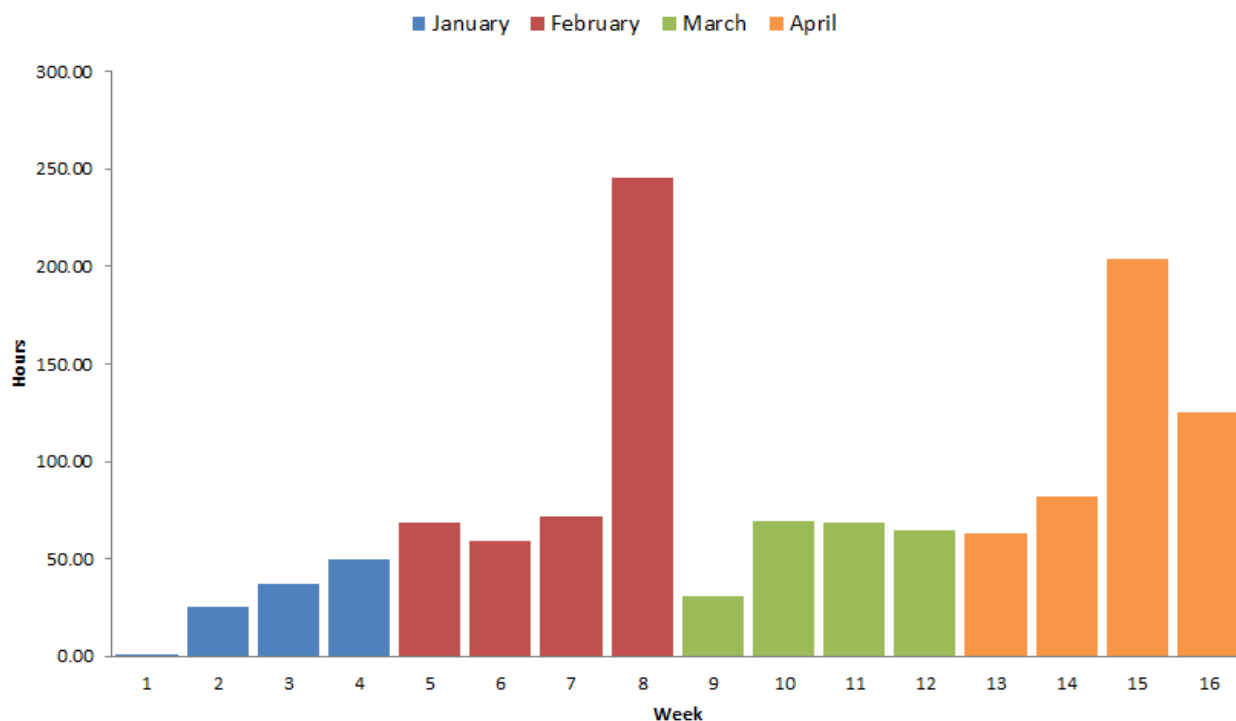


Figure 106: Weekly Personal Work Hours

The following pie chart (Figure 107) presents the distribution of the design team work hours by department. It can be observed that a majority of the costs are attributed to the Performance and Configuration Control departments, which have each had a significant workload establishing a functional first baseline, followed by consistent work throughout the semester to keep the design up to date. Systems occupies a large portion of the budgetary spending as well, due to the complexity of a MEA systems development.

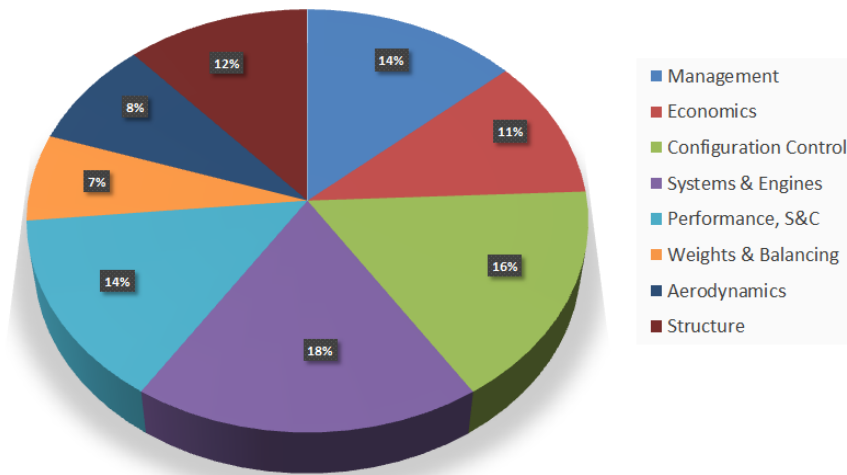


Figure 107: Departmental Budget Spending Distribution

The following pie chart (Figure 108) presents the overall distribution of budgetary spending. It can be easily observed that a significant portion of the budget (approximately 2/3) is currently being dedicated to departmental work.



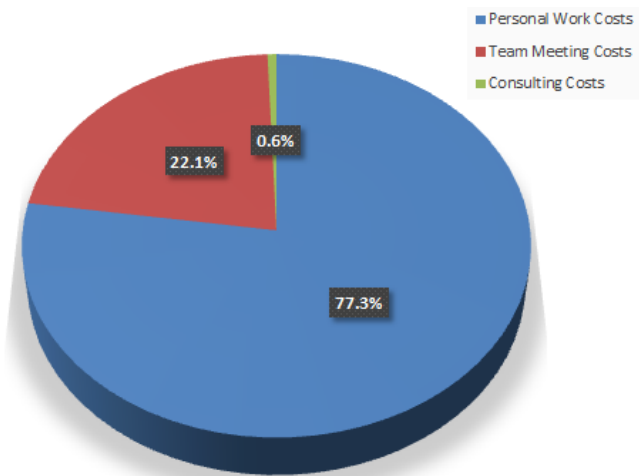


Figure 108: Overall Budget Distribution

The following chart (Figure 109) presents the weekly budget spending as compared to updated prediction with the 130 000\$ budget, as well as compared to the initial prediction with the 100 000\$ budget.

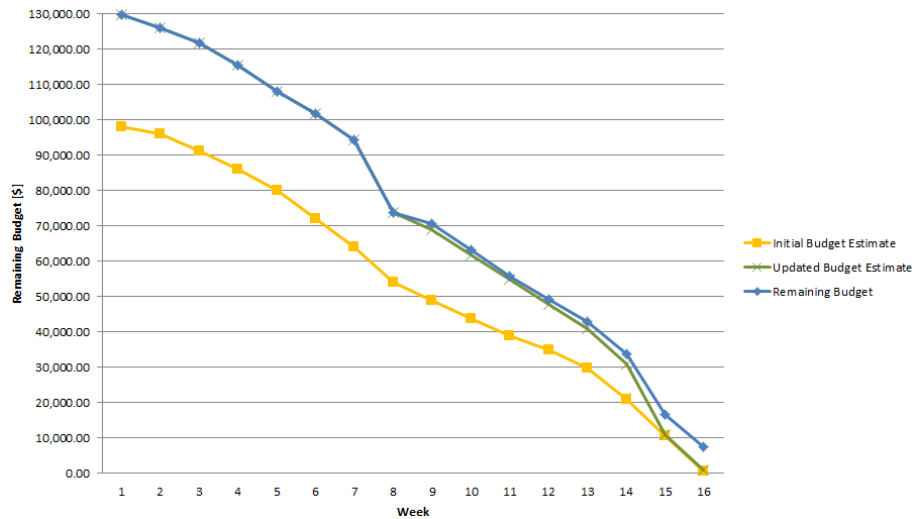


Figure 109: Weekly Budget Tracker

At the close of this project, the design team has spent 94.3% of the 130 000\$ budget, which leaves a margin of 7 375\$. The mid-semester budget update was therefore completely justified in order to allow the design team enough lee-way to complete their necessary tasks, seeing as budgetary spending surpassed the initial expectation by approximately 23 000\$. The remaining budget corresponds to approximately a full week's work by the entire design team - this money could therefore be used to fund another week of design work, if necessary.



14 Conclusion

14.1 Commonality

An important requirement stated in the MR&O was to respect commonality among parts at a ratio of at least 90%. This subject is addressed by assessing the commonality with regard to the structural components and systems configurations. Tables 59 & 60 display the high degree of commonality obtained for both ORCA aircraft.

Structural Components	
Wing	Common
Fuselage	Distinct
Horizontal Stabilizer	Common
Vertical Stabilizer	Common
Nacelle	Common
Pylon	Common
Main Landing Gear	Common
Nose Landing Gear	Common

Table 59: Structural Components Commonality

System Components	
Electrical System	Common
Hydraulic System	Common
ECS	Common
Ducting	Distinct
Fuel System	Common
Flight Controls	Common
Avionics	Common
Ice Protection	Common
APU	Common

Table 60: Systems Components Commonality

Table 59 indicates that the fuselage is the only element that will vary since two plugs are added to design ORCA 101. The structural components of the rest of the aircraft will be identical in order to simplify the manufacturing process. Hence, the production line will be able to work at a pace that meets the market demand. This is a standard practice when an aircraft family is designed.

Table 60 showcases how the systems are designed to meet the commonality requirement. The majority of them have been sized to satisfy the higher demand of the ORCA 101. The only



exceptions are associated with the ECS system and the electric hydraulic pump. The core ECS pack is similar inside both aircrafts, but the only deviation is related to the ducting and wiring for the ORCA 101 aircraft. These special cases won't interfere with the manufacturing efficiency related to commonality since the deviations are externally purchased products. Hence, it is correct to state that the 90% commonality requirement is met. In future phases, a mathematically precise assessment is recommended following the design of all parts of both aircraft.

14.2 Last Words

Following the design that the team has achieved so far, the product line is ready for official launch. After completing the preliminary aircraft design, we are able to visualise the standpoint of both aircraft regarding the competition and the MR&O. The fact that the use of optimization tools hasn't reached its full potential is an indication that the design refinement will be an ongoing operation in the next aircraft program phase. Also, integration is the main aspect that creates constraints between group activities because numerous interactions are required to complete most tasks. For example, the unification of the performance data center with the aerodynamics and weights codes resulted in a more centralized tool, but the complexity of the process greatly increased. The creation of specific groups and a team management role allows to recreate the environment present in the industry. When the team members become specialized in a particular field, it becomes increasingly arduous to track the advancement of the project as a whole. Hence, the design process described previously guided the team to achieve an aircraft design that complies with all the limiting factors of the MR&O.

The overall results are encouraging, but it is also very important to scrutinize the future aircraft that will attempt to replace our products. The team had the opportunity to present the preliminary aircraft design to a jury of professionals, and valuable feedback was given to improve our models regarding general morphology and configurations. While the jury appreciated our innovative vision, the main advice was to remember the ramifications that an unprecedented product technology would have on finance and certification. Despite the risks associated with integrating such advanced concepts throughout the aircraft, we believe that the ORCA family design presents various technological trends that will be applied in future aircraft as they continue to become more efficient, customer-oriented and environmentally friendly.



References

- [1] *Airport Planning manual.* Airbus, Fokker, Embraer, Bombardier, Boeing, Sukhoi, ATR, COMAC, -.
- [2] Auxiliary power system for the boeing 737. <https://hsapps.utc.com/powersystems/products/aps2000pds.htm>.
- [3] B737 autothrottle (a/t) - normal and non-normal operations. <http://www.flaps2approach.com/journal/2014/9/2/b737-autothrottle-at-normal-and-non-normal-operations.html>.
- [4] Boeing 727-63. <http://www.airliners.net/photo/Boeing/Boeing-727-63%28UDF%29/0001821/L/>.
- [5] Boeing 787 update. <http://www.compositesworld.com/articles/boeing-787-update/>.
- [6] Iata price analyses. <http://www.iata.org/publications/economics/fuel-monitor/Pages/price-analysis.aspx>.
- [7] Morichon's selected statistics in aircraft design. www.fzt.haw-hamburg.de/pers/Scholz/arbeiten/DataMorichon.xls.
- [8] Nasa sc(2)-0612 airfoil. <http://airfoiltools.com/airfoil/details?airfoil=sc20612-il/>.
- [9] Note de cours aer3640.
- [10] Open rotor noise not a barrier to entry: Ge. <http://www.flightglobal.com/news/articles/open-rotor-noise-not-a-barrier-to-entry-ge-373817/>.
- [11] FINANCIAL POST, mrj rolls out, but real test lies in certification. <http://business.financialpost.com/news/transportation/embraer-poised-to-extends-lead-in-regional-jet-as-over-bombardier>.
- [12] ROCKWELL COLLINS, head-up vision system. <http://rockwellcollins.com/~/media/134F7EDF74B04B4F9EE2DB435C1EC1C4.ashx>.
- [13] *Fibre metal laminates : an introduction.* Dordrecht, The Netherlands : Kluwer Academic Publishers, 2001.



- [14] *Aircraft design.* Cambridge aerospace series, Cambridge University Press, The Edinburgh Building, Cambridge CB2 8RU, UK, 2010.
- [15] B. Aerospace. Bombardier commercial aircraft market forecast 2014-2033, 2014.
- [16] B. Aerospace. Embraer commercial aircraft market outlook 2014-2033, 2014.
- [17] A. A. Baker. *Composite materials for aircraft structures.* Reston, VA : American Institute of Aeronautics and Astronautics, 2004.
- [18] N. BN. An overview of the boeing 777 high-lift aerodynamics design. *Aeronaut J*, 99:71, 1995.
- [19] Boeing. Fuel conservation strategies: Cost index explained. http://www.boeing.com/commercial/aeromagazine/articles/qtr_2_07/AERO_Q207_article5.pdf.
- [20] Bombardier. Bombardier engineering system. MEC8910A.
- [21] S. A. Brandt. *Introduction to aeronautics : a design perspective.* Reston, VA : American Institute of Aeronautics and Astronautics, 1953.
- [22] M. J. Brune GW. Computational aerodynamics applied to high-lift systems. *AIAA*, 125:389–433, 1989.
- [23] Butterworth-Heinemann. Data b : Engine data file. <http://booksite.elsevier.com/9780340741528/appendices/data-b/default.htm>.
- [24] S. Cham. Murdoc. *International Conference on Abstract State Machines, Alloy, B and Z. ABZ 2014 : the landing gear case study : proceedings.* 2014.
- [25] L. R. C. (Etats-Unis). *NASA acoustically treated nacelle program; a conference held at Langley Research Center.* Hyderabad, Inde :Leiden, Pays-Bas : BS Publications ; CRC Press, 1969.
- [26] C. K. Fassi Kafyeke, Francois Pepin. Development of high-lift systems for the bombardier crj-700. *ICAS 2002 Congress*, 2002.
- [27] D. G.E. Mabson, L.B.Ilcewicz. Cost optimization software for transport aircraft design evaluation. (*COSTADE*), 2000.
- [28] D. G.E. Mabson, L.B.Ilcewicz. New materials for next generation commercial transports. *Commission on Engineering and Technical Systems National Research Council*, 2000.



- [29] H. Gravel. On aircraft fuel systems: Conceptual design and modeling. 2007.
- [30] S. Gudmundsson. *General Aviation Aircraft Design: applies methods and procedures*. Oxford, Angleterre :Butterworth-Heinemann, 2014.
- [31] E. E. a. HENDRICKS. Performance and weight estimates for an advanced open rotor engine. <http://ntrs.nasa.gov/archive/nasa/casi.ntrs.nasa.gov/20120014381.pdf>.
- [32] N. J. Hoff. *Monocoque, sandwich, and composite aerospace structures : selected papers of Nicholas J. Hoff*. Lancaster, Pennsylvania : Technomic Pub, 1986.
- [33] D. Howe. *Aircraft Loading and structural layout*. Reston, Va. :Bury St Edmunds, U.K. : American Institute of Aeronautics and Astronautics ; Professional Engineering Publishing, 2004.
- [34] IATA. Fuel price analysis. <http://www.iata.org/publications/economics/fuel-monitor/Pages/price-analysis.aspx>.
- [35] IATA. Fuel price analysis. <http://www.iata.org/publications/economics/fuel-monitor/Pages/price-analysis.aspx>.
- [36] F. Jane. *Jane's All the World's Aircraft*. New York: McGraw-Hill, 2004.
- [37] A. e. a. KHALID. Open rotor aeroacoustic technology non-proprietary report. http://www.faa.gov/about/office_org/headquarters_offices/apl/research/aircraft_technology/cleen/reports/media/Open_Rotor_Public_Final_Report.pdf.
- [38] B. F. K.S. Wilden, C.G.Harris. Advanced technology composite fuselage-manufacturing. *The boeing Company Seatle*, 2002.
- [39] R. Langton and al. Aircraft fuel systems. Wiley, 2009.
- [40] T. L. Lomax. *Structural loads analysis for commercial transport aircraft : theory and practice*. Washington, D.C. : American Institute of Aeronautics and Astronautics, 1996.
- [41] Minco. Flexible heather design guide. http://www.minco.com/Heaters/~media/WWW/Resource%20Library/Minco_HeaterDesignGuide.ashx.
- [42] A. e. a. Moir. *Civil Avionics Systems*. AIAA, 2013.



- [43] G. C. Murthy, S. N. B. ; Paynter. *Progress in astronautics and aeronautics. V.102, Numerical methods for engine-airframe intégration.* New York : American Institute of Aeronautics and Astronautics, 1986.
- [44] N/A. Udf test flight. <http://www.frenchpainter.fr/?p=878>.
- [45] G. L. Narasaiah. *Aircraft structures.* Hyderabad, Inde :Leiden, Pays-Bas : BS Publications ; CRC Press, 2011.
- [46] NASA. Initial assessment of open rotor propulsion applied to an advanced single-aisle aircraft. <http://ntrs.nasa.gov/archive/nasa/casi.ntrs.nasa.gov/20110015875.pdf>.
- [47] NASA. Performance and weight estimates for an advanced open rotor engine. <http://ntrs.nasa.gov/archive/nasa/casi.ntrs.nasa.gov/20120014381.pdf>.
- [48] C.-Y. Niu. *Airframe structural design : practical design information and data on aircraft structures.* Cambridge aerospace series, Cambridge University Press, 1988.
- [49] C.-Y. Niu. *Composite airframe structures : practical design information and data.* Hong Kong : Commilit Press, 1992.
- [50] L. P Xue and C. Qiao. Crashwothiness study on fuselage section and struts under cabin floor.
- [51] R. PKC. High-lift systems on commercial subsonic airliners. *NASA CR 4746*, 1996.
- [52] D. Raymer. *Aircraft design: A conceptual approach.* American Institute of Aeronautics and Astronautics, 1999.
- [53] J. Roskam. *Airplane design.* Roskam Aviation and Engineering, 1985.
- [54] SBAC. Aviation and environment briefing papers. <http://www.sustainableaviation.co.uk/wp-content/uploads/open-rotor-engine-briefing-paper.pdf>.
- [55] M. Sinnett. 787 no-bleed systems: Saving fuel and enhancing operational efficiencies. http://www.boeing.com/commercial/aeromagazine/articles/qtr_4_07/AERO_Q407_article2.pdf.
- [56] H. Sundstrand. Auxiliary and ground power systems. http://hsapps.utc.com/powersystems/2190600_web.pdf.



- [57] J. A. Tanner. *Airframe structural design : practical design information and data on aircraft structures*. Warrendale, PA : Society of Automotive Engineers, 1997.
- [58] P. T.H.Walker. Advanced technology composite fuselage-performance. *The boeing Company Seatle*, 2002.
- [59] E. Torenbeek. *Synthesis of subsonic airplane design*. Dordrecht, Netherlands : Kluwer Academic Publishers, 1982, 1982.
- [60] E. Torenbeek. *Advanced Aircraft Design*. Aerospace Series, 2013.
- [61] E. Torenbeeki. *Development and application of a comprehensive, design-sensitive weight Prediction Method for Wing Structures of Transport Category Aircraft*. Dordrecht, Netherlands : Kluwer Academic Publishers, 1992.
- [62] C. van Dam. The aerodynamic design of multi-element high-lift systems for transport airplanes. *Progress in Aerospace Sciences*, 38:101–144, 2002.



A ANNEX

A.1 Materials

Initially, aluminum was used as the material choice for the principal structures as a safe benchmark, but in order to optimize the design, other material have been analysed. There are two tables with pros and cons for glare material and composite materials presented in this annex. Specifications are also giving for foam and honeycomb core material.

Pros	Cons
<ul style="list-style-type: none"> - Weight reduction - Low material cost - Lower manufacturing cost (less junction) - Less use of rivet (splice) Better finish - Low process temperature - Longer use - Fatigue resistant - Lightning protection 	<ul style="list-style-type: none"> - Mainly skin molded part - Low temperature use - Mainly skin molded part - Less data base & slightly more complex structural analysis

Table 61: Fuselage Structure Competitor Comparison

Pros	Cons
<ul style="list-style-type: none"> -Weight reduction -Lower manufacturing cost (less junction) -No use of rivet -Better finish -Better aeroelastic property -Low process temperature -No corrosion -Anisotropy -Fatigue resistant -Fretting resistant -More resistant to acoustic and service environnement 	<ul style="list-style-type: none"> - Mainly molded part - Low temperature use - Higher material cost : carbon fiber T8001 is 100\$/lbs compare to 5-20\$/lbs for aluminum) - Less data base & Complex structural analysis - Prone to delaminating - Sensitive to moisture, ultraviolet light, fuel, cleaning agent

Table 62: Fuselage Structure Competitor Comparison

The report shows a Pugh matrix which guides the material choices. Figure 110 shows the impact of cost of materials and manufacturing.



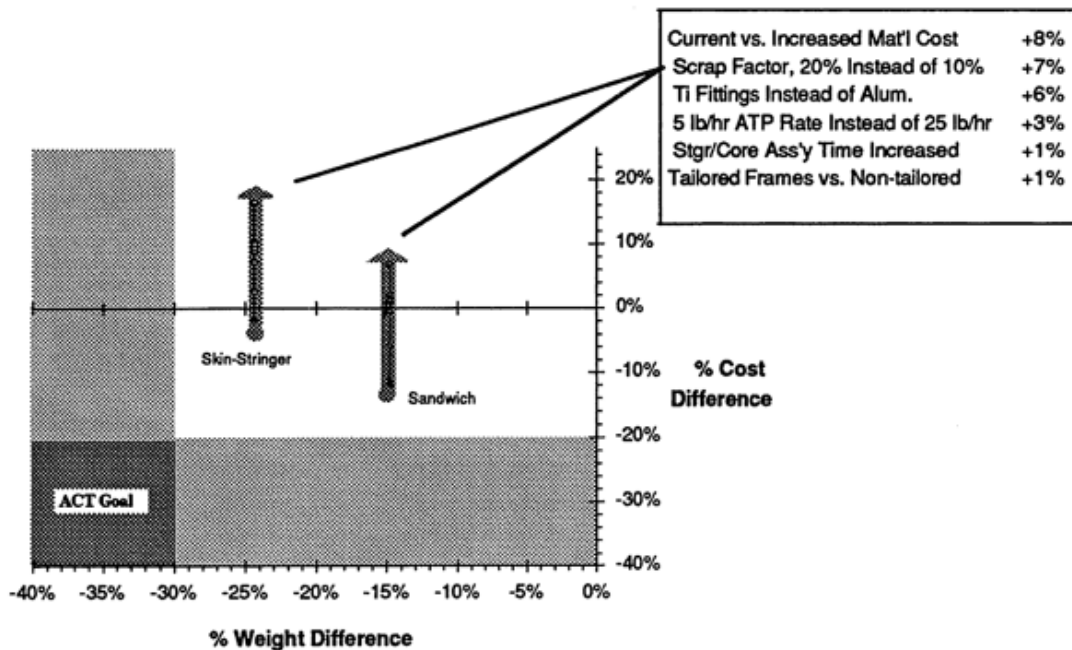


Figure 5-4. Cost and Weight Impact Based on Conservative Assumptions

Figure 110: Cost and Weight Impact Based on Conservative Assumptions

At this point of the design, choosing a complete composite structure without reinvesting this selection would be a blind choice. However, choosing an aluminum structure would be a big mistake considering possible weight reduction up to 30 % and cost reduction in long term perspective of nearly 50% shown in the figure 111.



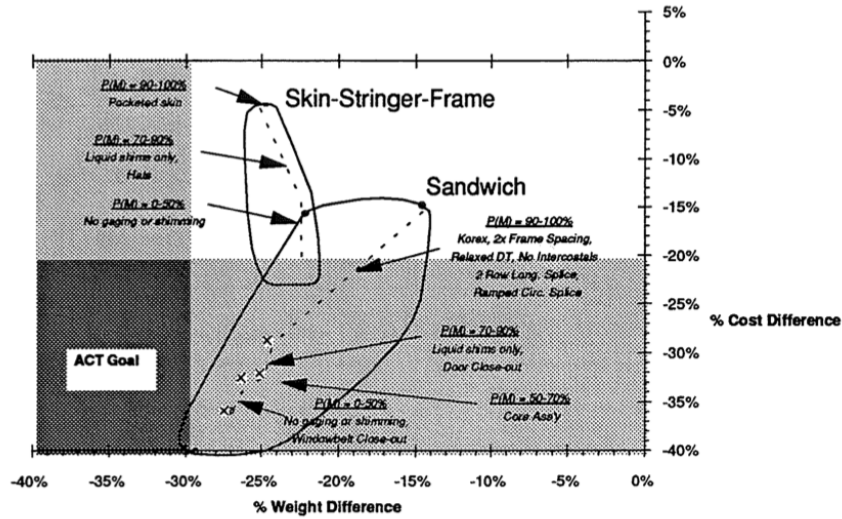


Figure 5-5. Range of Potential Cost and Weight Savings

Figure 111: Range of Potential Weight and Cost Savings

The sandwich design was benchmarked on a NASA analysis shown in the Figure 112. A slightly smaller thickness was chosen due to the smaller length of the fuselage. Regardless of sandwich design, the thickness was also compared with an aluminum skin.

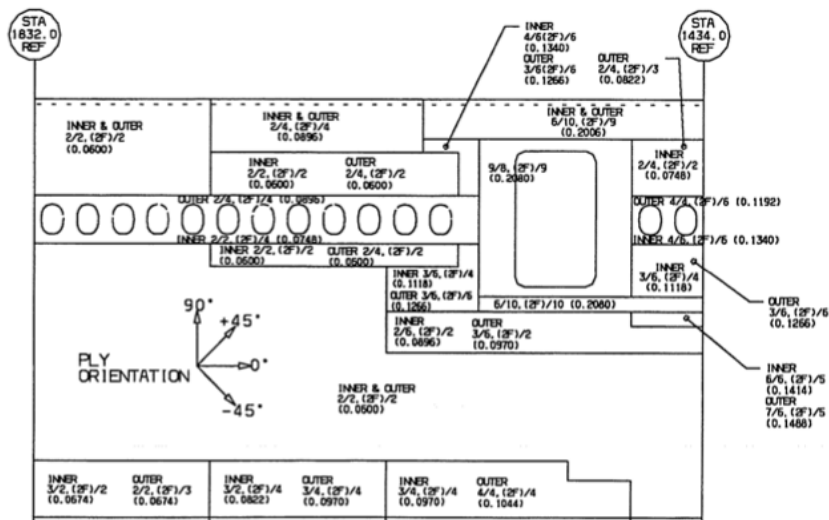


Figure 5-23. Ply Tailoring of Side Panel

Figure 112: Thickness Along a Sample Panel

All those impacts need to be considered and the manufacturing technology will be mainly



based upon the current company capacity and little improvement.

A.2 Structure

The initial stringer and frame structure is shown in the Figure 113 along with the table 63 that shows the benchmark made on similar aircraft with an aluminum structure.

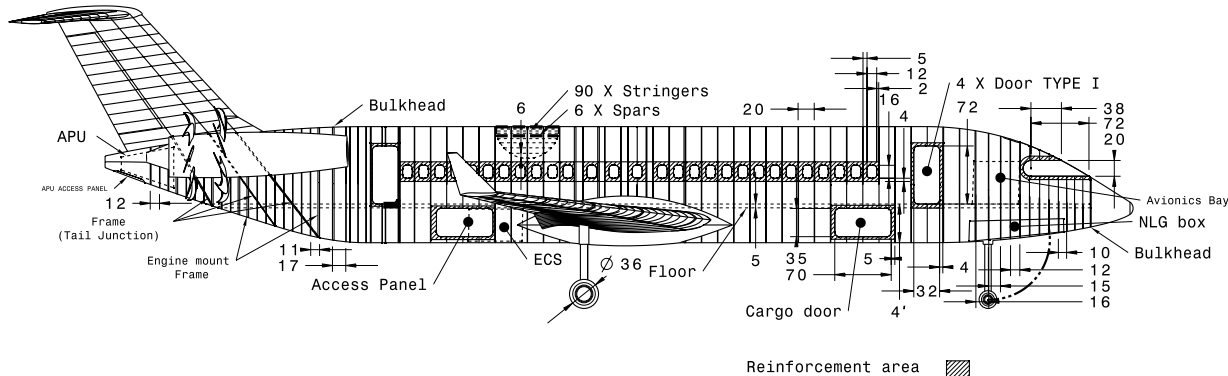


Figure 113: Initial Conventional Structure

The structure selected is shown at the beginning of Section 6.

Fuselage analysis		Design 77 & 101 PAX	Fokker100	Embraer-190	CRJ900	A319	717-200
Fuselage	Height	144	130	118.5	110	152	132
	width	144	130	132	110	152	142
Frame spacing	Nose	10-16	TBD	8-18	TBD	8-16	TBD
	Cabine section	16	20	16	TBD	16	16-18?
	Tail	8-20	16-18	8-18	TBD	10-16	TBD
Stringer	Nb	90	80 (5/L)	52 (7.5/Z)	52 (6.7/Z)	100 (Z)	65
	Spacing	5	5	7.5	6.7	5	4.3
	Type	Z	L	Z	Z	Z	TBD
Window size	10 X 14	10 X 13.5	12.8 X 14	10 X 14	TBD	10 X 14	TBD
Fuselage length	105/117	116.5	119	110	111	113	TBD
Configuration	Door Type	Sliding	Rotational	Sliding Door forward	Rotational	Slidding Forward	TBD
	Engine position	fuselage	fuselage	underwing	fuselage	under wing	fuselage
	Fuselage	circular	double bubble	circular	circular	double bubble	TBD
	Seat	3-2	3-2	2-2	2-2	3-3	3-2
	Toilet	3	2	2	1	3	2
	Galley	2	2	2	1	2	2

Table 63: Fuselage Structure Competitor Comparison

Wing/Stab.	Main component	Design 77 & 101 PAX	Fokker100	Embraer-190	CRJ900	A319	717-200
Area (ft²)/span (ft)	Wing	910/97	1006/92	996/94	647/81.5	1073/112	1001/93
	H-Stab	170/27.5	TBD	280/39.7	171/28	275/41	TBD/37
	V-Stab (1/2 b)	152/10.6	TBD	174/TBD	122	238/19.3	TBD
Spacing (Number of Ribs)	Outer Wing (1/2)	20-30 (25)	30 (18)	20-28 (28)	18-26 (20)	20-28 (25)	20-30 (18)
	V-stab	13 (9)	20 (5)	10 (13)	11(8)	25 (9)	15(8)
	Outer H-Stab (1/2)	20 (10)	22 (8)	30 (11)	18 (12)	35 (10)	30 (12)
Spacing (Number of	Wing box	6 (12)	7 (12)	5 (15)	6 (12)	7 (14)	5 (8)
	V-Stab box	6 (6)	(9)	(8)	(6)	(7)	TBD
	H-Stab box	6 (6)	TBD	TBD	(6)	(4)	(6)
Stringers) Spar Position	Wing	13/66/80	15/(50-60)/75	15/50/70(A)	15/70/75(A)	15/60/75(A)	15/60
	V-stab	13/33/62	TBD	15/25/60/65	20/50/75	20/55/70	15/55
	H-stab	15/70	10/70	15/40/70	15/70	15/50/70	15/55
Empennage Type	-	T-Tail	T-tail	conventional	T-tail	conventional	T-Tail

Table 64: Wing & Tail Structure Competitor Analysis



Actuator, Track and Hinges Competitor Analysis							
Control surfaces	Main component	Design 77 & 101 PAX	Fokker100	Embraer-190	CRJ900	A319	717-200
# Flap Track	4	4	6	8	6		
Number of Actuators	Ailerons	2	2	TBD	TBD	4	TBD
	Rudder	2	1	2	TBD	2	TBD
	Elevator	4	1	4	2	4	TBD
	Spoiler	10	10	TBD		10	TBD
	Slat	16	TBD	16	18	16	TBD
	Flap	6	6	6	TBD	6	TBD
Number of Hinges	Ailerons	4	TBD	5	4	4	TBD
	Rudder	4	3	5-10	TBD	3	TBD
	Elevator	4	3	TBD	3	4	TBD
	Spoiler	2	TBD	2	2	4	TBD
	Slat	2	TBD	2	3	2	TBD
	Flap	1	3	TBD	TBD	1	TBD

Table 65: Control Surfaces Competitor Analysis



A.3 Barrel and Panel Design Analysis

The barrel and panel design are shown in the Figure followed by an analysis contain in a Pugh matrix analysis in Table 66. The first design, Figure 114, is mainly used in an aluminum fuselage assembly.

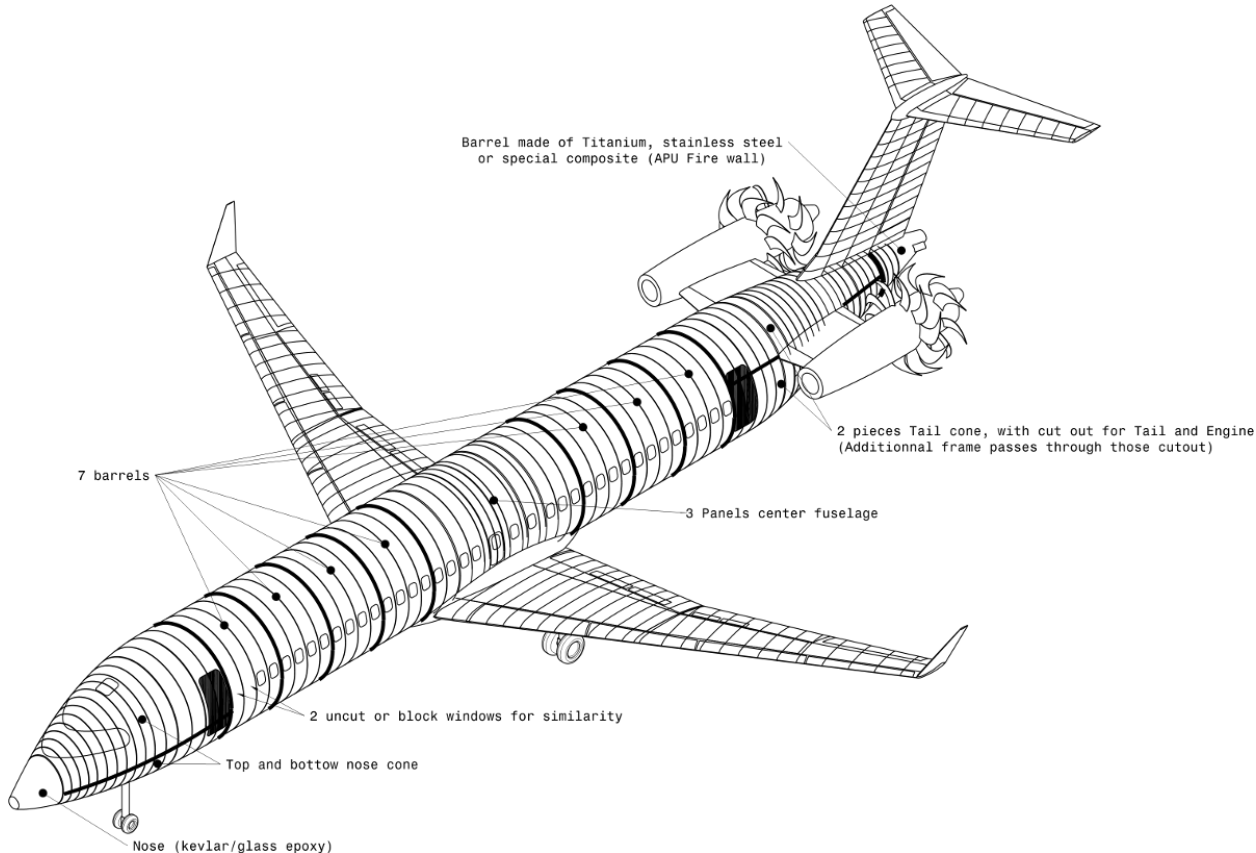


Figure 114: Barrel Design

The design below shows a 7 barrels design along the fuselage. The main advantage is the repetition of this barrel that is similar to the two plugs. That implies a same manufacturing process which reduces manufacturing cost but increase assembly complexity. Figure 115 shows another design with smaller panels instead of the barrel.

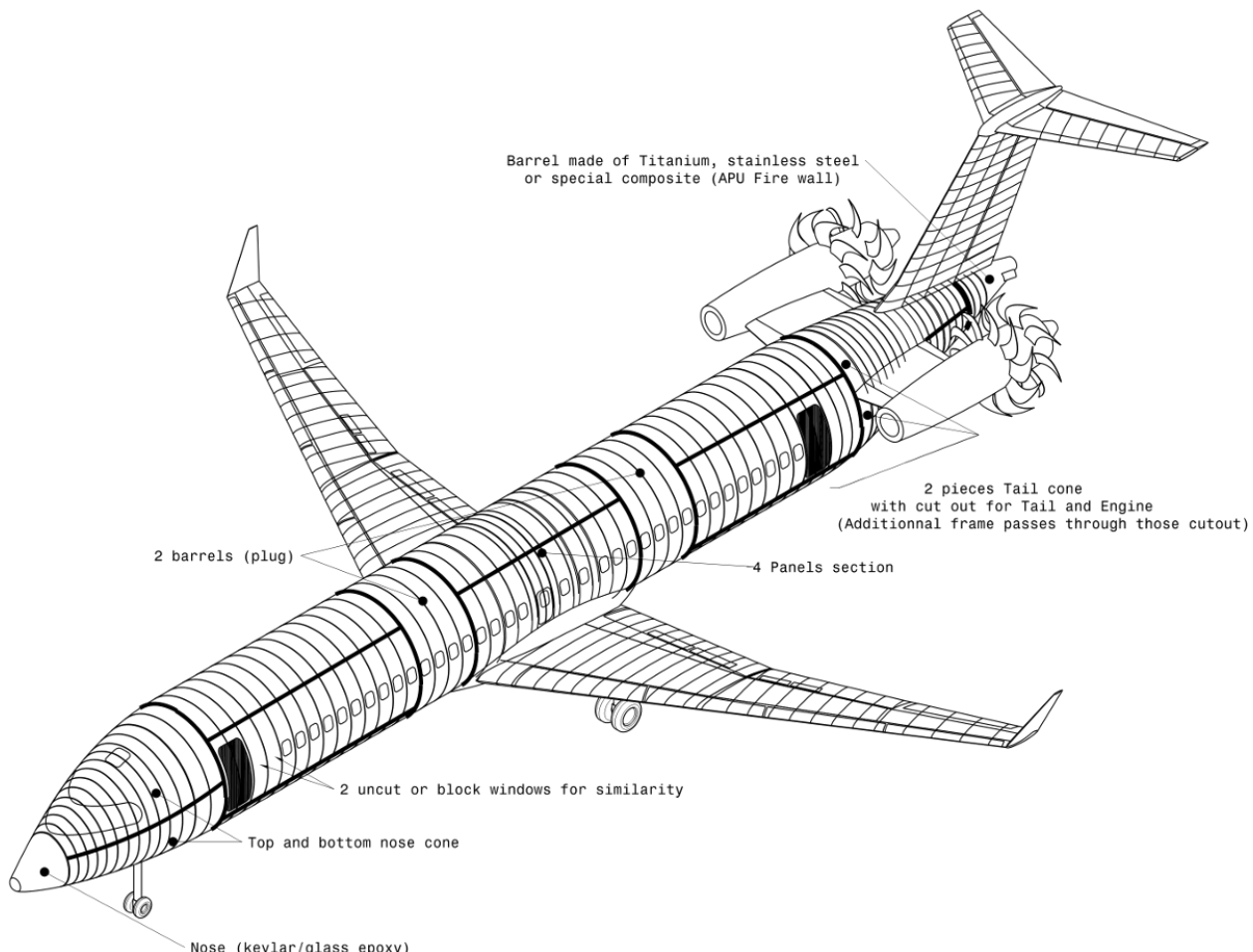


Figure 115: Three Sections Panels with Plugs

This design with a plug next to the wing junction proposed three sections of four panels. The assembly will be complex and the additional weight due to the junctions is a drawback of this design. The Figure 116 shows a full panel design with a plug at the end.

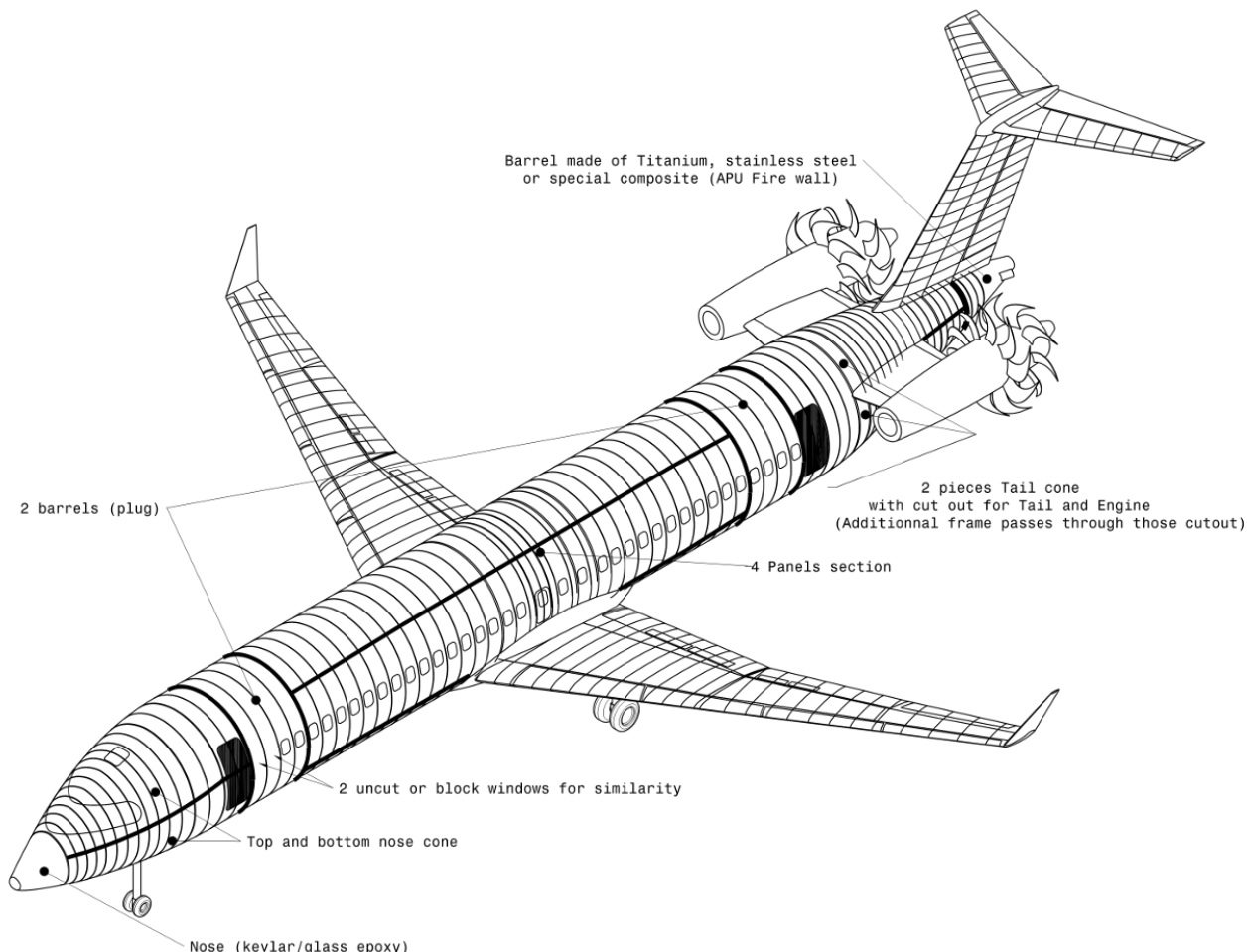


Figure 116: Full Panels Design with Plugs

Using full panels could improve manufacturing simplicity, but increase the amount of tooling. The next design proposed in Figure 117 shows a full length panel design with integrated plugs.

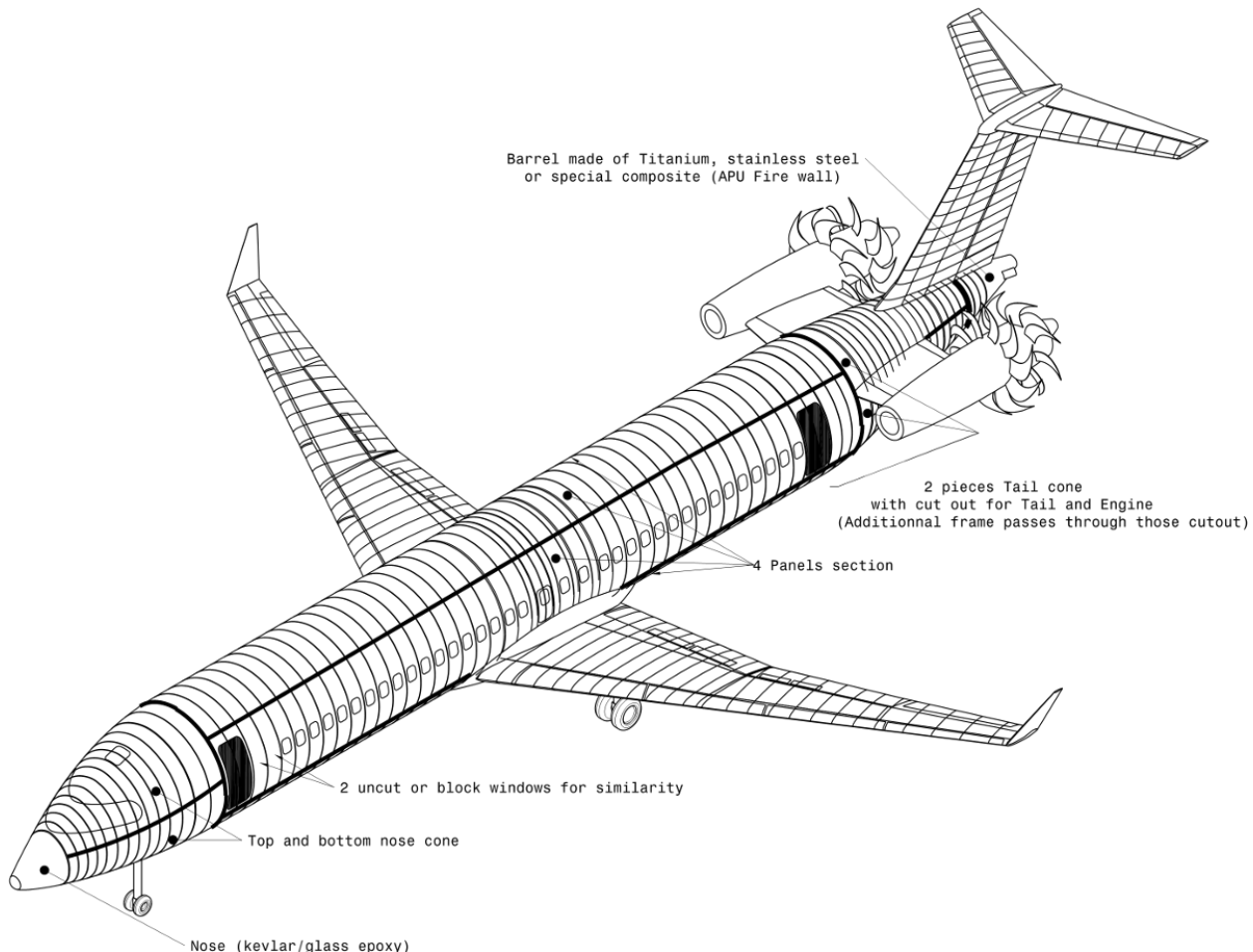


Figure 117: Full Length Panel Design

This last design was chosen for its simplicity due to less junctions and less panels. However, a drawback is the higher price for tooling due to the panel dimensions. Considering feasibility, same size panels are already made by Airbus for the A-350. The Pugh matrix (Figure 66) below show the analysis result.

	Complexity	Part size	Weight	Junction	Price	Commonality	Total	Comments
Criteria	Total Parts / Distinct Parts	(+, big)	(+, heavy weight)	(+, tolerancing issue)	(+, expensive)	(++ = Non-commonality)		
Barrel Design	16/10(+++)	+++	+	+	+++	++++	25	Small dimension and repeatability, trouble with assembly
Three Section panels with plugs	20/19 (+)	++	+	++	+	++++	17	More easy to assemble, average size part, lots of parts, easier for maintenance to change a panel.
Full Panels Design (barrels and plugs)	12/11(+++)	+	++	++	++	++++	25	Longer Nose cone & hard assembly between nose/tail cone and plug
Full Panels Design (No plugs, different panels for 101 PAX& 77 PAX)	10/10(++++)	+	+++	++	+++	++	29	Less panels, lighter panels (less junctions), easy to manufacture, to store, possibility of easier repair (due to a panel replacement)
Weight	2	1	3	1	2	1.5		

Table 66: Panel & Barrel Comparison

The integration of many other system was a the next task; specifically, the wing and the empennage have actuators for control surfaces that may required more space than there actual space between the skins or sandwich layer. The task of sizing those actuator required to estimated the maximum load required. The load shown in the Figure 118 & 121 bellow were use.



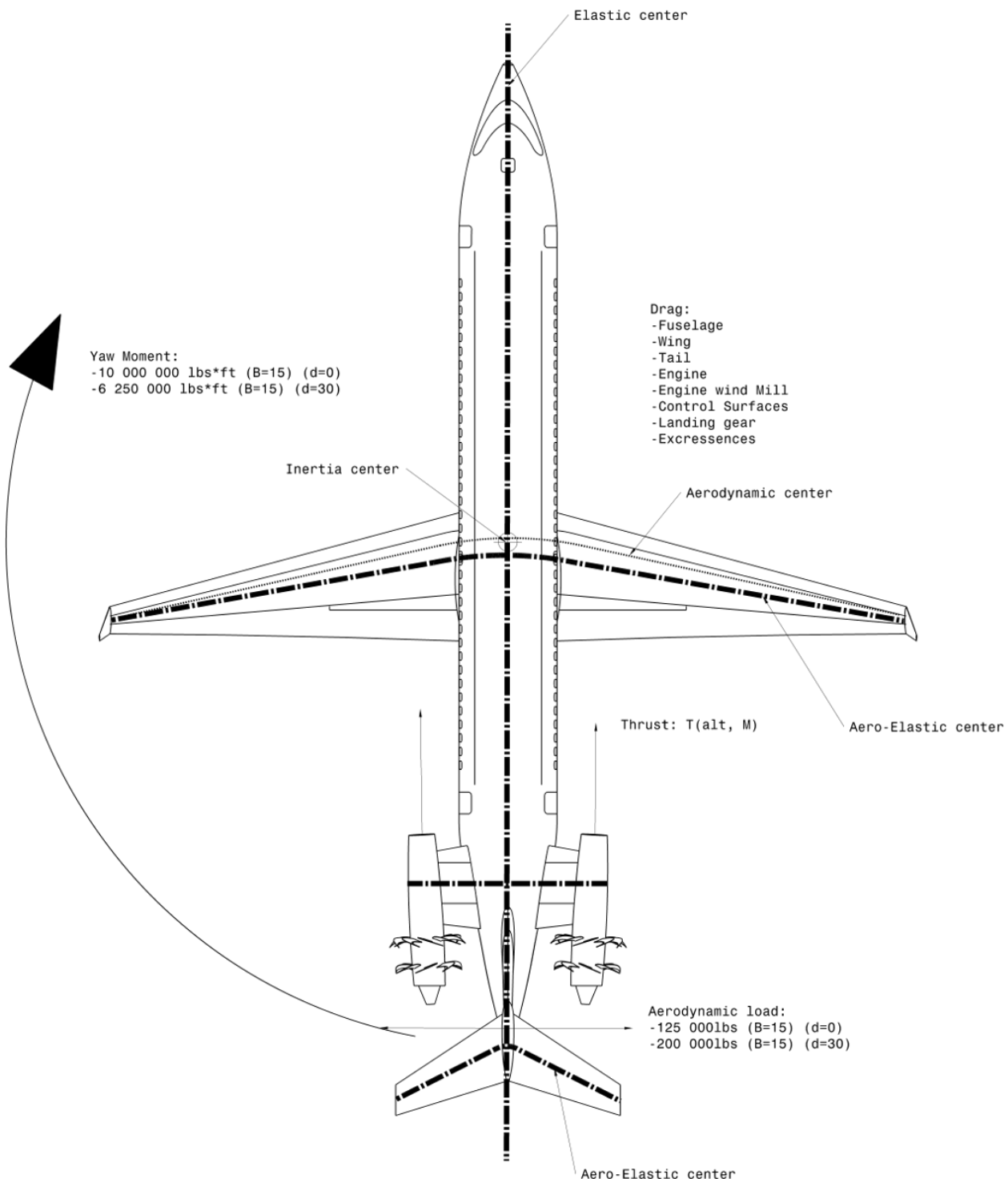


Figure 118: Top View Load Path

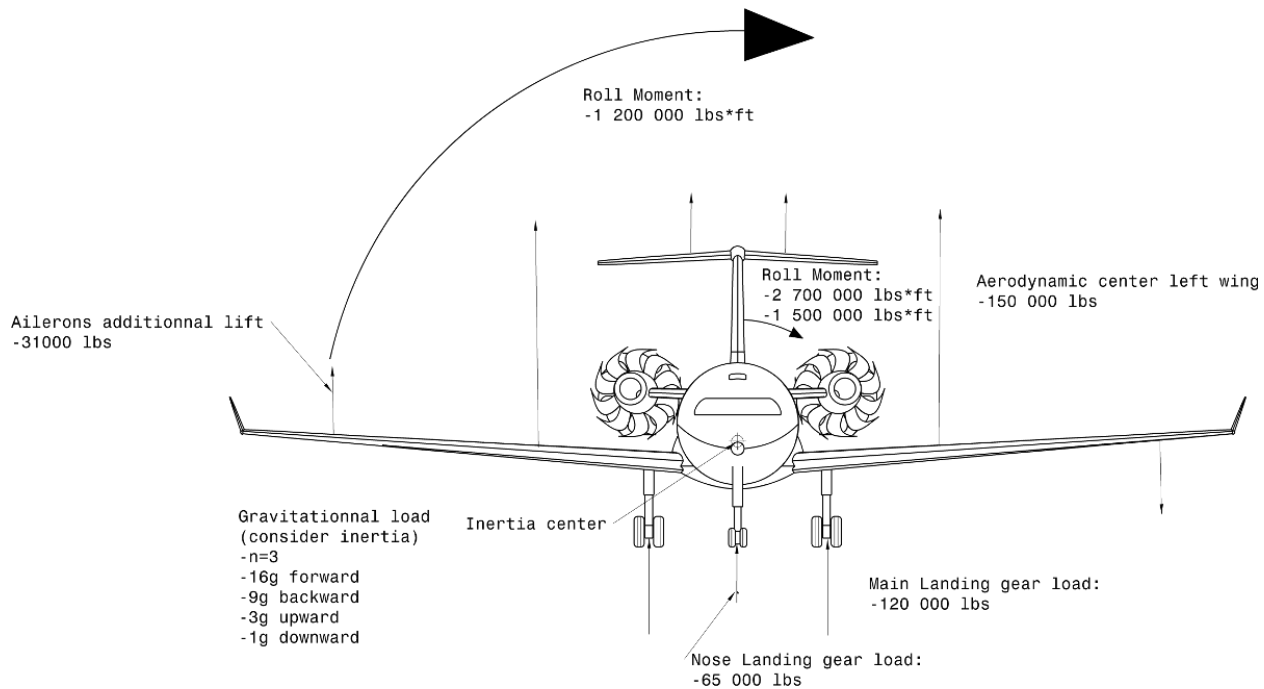


Figure 119: Frontal Load Path

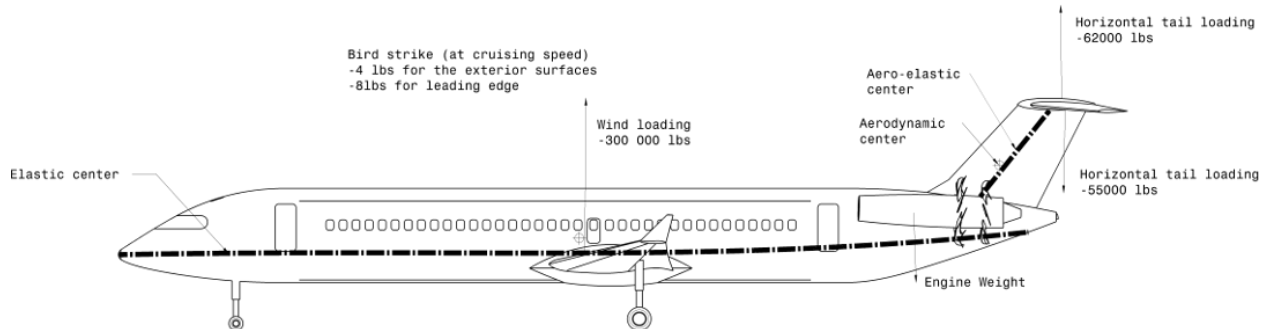


Figure 120: Longitudinal Load Path

Loads were considered for two extreme conditions: dive and step turn at Clmax. More extreme conditions could be explored considering an error from the pilot or the control system; an additional security factor was chosen. The table 67 below shows the actuator initial sizing.



	Maximum required volume (in)	# Actuators under critical load	Lever (ft)	Load (lbs)	Condition
Rudder	8 X 13 X 19	1	0.7	25000	Dive (Climax V-tail)/Dive (B=15°)
Elevator	7 X 10 X 14	1	0.3	22000	Recovery Dive (n=3)
Ailerons	5 X 8 X 12	1	0.3	8500	Recovery Dive (n=3)
Flap	25175	2	1	63000	n=3
Spoiler	4 X 7 X 10	8	0.50	7000	Dive
Slat	4 X 6 X 10	8	3.5	6000	n=3
H-stab	9 X 15 X 22	1	2	35000	

Table 67: Actuator Initial Sizing

This Table was use to size the actuator show in the view. The more critical were: the flap actuator, the ailerons actuator, the horizontal incidence actuator and both rudder and elevator actuator. Two type of actuator were considered electro/hydraulic and hydraulic actuator.

A.4 Landing Gear Design

The landing gear was design considers an MTOW of 90 000 lb and a landing weight of 80 000 lb. The table below [68](#)

		Nose landing gear	Main landing gear
Stroke (in)		16	16
Overlap (in)		18	11
Tire type		24 X 7.7-12	36 X 11.5-16
Rolling radius (in)		10.7	16.5
Wheel	Diameter (in)	10	16
	Width (in)	5.5	9
Heat sink	Width (in)	NA	6.00
	OD (in)	NA	4.38
	ID (in)	NA	6.88
Number of disk		NA	4
Brake width (in)		NA	8.75
Rolling radius (in)		10.72	16.53

Table 68: Landing Gear Sizing

One important point of this sizing was to ensure that the heat sink is small enough to fit in the wheel. In another order of ideas, a design proposal was made with electrical motor powering the aircraft for takeoff. Table [69](#) show the pros and cons of this proposition.



Pros	Cons
<ul style="list-style-type: none"> -Reduce the takeoff distance (Maybe a down size for the motor) -Energy can restore in the batteries during landing -Use for displacement on land 	<ul style="list-style-type: none"> -More weight -Slightly more drag for take off -More maintenance

Table 69: Landing Gear Sizing Electrical Motor Integration Analysis

Overall Weight (lbs)	2582	Aircraft to landing gear weight ratio	3.11%
Component	NLG Weight	(% overall)	MLG Weight
structure	77	3.0%	464
Wheel	34	1.3%	252
Tire	53	2.1%	402
brake	0	0.0%	286
actuator	52	2.0%	181
direction actuator	26	1.0%	0
Shock absorber strut	164	6.4%	591

Table 70: Landing Gear Weight Breakdown

Main Landing Gear Weight distribution: ORCA101



- structure
- Tire
- actuator
- Shock absorber strut
- Wheel
- brake
- direction actuator

Nose Landing Gear Weight distribution: ORCA101



- structure
- Tire
- actuator
- Shock absorber strut
- Wheel
- brake
- direction actuator

Figure 121: Landing Gear Weight Breakdown

The landing gears are designed to confer the right rigidity at high temperature. Also, height and material selection were considered. The overall weight is slightly lower than initial sizing using many equations as described in the Figure 122.



- Landing weight meets the Douglas and GD predictions

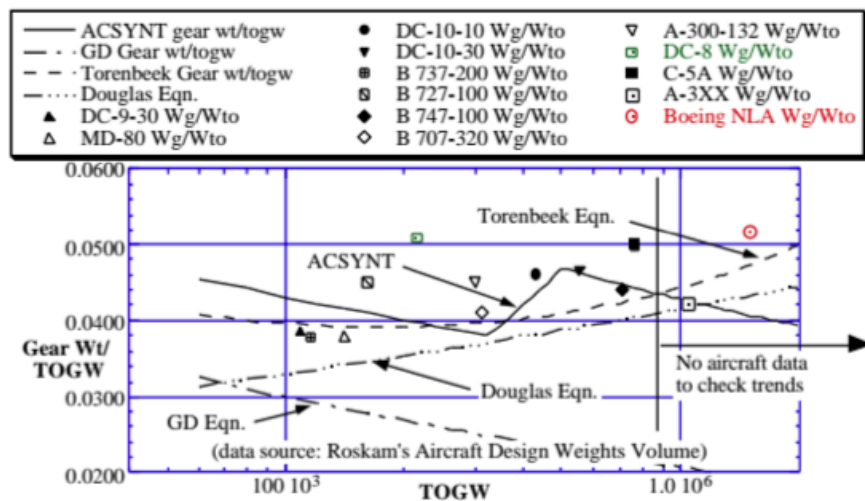


Figure 1-1. Initial comparison of weight equations with aircraft weights data.

Sonny T. Chai & William H. Mason, **Landing Gear Integration in Aircraft Conceptual Design**, MAD Center Report: MAD 96-09-01, September 1996. NASA Ames Research Center under Grant NAG-2-919

Figure 122: Landing Gear Weight Initial Sizing

